EG&G

EGG-1183-1661
15 April 1975

0014281

AN AERIAL RADIOLOGICAL SURVEY OF THE U.S. ENERGY RESEARCH AND DEVELOPMENT ADMINISTRATION'S HANFORD RESERVATION

(SURVEY PERIOD: 1973 - 1974)

by

W. John Tipton

Approved for Publication:

J. R. Doyle, III, Manager
Aerial Surveillance Dept.

C. Jupiter, Manager
Radiation and Environmental Sciences Dept.

This Document is
UNCLASSIFIED

G. P. Stobie
Classification Officer

JUN 1991
RECEIVED
EDMC

Prepared by EG&G, Inc. for the United States Energy Research and Development Administration, Division of Operational Safety.

ACKNOWLEDGMENTS

Appreciation is given to L. J. Deal, Assistant Director of the U. S. Energy Research and Development Administration's Division of Operational Safety, for his support and encouragement in this survey project.

Correlation of the aerial results with source location on the ground was provided by L. V. Barker (UNI), L. E. Bruns (ARHCO), J. P. Corley (BNW), R. B. Hall (WHC) and B. J. McMurray (ARHCO).

Acknowledgment is given for the excellent contribution of the EG&G survey team: L. R. Arambula, J. R. Cleland, I. F. Harris, J. T. Hess, R. J. Mazurkewiz, G. E. Menkel, M. D. Sevart, W. F. Verheyden & G. G. Wallace. Computer data reduction and analysis was carried out with the assistance of C. M. Bluitt, J. W. Cates, E. L. Feimster and T. J. Hendricks. Photographic support was provided by G. H. Bull Jr., M. K. Knighten, R. A. Meibaum and M. D. Pelan.

Appreciation is given to CDR. Reed Carelton and the men of the U.S. Navy ASW WING PAC, San Diego for their excellent helicopter support.

Special appreciation is given to R. B. St. John of the ERDA's Richland Operations Office for his aid in coordinating the operational aspects of the surveys.

CONTENTS

		Page
TABLES		v
ILLUSTRATIONS		vi
ABSTRACT		x
1.	INTRODUCTION	1
2.	SYSTEMS AND PROCEDURES	4
2.1	Data Acquisition System	4
2.2	Data Reduction System	10
2.3	Survey Procedures	12
2.4	Data Reduction Procedures	13
2.5	Calibration Procedures	19
3.	SURVEY RESULTS	25
3.1	Hanford Reservation Survey	25
3.2	Reactor Areas	30
3.2.1	B and C Reactor Areas	32
3.2.2	KW and KE Reactor Areas	32
3.2.3	N Reactor Area	39
3.2.4	D and DR Reactor Areas	39
3.2.5	H Reactor Area	43
3.2.6	F Reactor Area	43
3.3	200 Area Plateau	55
3.3.1	200-West Area	55
3.3.2	200-East Area	59
3.3.3	Waste Transfer Line	65
3.3.4	Gable Mountain Pond	65
3.3.5	BC-Crib Area	65
3.3.6	200-North Area	70
3.4	Burial Grounds	70
3.5	300 Area	73
3.6	Columbia River	73
3.7	Special Surveys	93
3.7.1	^{241}Am Survey	93
3.7.2	Neutron Survey	95
3.7.3	Ge(Li) Survey	95

Contents (cont.)

Page

4. SUMMARY. 101

APPENDIX DERIVATION OF CONVERSION FACTORS RELATING AERIAL MEASUREMENTS TO GROUND CONCENTRATION FOR A VARIETY OF SOURCE GEOMETRIES 103

REFERENCES

TABLES

Table		Page
1.	Conversion factors used during the Hanford survey to relate photopeak window count rate data to radionuclide concentration on the ground.	23
A.1	Conversion factors relating aerial photopeak count rate data to radionuclide concentration on the ground for a variety of source distribution geometries	110

ILLUSTRATIONS

Figure		Page
1.	Area map of the Hanford Reservation.	2
2.	Block diagram of the data acquisition system	5
3.	Photograph of the REDAR (Radiation and Environmental Data Acquisition and Recorder)	6
4.	The SH-3 helicopter shown with the NaI(Tℓ) detector pods attached.	7
5.	One of the gamma radiation detector pods with the hatch cover removed.	8
6.	Photograph of the REDAC (Radiation and Environmental Data Analyzer and Computer)	11
7.	A typical gamma ray spectrum showing the pulse-height windows used to extract ^{137}Cs and ^{60}Co photopeak count rate data	16
8.	Line plots illustrating the stripping technique used to extract ^{60}Co and ^{137}Cs photopeak count rate data	18
9.	Gamma ray spectra obtained along three segments of the flight line shown in Figure 8	20
10.	Flight lines flown during the fixed-wing (150-meter altitude) survey	26
11.	Isopleth map of the total gamma ray count rate obtained during the fixed-wing survey	27
12.	Concentration and gamma exposure rate isopleths for ^{137}Cs obtained during the fixed-wing survey	28
13.	Concentration and gamma exposure rate isopleths for ^{60}Co obtained during the fixed-wing survey	29
14.	Facility map of the 100-B and 100-C reactor areas.	33
15.	Isopleth map of the total gamma ray count rate obtained over the 100-B and 100-C reactor areas. . .	34
16.	Concentration and gamma exposure rate isopleths for ^{60}Co obtained over the 100-B and 100-C reactor areas.	35
17.	Facility map of the 100-KW and 100-KE reactor areas.	36
18.	Isopleth map of the total gamma ray count rate obtained over the 100-KW and 100-KE reactor areas.	37

Figure | Page

19. Concentration and gamma exposure rate isopleths for ^{60}Co obtained over the 100-KW and 100-KE reactor areas. 38
20. Facility map of the 100-N reactor area 40
21. Isopleth map of the total gamma ray count rate obtained over a portion of the 100-N reactor area. . . . 41
22. Concentration and gamma exposure rate isopleths for ^{60}Co obtained over a portion of the 100-N reactor area. 42
23. Facility map of the 100-D and 100-DR reactor areas . . 44
24. Isopleth map of the total gamma ray count rate obtained over the 100-D and 100-DR reactor areas . . . 45
25. Concentration and gamma exposure rate isopleths for ^{60}Co obtained over the 100-D and 100-DR reactor areas 46
26. Facility map of the 100-H reactor area 47
27. Isopleth map of the total gamma ray count rate obtained over the 100-H reactor area 48
28. Concentration and gamma exposure rate isopleths for ^{60}Co obtained over the 100-H reactor area 49
29. Facility map of the 100-F reactor area 51
30. Isopleth map of the total gamma ray count rate obtained over the 100-F reactor area 52
31. Concentration and gamma exposure rate isopleths for ^{60}Co obtained over the 100-F reactor area 53
32. Gamma ray spectrum obtained over the 1707-F, FA Inhalation Laboratory 54
33. Facility map of the 200-West Area 56
34. Isopleth map of the total gamma ray count rate obtained over the 200-West Area 57
35. Concentration and gamma exposure rate isopleths for ^{137}Cs obtained over the 200-West Area. 58
36. Physical location of the areas where elevated activity was observed during the 200-West Area survey. 60
37. Gamma ray spectra obtained over four of the areas of elevated activity identified in Figure 36 61
38. Facility map of the 200-East Area 62
39. Isopleth map of the total gamma ray count rate obtained over the 200-East Area 63
40. Concentration and gamma exposure rate isopleths for ^{137}Cs obtained over the 200-East Area 64

Figure | Page

41. Physical location of the areas where elevated activity was observed during the 200-East Area survey. 66
42. Concentration and gamma exposure rate isopleths for ^{137}Cs obtained over the waste transfer pipeline . . . 67
43. Isopleth map of the total gamma ray count rate obtained over the Gable Mountain Pond area 68
44. Concentration and gamma exposure rate isopleths for ^{137}Cs obtained over the Gable Mountain Pond area 69
45. Isopleth map of the total gamma ray count rate obtained over the BC-Crib area 71
46. Concentration and gamma exposure rate isopleths for ^{137}Cs obtained over the BC-Crib area 72
47. Facility map of the 300 Area. 74
48. Isopleth map of the total gamma ray count rate obtained over the 300 Area 75
49. Concentration and gamma exposure rate isopleths for ^{60}Co obtained over the 300 Area. 76
50. A photo mosaic of the Columbia River showing the twelve areas surveyed 78
51. Concentration and gamma exposure rate isopleths for ^{60}Co obtained along the Columbia River between the Vernita Bridge and the 100-B Area 79
52. Concentration and gamma exposure rate isopleths for ^{60}Co obtained along the Columbia River between the 100-B and 100-D reactor areas 80
53. Concentration and gamma exposure rate isopleths for ^{60}Co obtained along the Columbia River between the 100-D and 100-F reactor areas 81
54. Concentration and gamma exposure rate isopleths for ^{137}Cs obtained along the Columbia River between the 100-D and 100-F reactor areas 82
55. Concentration and gamma exposure rate isopleths for ^{60}Co obtained along the Columbia River between the 100-F Area and the old Hanford townsite. 83
56. Concentration and gamma exposure rate isopleths for ^{137}Cs obtained along the Columbia River between the 100-F Area and the old Hanford townsite. 84

Figure Page

57. Concentration and gamma exposure rate isopleths for ^{60}Co obtained along the Columbia River in the vicinity of Savage Island. 85
58. Concentration and gamma exposure rate isopleths for ^{60}Co obtained along the Columbia River in the vicinity of Wooded Island 86
59. Concentration and gamma exposure rate isopleths for ^{60}Co obtained along the Columbia River between the 300 Area and North Richland 87
60. Concentration and gamma exposure rate isopleths for ^{60}Co obtained along the Columbia River near its intersection with the Yakima River. 88
61. Concentration and gamma exposure rate isopleths for ^{60}Co obtained along the Columbia River between Pasco and Kennewich. 89
62. Concentration and gamma exposure rate isopleths for ^{60}Co obtained along the Columbia River near its intersection with the Snake River 90
63. Concentration and gamma exposure rate isopleths for ^{60}Co obtained along the Columbia River just below McNary Dam. 91
64. Concentration and gamma exposure rate isopleths for ^{60}Co obtained along the Columbia River near Irrigon. 92
65. Concentration isopleths for ^{241}Am obtained during a special low energy survey over a portion of the 200-West Area 94
66. Isopleth map of the neutron count rate (at an altitude of 30 meters) obtained during a special survey over a portion of the 200-West Area. 96
67. Isopleth map of the total gamma ray count rate obtained during a special survey over a portion of the 200-West Area utilizing a 77 cm^3 Ge(Li) detector . . 98
68. Isopleth map of the ^{137}Cs photopeak count rate obtained during a special survey over a portion of the 200-West Area utilizing a 77 cm^3 Ge(Li) detector . . 99
69. Isopleth map of the ^{60}Co photopeak count rate obtained during a special survey over a portion of the 200-West Area utilizing a 77 cm^3 Ge(Li) detector . .100
A.1 Geometry used in the derivation of conversion factors relating aerial photopeak count rate data to ground concentrations 104

ABSTRACT

During the period from May 1973 to April 1974, four aerial radiological surveys were conducted over the United States Energy Research and Development Administration's Hanford Reservation. These surveys, conducted at the request of the ERDA's Division of Operational Safety, were made utilizing the Aerial Radiological Measuring System (ARMS) operated for the ERDA by EG&G, Inc. The surveys were conducted as part of a continuing nationwide ARMS program, started in 1958, to monitor radiation levels in and around facilities utilizing or producing radioactive material. Two distinct types of surveys were performed. The first, utilizing a fixed-wing aircraft, covered the entire site and an area extending approximately eight kilometers in each direction from the site boundary. This survey was flown at an altitude of 150 meters with line spacings varying from 0.4 to 1.6 kilometers. The second type of survey utilized a helicopter platform to provide detailed coverage over selected areas. These surveys were flown at an altitude of 45 meters with 45 meter line spacings. Detailed helicopter surveys were flown over each of the major facilities located within the Hanford Reservation as well as along a section of the Columbia River. The river survey extended from the Vernita Bridge upstream of the site to the intersection of the Snake and Columbia Rivers approximately 35 kilometers downstream from the site boundary. The aerial results are presented in the form of radioisotope concentration and gamma ray exposure rate isopleths plotted over aerial photographs of each area surveyed.

1. INTRODUCTION

During the period from May 1973 to April 1974, four aerial radiological surveys were conducted over the United States Atomic Energy Commission's* Hanford Reservation. These surveys were performed using the Aerial Radiological Measuring System (ARMS), operated for the AEC by EG&G, Incorporated. The surveys were made at the request of the AEC's Division of Operational Safety as part of a continuing nationwide ARMS program, started in 1958, to monitor radiation levels in and around facilities producing or utilizing ratioactive material. Recently this program has been extended to making detailed surveys, utilizing a helicopter platform, over selected areas within all major AEC facilities. The purpose of these surveys is twofold: first, to document, at a given point in time, the location of all areas containing gamma emitting radioactivity (visible at the surface); second, as an aid to local personnel in evaluating the magnitude and spatial extent of any radioactive contaminants released into the environment.

The Hanford Reservation is located in south-central Washington state (see Figure 1) and covers an area of approximately 1500 km^2. This is a semi-arid region with an average annual rainfall of 16 cm. The area has a sparse covering of natural vegetation, primarily suited for grazing. Large areas near the site, however, have recently been put under irrigation. The Columbia River flows through the northern edge of the site and forms part of the eastern boundary. The nearest large population center is the Tri-Cities area (Richland, Pasco and Kennewick), located directly downstream from the site boundary. This area, along with the other smaller communities and agricultural areas surrounding the site, contains a population of approximately 100,000.

Since the facility began operation in 1944, activities at the Hanford Reservation have centered around the production of plutonium. Nine graphite moderated production reactors, located within the six 100 Areas along the Columbia River (see Figure 1), have been operated during this time. Located in the center of the reservation are two large

*The Hanford Reservation is now under the direction of the newly created Energy Research and Development Administration. The work described in this report which has been supported by the U. S. Atomic Energy Commission (AEC) is now under the cognizance of the Energy Research and Development Administration (ERDA).

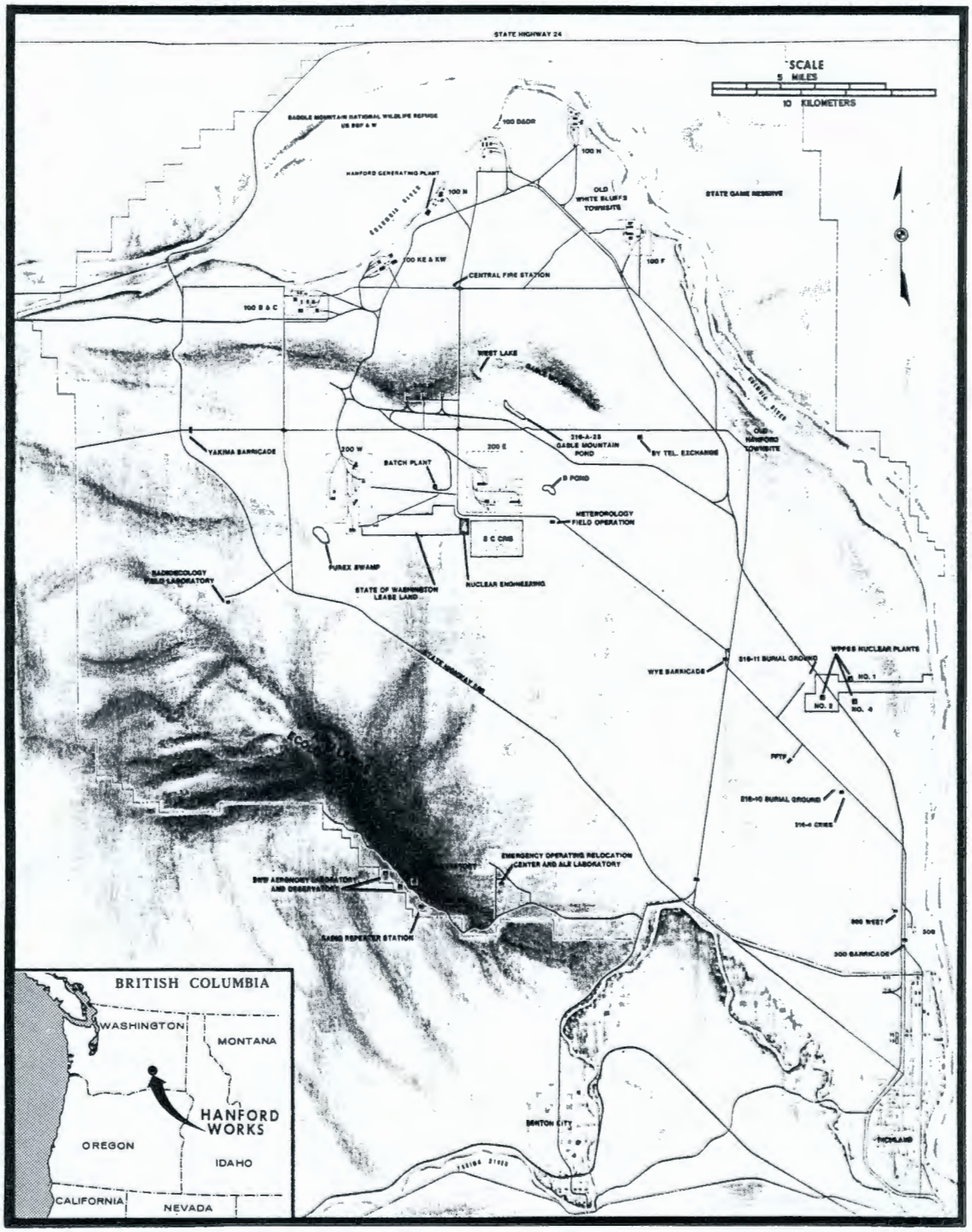

Figure 1. Area map of the Hanford Reservation

chemical separation areas (200-East and 200-West) where plutonium (and later uranium) is extracted from irradiated uranium fuel elements. Large quantities of radioactive wastes, generated in the separation processes, are also stored within these areas.

Two distinct types of aerial surveys were performed over the Hanford Reservation. A general survey, conducted between July 10 and July 16, 1973, utilized a fixed-wing aircraft flying at speeds ranging from 60 to 75 meters per second. Flight lines were flown at an altitude of 150 meters, with line spacings varying from 0.4 to 1.6 kilometers. This survey covered the entire site, as well as an area off-site extending approximately eight kilometers on each side of the site boundary. The purpose of the 150 meter survey was to provide a broad overview of the entire reservation and to locate general areas of activity. A second type of survey utilized a helicopter platform in order to survey at lower altitudes (typically 45 meters) and at slower speeds (typically 30 to 40 meters per second). This type of survey was used to provide detailed coverage of selected areas within the site. Line spacings of 45 meters allowed for complete overlap and provided a spatial resolution on the order of 30 meters. The detection sensitivity for activity spread out over a large area was improved by a factor of 3 to 4, while the sensitivity for localized "point" sources was improved by an order of magnitude in the 45 meter survey versus the 150 meter survey.

Three helicopter surveys were flown. The first was a special survey conducted between May 22 and June 6, 1973 at the request of the Atlantic Richfield Hanford Company (ARHCO). This survey covered eight areas in and around the two chemical separation areas operated by ARHCO. All but one of these areas (the BC-Crib area) were resurveyed as part of a more complete series of helicopter surveys conducted between October 15 and October 27, 1973 and between March 26 and April 8, 1974.

The results of the aerial surveys are presented in the form of gamma radiation isopleths plotted over photographs of each area. Two types of isopleth maps are provided for each area surveyed. The first gives the total gamma count rate, at the survey altitude, for gamma rays between 50 keV and 3 MeV. The second is a plot of the isoactivity and isoexposure rate for all major man-made isotopes. Only a single isopleth map is presented for those areas where one isotope dominates. The results are expressed in terms of an equivalent "surface" concentration, given in $\mu Ci/m^2$. (This surface concentration would lead to the same gamma ray count rate as that actually measured). The exposure rate at one meter above the ground, derived from the surface concentrations, is also given (in $\mu R/h$).

2. SYSTEMS AND PROCEDURES

2.1 Data Acquisition System

The data acquisition system was composed of a detector package, a data recording system called REDAR (Radiation and Environmental Data Acquisition and Recorder), and a navigation unit which provided position information. The REDAR system contained four memories for data storage. The first stored a variety of information, such as the gross count data, single-channel data, position information, live-time, radar altitude, and various meteorological information if the appropriate transducers were employed. The second and third memories operated in a flip-flop mode to store spectral information. Memories one and alternately either two or three were stored every three seconds on a 9-track magnetic tape. The fourth memory was used solely for real time analysis on board the aircraft, and was not stored on magnetic tape. Figure 2 is a block diagram showing the major components of the acquisition system in the normal helicopter configuration, and Figure 3 shows the REDAR system.

During the Hanford survey, four different detector packages were employed. The major portion of the gamma ray information was obtained using NaI(Tℓ) scintillation detectors. For the large area survey, three arrays, each containing seven 10 cm. diameter by 10 cm. thick NaI(Tℓ) detectors, were mounted inside a Martin-404 fixed-wing aircraft operated by EG&G, Inc. for the Atomic Energy Commission (AEC). In the low altitude detailed surveys two pods, each containing twenty 12.7 cm. diameter by 5 cm. thick NaI(Tℓ) detectors, were mounted externally on a Navy SH-3 helicopter. Figure 4 shows the helicopter with the pods attached and Figure 5 shows one of the detector pods with the hatch cover removed. Two additional detector packages were briefly employed during two special surveys conducted over a portion of the 200-West Area. One contained an array of four BF_3 neutron counters, each 1.8 meters long and 15 cm. in diameter, filled to a pressure of 50 cm. of Hg. These were mounted in two pods which hung externally on the helicopter in the same position as the gamma pods. The total thermal neutron sensitivity for the array was 6000 counts/second per neutron/cm^2-second. For the second special survey a high resolution lithium-drifted germanium solid-state detector was mounted inside the helicopter. This detector had an efficiency of 14.5% with a total active volume of 77 cm^3.

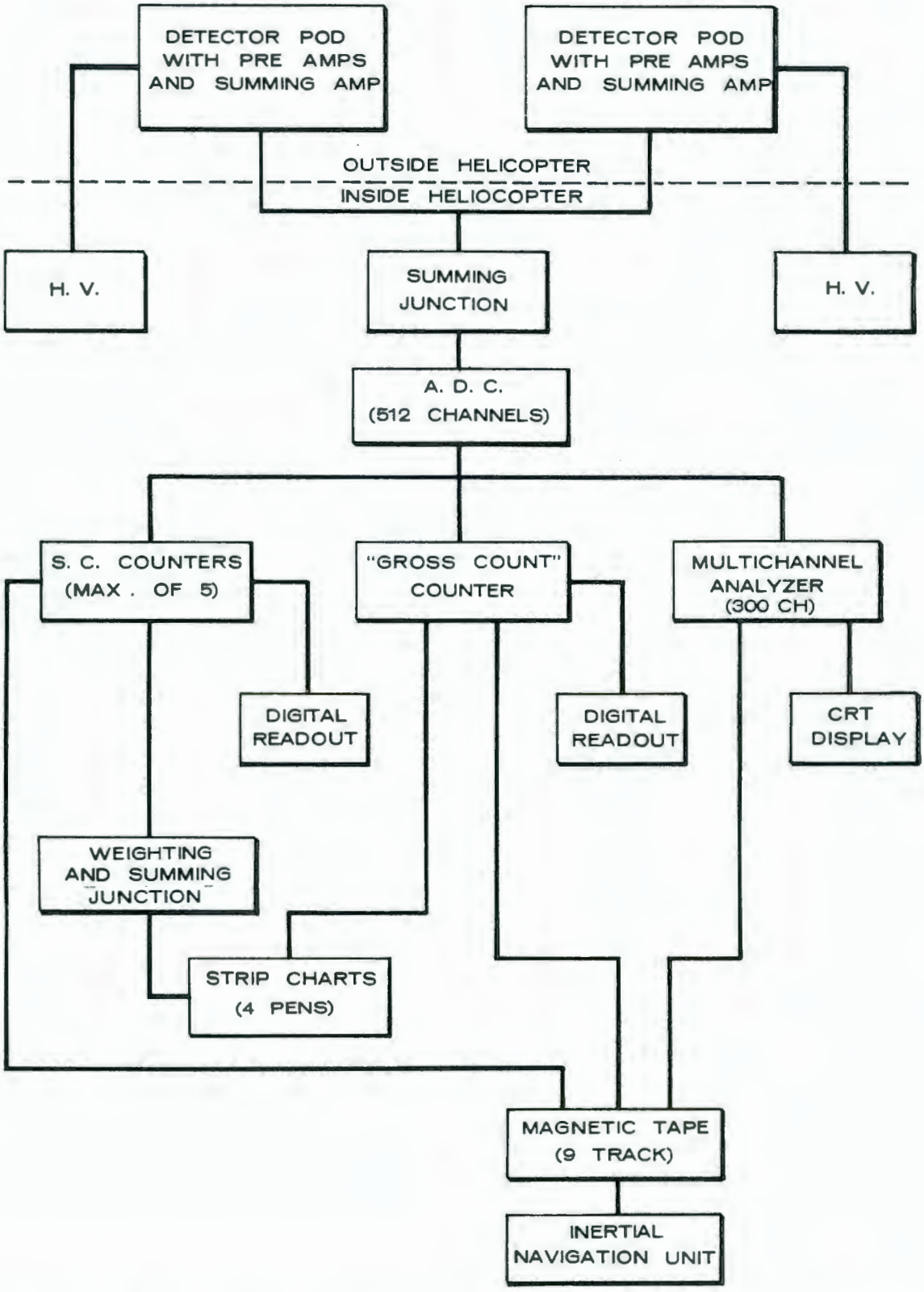

Figure 2. Block diagram of the data acquisition system as employed during the helicopter portion of the Hanford survey.

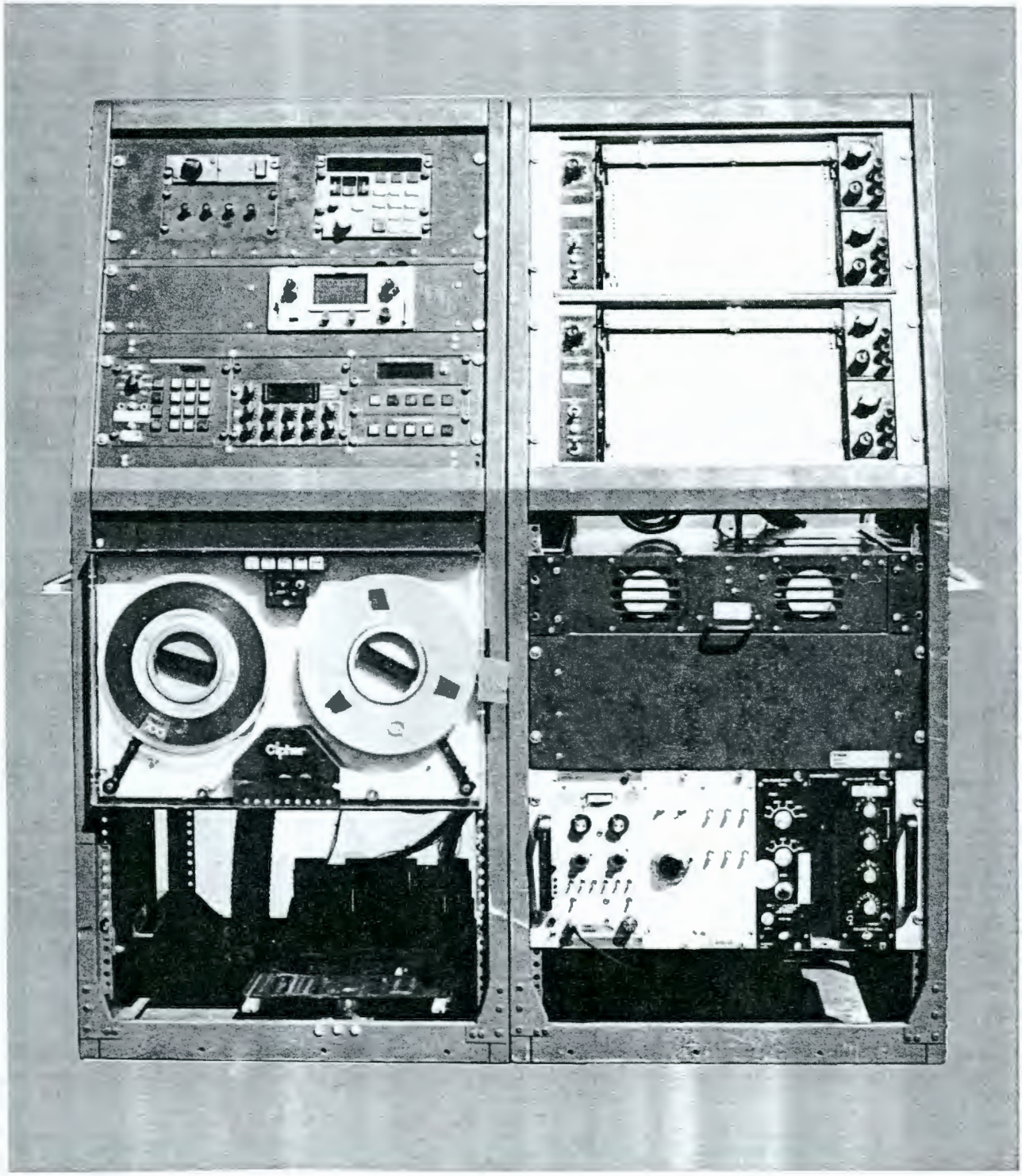

Figure 3. Photograph of the REDAR (Radiation and Environmental Data Acquisition and Recorder) system used during the Hanford survey.

Figure 4. The SH-3 helicopter shown with the NaI(Tℓ) detector pods attached.

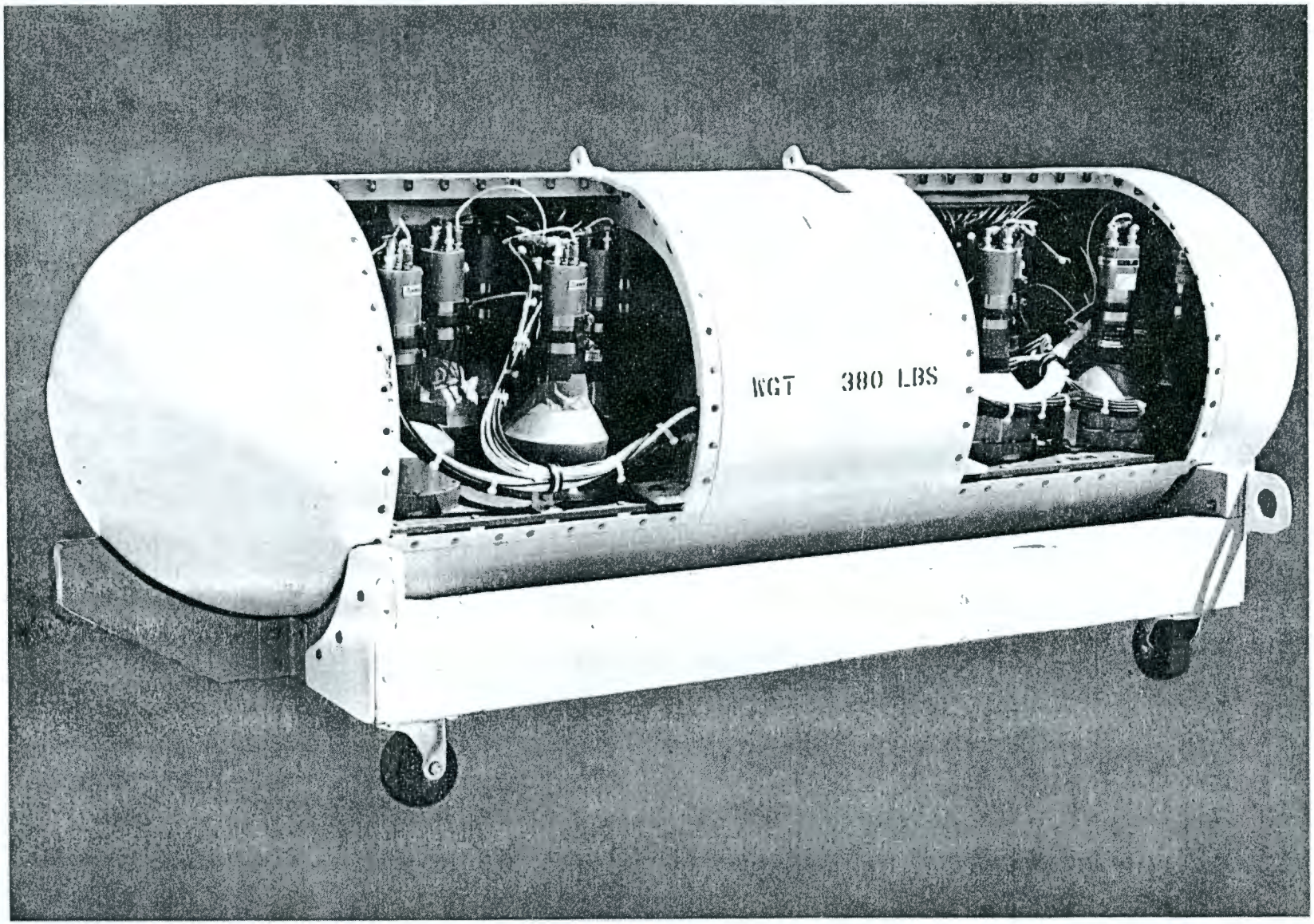

Figure 5. One of the gamma radiation detector pods with the hatch covers removed. Each pod contained twenty 12.7 cm diameter by 5 cm thick NaI(Tℓ) scintillation detectors.

Preamplifier signals from each detector within an array were fed into a summing amplifier. The summing amplifier output for each array was then fed into a summing junction from which the total signal was fed into an analog-to-digital converter (ADC). After the ADC, the signal was split into three paths. All counts passing the ADC were recorded in a "gross count" scaler. This information was updated every 0.1 second. The second path lead to a set of five adjustable window single-channel analyzers (SCA) which could be individually set over any region of the spectrum. The resulting counts within each window were recorded in a scaler which was updated every 0.2 second. The third path lead to a 300 channel multichannel analyzer (MCA) where spectral information was acquired and updated every 3 seconds. All these results were stored on magnetic tape. Other parameters, such as the altitude* and position information, were updated every 1 second and also stored on magnetic tape.

The radiation results could also be viewed in real time on board the aircraft. Spectral information was monitored on a CRT display. The gross count information was displayed on a digital readout and could be monitored on a strip chart. Any one of the single-channel outputs could be monitored on a digital readout. The results from all the single-channel analyzers could be routed into a weighting and summing junction. From here, weighted combinations of the SCA data could be displayed on strip charts. This allowed for some real time data manipulation, such as the background subtraction technique described in Section 2.4.

Position information was provided by a Litton inertial navigation system, LTN-51. The LTN-51 utilizes two accelerometers to measure aircraft acceleration along two perpendicular axes. During automatic preflight alignment, the accelerometers are leveled and the system determines its orientation to true north. As the aircraft moves, the accelerations are integrated once to obtain aircraft velocity and then a second time to determine distance traveled. This integration occurs in both the north-south and east-west directions. The distance traveled is then summed with the initial position of the aircraft and resolved in the latitude-longitude grid to determine the aircraft's present position. Special software, prepared by Litton, allowed these data to be recorded with a minimum detectable distance increment of 4.5 meters.

*Altitude information was only obtained during the fixed-wing portion of the Hanford survey.

2.2 Data Reduction System

The data reduction system, called REDAC (Radiation and Environmental Data Analyzer and Computer), consisted of a NOVA 840 minicomputer, a Tektronix CRT terminal with a hard copy unit, a high speed paper tape reader, two magnetic tape transports and two Cal-Comp plotters. This equipment was mounted in a large step van which was driven to the survey site.* Figure 6 shows the system mounted inside the step van.

A large variety of software routines were available for analyzing the data. Line plots giving count rate as a function of time or position could be plotted on the CRT terminal or on the CalComp plotters. The count rate could come from the gross count data, any of the five pre-selected SCA data, or from up to eight software selected windows set over any region of the spectrum. Combinations of single-channel data in the general form

$$\frac{\sum_i a_i A_i + C_1}{\sum_j b_j B_j + C_2},$$

where A and B represent the single-channel information, a and b are weighting factors, and C_1 and C_2 are constants, could also be plotted.

Spectral information, in data blocks representing 3 seconds of clock time, could be accumulated over any portion of a flight line and plotted on the CRT terminal or the CalComp plotter. Two spectra could be accumulated and stored. Weighted combinations of these spectra could be formed and then plotted. The integrated counts over any window within the spectrum could be obtained and summed in 3-second data blocks over any portion of a flight line.

Two types of software generated correction factors were generally applied to the data. The first corrected for counting losses

* The data reduction system remained in Las Vegas during the fixed-wing portion of the Hanford survey.

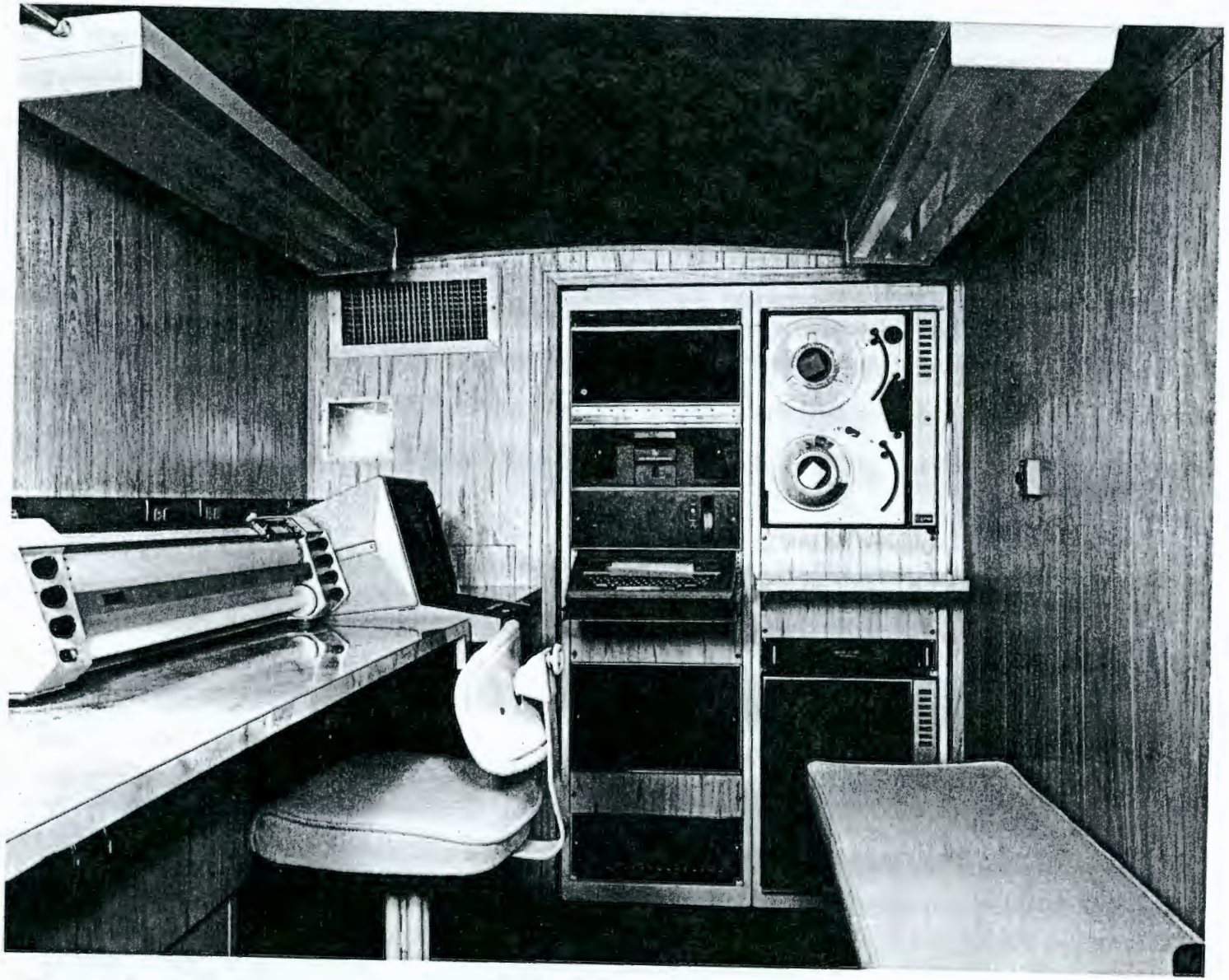

Figure 6. Photograph of the REDAC (Radiation and Environmental Data Analyzer and Computer) system mounted in the mobile step van.

due to dead time within the ADC. The second corrected for altitude fluctuations and normalized the data to the standard survey altitude.*

Details and examples on how these software routines were utilized are given in Section 2.4.

2.3 Survey Procedures

Flight lines, laid out prior to each flight, were flown using visual navigation. Because of the rather wide line spacings used in the large area survey (0.4 to 1.6 kilometer spacings), a sufficient number of reference points could be identified on a standard 1:62,500 scale map to allow the navigator to keep the aircraft on course. Deviations of 50 to 100 meters on either side of a flight line were not a serious problem for this type of survey.

For the small area detailed surveys flight lines spaced 45 meters apart had to be maintained over distances as long as 10 kilometers. Two different methods were used to fly these lines. For the majority of the areas surveyed ground crews were used to provide reference points for the pilots. Pickup trucks, carrying large painted boards in the bed, were spaced at intervals of 1.5 to 3 kilometers. These could be easily seen by the pilots and used as a reference for maintaining straight lines. Reference markers giving the line number were placed on the ground at 45 meter intervals along the path of each truck. Constant radio communication between the helicopter and the ground crew assured that each truck was in the proper position before a given line was flown.

A second method was used for the detailed surveys along the banks and over the islands of the Columbia River. The use of ground crews was not considered practical for this type of survey. Since sufficient detail did not exist on any maps, use was made of high resolution aerial photographs taken just prior to the survey. Flight lines drawn on the photographs could be followed without much difficulty.

A reference signal, called an on-top mark, was placed on the magnetic tape by the navigator as the aircraft passed over certain known locations on the ground. A minimum of two on-top marks were

* This correction factor was only applied to the data from the fixed-wing portion of the Hanford survey.

placed on the tape along each flight line. In this manner, a correlation could be made between the position data, given in latitude and longitude coordinates, and certain known reference points along each flight line.

In order to avoid pulse pile-up problems, the maximum count rate coming into the ADC had to remain below 50,000 counts per second. With all the detectors turned on, this count rate was approximately four to five times that due to natural background radiation. Whenever the count rate exceeded this level, the line was reflown with some of the detectors turned off. Ideally, each line should be flown with all the detectors on, maximizing sensitivity for the low activity areas, and then reflown with some of the detectors shut off to keep the count rate in the higher activity regions below 50,000 counts/second. Due to time limitations, this could not be done in all cases, especially for some of the longer flight lines. A compromise was generally made between maintaining maximum sensitivity in the low activity regions and keeping the count rate below 50,000 cps in the higher activity regions.

2.4 Data Reduction Procedures

The aerial radiation survey accumulated an enormous amount of data over rather large areas in a very short period of time. A semi-automated, computer based, data reduction system was therefore necessary to reduce this data to a usable form in a reasonably short time. The system employed during the Hanford survey has been described in Section 2.2. The present section will describe in more detail the methods employed in the data reduction.

Radiation data is generally presented in the form of isopleth maps which overlay a map or photograph of the area surveyed. This allows a rapid, visual correlation to be made between the measured activity and its origin on the ground. The isopleths are constructed by plotting, on a second-by-second basis, the radiation data as a function of position.

For the Hanford survey position information was stored on the magnetic tape once each second in the form of latitude and longitude coordinates. By using the on-top marks placed on the tape during the flight, this information could be scaled to any map or photograph of the area. First the latitude and longitude coordinates (tagged by the on-top mark) for each ground reference point were obtained. From this the separation in arc seconds of latitude and longitude between reference points was obtained. Next an x-y grid was laid over the photograph, with

the x-direction being that of true north. The separation, in centimeters, in the x and y directions were then measured between the reference points. These data were used to compute a scaling factor in arc seconds per centimeter of latitude and longitude. Each flight line was processed separately and then positioned over the photograph using the on-top marks to assure proper alignment.

Once the position information was properly scaled, the radiation data could be processed. Alphabetic symbols, designating count rate intervals, were plotted each second along the flight line with a position uncertainty related to the flying time of ± 1/2 second. Isopleths were drawn after all flight lines had been processed and properly positioned over the photograph.

A "gross count" isopleth map was generally processed first. The total gamma ray counts (between 50 keV and 3 MeV) recorded at the survey altitude were summed over each 1-second time interval. The count rate data could come from the gross count scaler (updated every 0.1 second) or from the spectral data which was recorded every 3 seconds. Some spatial resolution was sacrificed in the latter case. However, an excellent approximation to the equivalent 1 second count rate could be obtained from the 3 second spectral data by separating the 3 second total into 1 second parts according to the ADC live time, which was recorded every second. The lowest count rate interval, generally designated as an A level, was chosen to include all contributions from natural background. Generally count rates corresponding to a B level or greater represent man-made activity superimposed upon the natural background. Once the gross count contour was processed, spectral plots were taken over each area showing an increased activity over natural background. In this manner, the specific isotopes contributing to the man-made activity were identified.

Specific isotope isopleth maps, generated from photopeak count rate data, were processed next. By removing the background within the photopeak pulse height window due to other sources, the resulting count rate data could be converted into isotope concentrations on the ground (see Section 2.5). The background subtraction procedure employed was based on the fact that the spectral shape for any given isotope or combination of isotopes remained remarkably constant over rather large variations in intensity. This was true as long as pulse pile-up problems were minimized.

The situation encountered most often during the Hanford survey was a mixture of ^{137}Cs, ^{60}Co and the natural terrestrial radioisotopes. Figure 7 shows a typical spectral plot for this case. Four pulse-height windows are also shown in this figure. Window 1 (from 600 to 750 keV) is centered on the ^{137}Cs photopeak. Window 2 (from 750-1000 keV) defines a background region between the ^{137}Cs and the ^{60}Co photopeaks. Window 3 (from 1100-1400 keV) spans both photopeaks from ^{60}Co. Window 4 (from 1400 keV to 3 MeV) defines the window used to monitor changes in the natural terrestrial radiation background. Four stripping coefficients were defined as follows:

$$\alpha \equiv \frac{\text{Window 1}}{\text{Window 4}} \quad \text{, for a natural background spectrum}$$

$$\beta \equiv \frac{\text{Window 2}}{\text{Window 4}} \quad \text{, for a natural background spectrum}$$

$$\gamma \equiv \frac{\text{Window 3}}{\text{Window 4}} \quad \text{, for a natural background spectrum}$$

$$\delta \equiv \frac{\text{Window 1}}{\text{Window 2}} \quad \text{, for a pure } ^{60}\text{Co spectrum}$$

The ^{60}Co photopeak count rate (CR) is then given by

$$\text{CR } (^{60}\text{Co}) = [\text{Cts. in 3}] - \gamma\,[\text{Cts. in 4}], \tag{1}$$

where the second term represents the contribution due to natural background gamma rays within the ^{60}Co photopeak window.

For ^{137}Cs both the natural background contributions and that due to Compton scattered gamma rays from ^{60}Co must be removed from the photopeak window. Thus

$$\text{CR } (^{137}\text{Cs}) = [\text{Cts. in 1}] - [\text{Contribution in 1 due to natural background}] - [\text{Contribution in 1 due to } ^{60}\text{Co}].$$

Using the coefficients and windows defined above, this can be written as

$$\text{CR } (^{137}\text{Cs}) = [\text{Cts. in 1}] - \alpha\,[\text{Cts. in 4}] - \delta\,[(\text{Cts. in 2}) - \beta(\text{Cts. in 4})]. \tag{2}$$

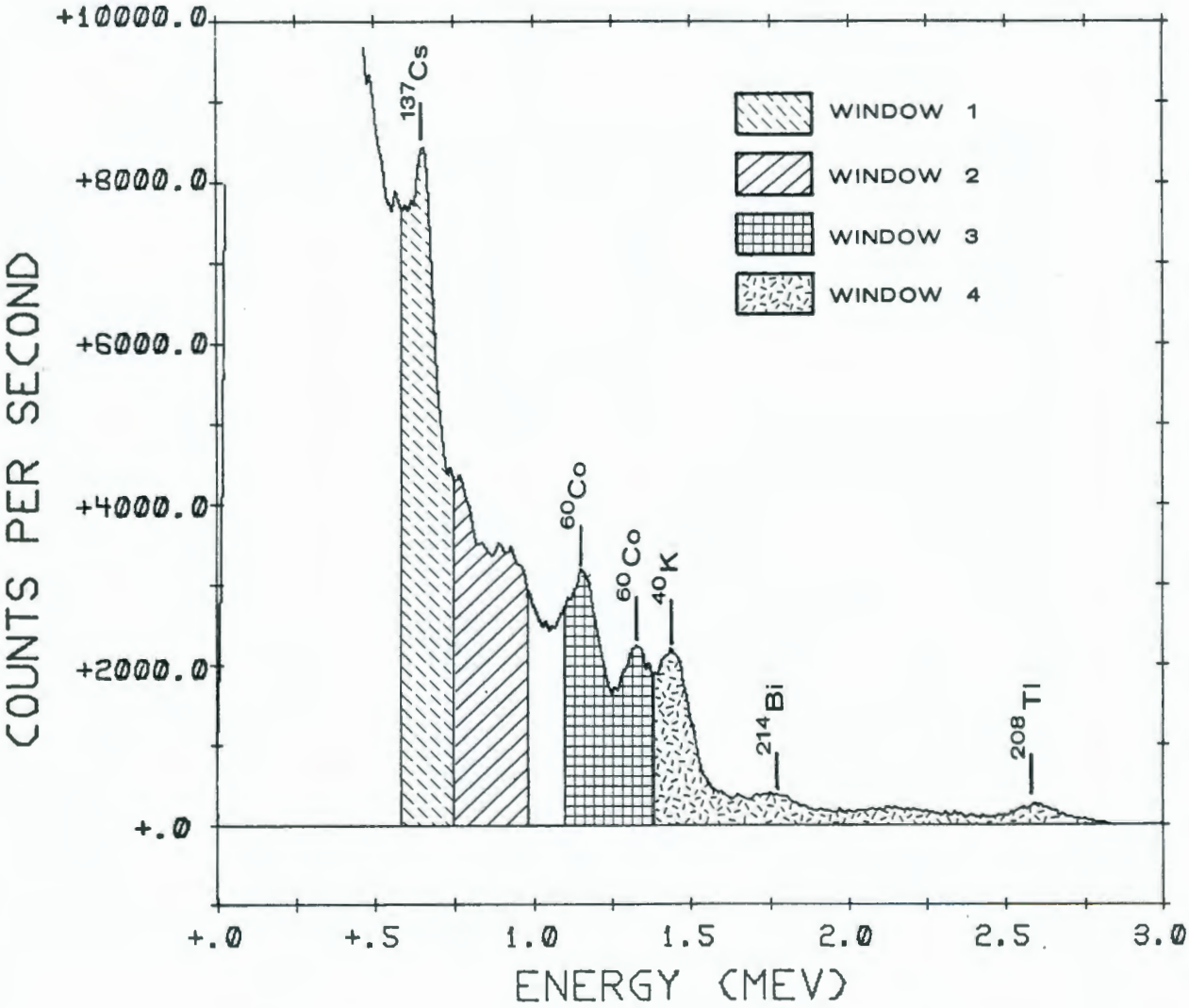

Figure 7. A typical gamma ray spectrum from the NaI(Tl) detector array showing the pulse-height windows used to extract ^{137}Cs and ^{60}Co photopeak count rate data.

In the third term, the background counts in Window 2 must first be subtracted away. The remaining counts are due to ^{60}Co gamma rays. These are then used to subtract away the ^{60}Co contribution within the ^{137}Cs photopeak window. Equation (2) can be rewritten as

$$CR\,(^{137}Cs) = [\text{Cts. in } 1] - \delta\,[\text{Cts. in } 2] - [\alpha - \delta\,\beta]\,[\text{Cts. in } 4]. \qquad (3)$$

Equations (1) and (3) were those used to process the photopeak count rate data for ^{60}Co and ^{137}Cs, respectively. The window data could come from the pre-selected SCA data, summed over one second time intervals, or from software selected windows placed over the appropriate pulse-height regions in the spectral data. Although the latter information came in three-second data blocks, a close approximation to the equivalent one-second count rate could be obtained using the ADC live time, as in the gross count case. The stripping coefficients α, β, and γ were obtained by taking an average value over some typical regions within the survey area which were free of man-made activity. To obtain the stripping coefficient δ, a region containing ^{60}Co as the only non-natural isotope had to be found. The counts in Windows 1 and 2 due to natural background were first subtracted away leaving only those counts due to Compton scattered gamma rays from ^{60}Co. This could be done by using the α and β coefficients or by subtracting away the entire natural background portion of the spectrum. In the latter method, two spectra were accumulated, one consisting of natural background gamma radiation only and one consisting of natural background plus ^{60}Co. A weighting factor was applied to one of the spectra to equate the total counts within Window 4. The two spectra were then subtracted leaving a pure ^{60}Co spectrum. The stripping coefficient δ could then be obtained.

Count rate levels for the isotope isopleth maps were selected in a manner similar to that described for the gross count case. An A level was chosen to include all the purely statistical fluctuations around zero. The magnitude of these statistical fluctuations determined the minimum detectable activity for the isotope in question. All levels B and above generally indicated the presence of the isotope under consideration.

Figure 8 illustrates the stripping technique for a line flown along the Columbia River shoreline between the 100-D and 100-F Areas. Also shown are the count rate intervals selected in each case for the count rate isopleths. This example illustrates one of the worst cases for the gross count data. Large variations are observed in the count rate as a function of position along the flight line, due mainly to

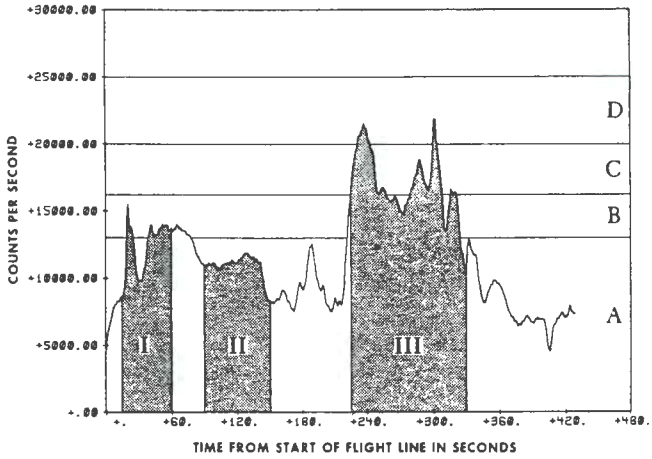

(a) Total gamma ray count rate

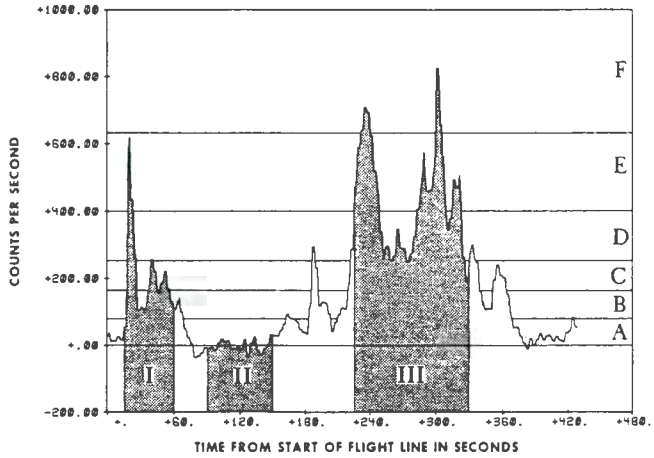

(b) ^{60}Co photopeak count rate

(c) ^{137}Cs photopeak count rate

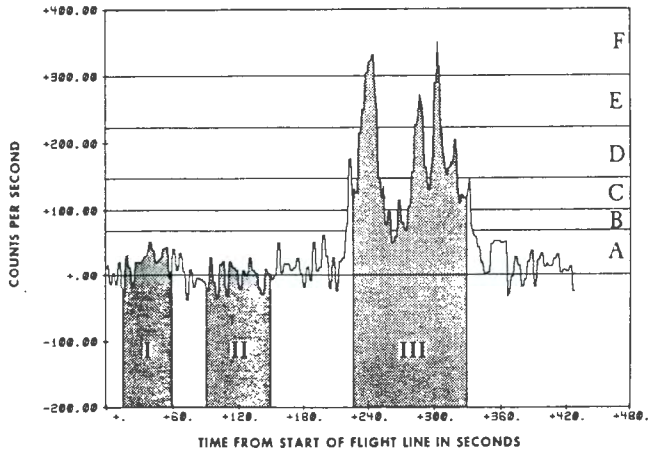

Figure 8. Line plots obtained from data taken along a flight line located near the Columbia River shoreline illustrating the stripping technique used to extract ^{60}Co and ^{137}Cs photopeak count rate data. Also shown are the count rate intervals selected in each case for the count rate isopleths. Gamma ray spectra obtained over segments I, II and III of the flight line are shown in Fig. 9.

the presence of water over portions of the flight line. Several sources of man-made radioactivity were completely missed because they occurred in regions of reduced natural background. It is obvious from Figure 8a that under certain circumstances very little quantitative information on man-made radioactivity can be extracted from the gross count data. Using the background stripping technique, however, quantitative results are possible even in areas having large fluctuations in the natural background count rate.

Using Equation (1), the natural background component was subtracted away leaving only the counts due to ^{60}Co within the photopeak window. These results are shown in Figure 8b. The count rate variations due just to natural background radiation have been removed and the areas of ^{60}Co activity stand out quite well.

Using Equation (3), both the natural background and the ^{60}Co contributions in the ^{137}Cs photopeak window have been subtracted away. The resulting count rate, due just to ^{137}Cs, is shown in Figure 8c. The large variations in count rate due to natural background changes are no longer present. In addition, the activity near the beginning of the flight line, which was due to ^{60}Co, has been eliminated.

Figure 9 shows spectral plots taken near the beginning, middle, and end, respectively, of the flight line. Both ^{60}Co and the naturally occurring terrestrial isotopes are identified in Figure 9a. Figure 9b is a spectrum taken over a region containing only natural background radiation. In Figure 9c, ^{137}Cs and ^{60}Co can both be seen.

2.5 Calibration Procedures

Extraneous radionuclides manifest themselves as photopeaks superimposed on a background spectrum due to naturally occurring terrestrial radioisotopes, natural radioactivity within the aircraft and cosmic rays. In addition, higher energy contaminants contribute to the background for all photopeaks of lower energy. The previous section describes how these background contributions were removed from the photopeak pulse-height window of interest. Relatively simple expressions can be derived relating the resulting photopeak count rate to radioisotope concentration on the ground.

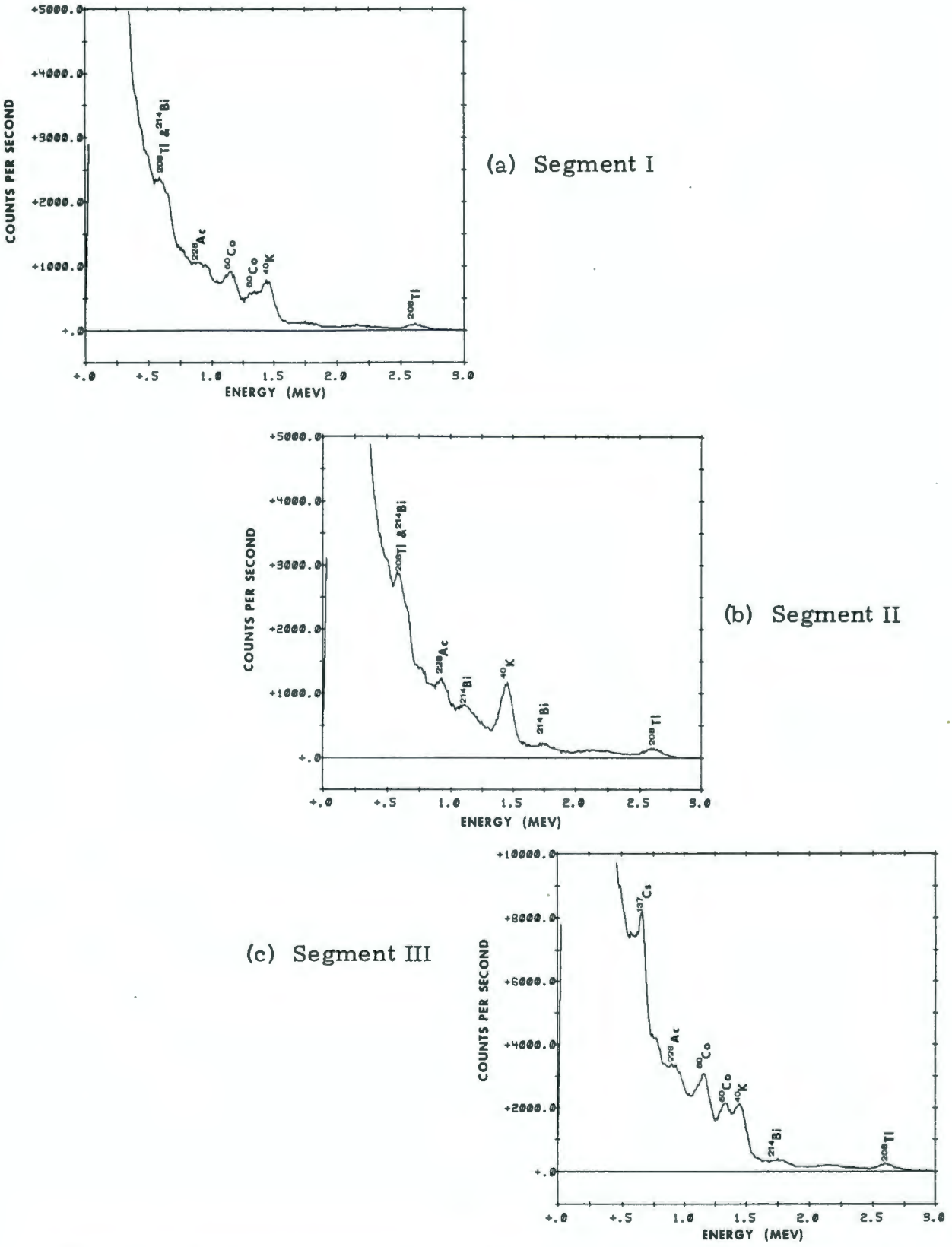

Figure 9. Gamma ray spectra obtained over three segments of the flight line shown in Figure 8.

Consider a point source placed directly under the detector array. The photopeak count rate (CR_φ) can be written in terms of an effective detector area as

$$CR_\varphi = \frac{S_0 A}{4\pi h^2} e^{-h/\lambda a} , \tag{4}$$

where

S_0 = the source strength in gammas per second,

h = the height of the detector above the source,

λa = the gamma ray mean free path in air and

A = the effective detector area for gamma rays incident normal to the detector face.

The effective area takes into account factors such as the attenuation in the detector housing and the photopeak efficiency of the detector.

For a source uniformly distributed over a smooth surface, with surface concentration η, a similar expression may be written. The photopeak count rate (CR), at an altitude d above the surface, is given by

$$CR = \int_0^\infty \frac{\eta A^* e^{-r/\lambda a}}{4\pi r^2} 2\pi x dx , \tag{5}$$

where

r = $\sqrt{x^2 + d^2}$ = the distance from each element of surface area to the detector position and

A^* = the effective detector area for gamma rays incident at an angle $\theta = \arccos\left(\frac{d}{r}\right)$.

In order to evaluate Equation 5, the variation of A^* with θ must be known. Two limiting cases of interest are that of an isotropic detector response and that of a cosine angular response. In the first case $A^* = A$ and in the second case $A^* = A \cos\theta$. Using these two cases, Equation 5 may be put in the form

$$CR = \frac{\eta A}{2} E_1\left(\frac{d}{\lambda a}\right) \tag{6}$$

for the isotropic detector response and

$$CR = \frac{\eta A}{2} E_2\left(\frac{d}{\lambda a}\right) \tag{7}$$

for the cosine response. Here $E_1(d/\lambda a)$ and $E_2(d/\lambda a)$ are exponential integrals defined by

$$E_n(a) \equiv a^{n-1} \int_a^{\infty} \frac{e^{-x}}{x^n} dx \ .$$

Eliminating the effective area between Equation 4 and Equations 6 and 7, the surface concentration can be written as

$$\eta = \left[\frac{S_0 e^{-h/\lambda a}}{2\pi h^2 (CR_p) E_1(d/\lambda a)} \right] CR \tag{8}$$

for the isotropic response and

$$\eta = \left[\frac{S_0 e^{-h/\lambda a}}{2\pi h^2 (CR_p) E_2(d/\lambda a)} \right] CR \tag{9}$$

for the cosine response. The expression within the bracket in Equations 8 and 9 can be evaluated for any survey altitude d by experimentally measuring the photopeak count rate at a distance h above a known source and using the tabulated values for the exponential integrals[1]. Table 1 gives the resulting conversion factors for ^{137}Cs, ^{60}Co and ^{241}Am for the detector arrays and survey altitudes employed during the Hanford survey.

A previous experimental measurement of the detector angular response for ^{137}Cs[2] showed that an excellent approximation to the angle-dependent response function could be obtained by averaging the results of the two limiting cases given in Equations 8 and 9. This approximation was employed in the case of ^{137}Cs and ^{60}Co. The result obtained assuming a cosine response function was used in the case of ^{241}Am. This was done because the detectors used during the ^{241}Am survey were surrounded on the sides with 0.9 mm thick cadmium, which is essentially opaque to 60 keV gamma rays.

Table 1. Conversion factors used during the Hanford survey to relate photopeak window count rate data to radionuclide concentration on the ground.

Radionuclide	Conversion Factor			
	Surface Concentration $\left[\frac{\mu Ci/m^2}{cps}\right]$			Exposure rate at 1 meter as calculated from previous column $\left[\frac{\mu R/h}{cps}\right]$
	Isotropic detector angular response	Cosine detector angular response	Average of previous two columns	
^{137}Cs [a]	4.0 (10^{-4})	7.2 (10^{-4})	5.6 (10^{-4})	5.9 (10^{-3})
^{60}Co [a]	2.2 (10^{-4})	4.3 (10^{-4})	3.2 (10^{-4})	1.4 (10^{-2})
^{241}Am [b]	-	2.9 (10^{-3})	-	-
^{137}Cs [c]	4.7 (10^{-3})	6.6 (10^{-3})	5.6 (10^{-3})	6.0 (10^{-2})
^{60}Co [c]	1.8 (10^{-3})	2.5 (10^{-3})	2.1 (10^{-3})	9.3 (10^{-2})

[a] Forty 12.7 cm x 5 cm NaI(Tℓ) array at 45 meter altitude.

[b] Forty 12.7 cm x 5 cm NaI(Tℓ) array at 30 meter altitude.

[c] Twenty-one 10 cm x 10 cm NaI(Tℓ) array at 150 meter altitude.

The cadmium shielding was used to improve the signal-to-noise ratio for low energy surveys. With this shield, the signal-to-background ratio at 60 keV for a 12.7 cm diameter by 5 cm thick detector is essentially the same as that of a 12.7 cm diameter by 0.16 cm thick detector[3].

Using previously derived data[4], the isotope concentrations can be converted to exposure rates at one meter above the ground. These results are also given in Table 1 for ^{137}Cs and ^{60}Co.

The conversion factors given in Table 1 are good to within ±15%, considering only sources of error associated with the actual calibration measurement. In using these conversion factors to infer a ground concentration, a major source of error lies in how closely the actual source geometry is represented by the idealized case considered in the derivation (namely, that of a uniformly distributed source over an infinite smooth plane). In situations where the actual source distribution is known, a correction factor can be applied (see the Appendix) to obtain a more realistic value for the ground concentration. This source geometry correction should be made prior to utilizing the aerial results to obtain a value for the total activity contained within a given area. In addition to the source geometry correction, it is also necessary to take into account any additional photopeak attenuation which may exist due to earth or structural shielding between the source and the aircraft.

When comparing the aerial results with localized ground measurements, it is imperative that the averaging properties of the aerial system be carefully considered. For any meaningful comparison to be made, a statistically significant number of random sampling locations covering an area which spans the field of view of the airborne system (approximately 150 meters in diameter for the helicopter surveys) must be analyzed and averaged together.

3. SURVEY RESULTS

3.1 Hanford Reservation Survey

The results of the large area survey over the entire reservation, conducted between July 10 and July 16, 1973, are given in Figures 10 to 13. These results are superimposed on a photo mosaic of the site constructed from photos taken during the same period of time as the radiation survey. The dotted line indicates the area covered during the radiation survey.

Figure 10 shows the actual flight lines flown during the survey. Over the center portion of the site, around the chemical separation areas, reasonably straight lines, spaced 0.4 kilometers apart, were flown. With this line spacing some side overlap exists in the radiation data. The photopeak count rate from a point source of ^{137}Cs or ^{60}Co placed midway between the lines would be approximately 30% of that obtained with the source placed on the line. The remaining portion of the site bound on the north and east by the Columbia River and on the south by the 300 Area, was flown with 0.8 kilometer line spacings. In this case the point source count rate for a source midway between the lines is only 2% of that for a source on the line. Thus, localized areas of activity between the lines might not be detected. The remainder of the survey area was flown with lines spaced 1.6 kilometers apart. In this case interpolations between flight lines are only valid for large area, slowly varying, sources of activity, such as that due to the natural terrestrial radiation background.

Figure 11 shows the results for the total gamma count rate between 50 keV and 3 MeV (in counts per second at 150 meter altitude). For this particular survey a C level was chosen to represent the normal background count rate interval. Although corrections were made for altitude variations, rapidly changing terrain elevation may show up as a surface anomaly. Several examples of this can be seen, notably around the Gable Mountain and Saddle Mountains areas. The terrestrial count rate is somewhat higher in the area north of the Columbia River. A few D areas show up in this region. These were investigated and found to be due to natural background, where the count rate just triggered the D level. Several isolated D levels show up in the Wooded Island area, just north of the 300 Area. These were investigated and identified as areas of ^{60}Co activity (see Figure 13). All levels greater

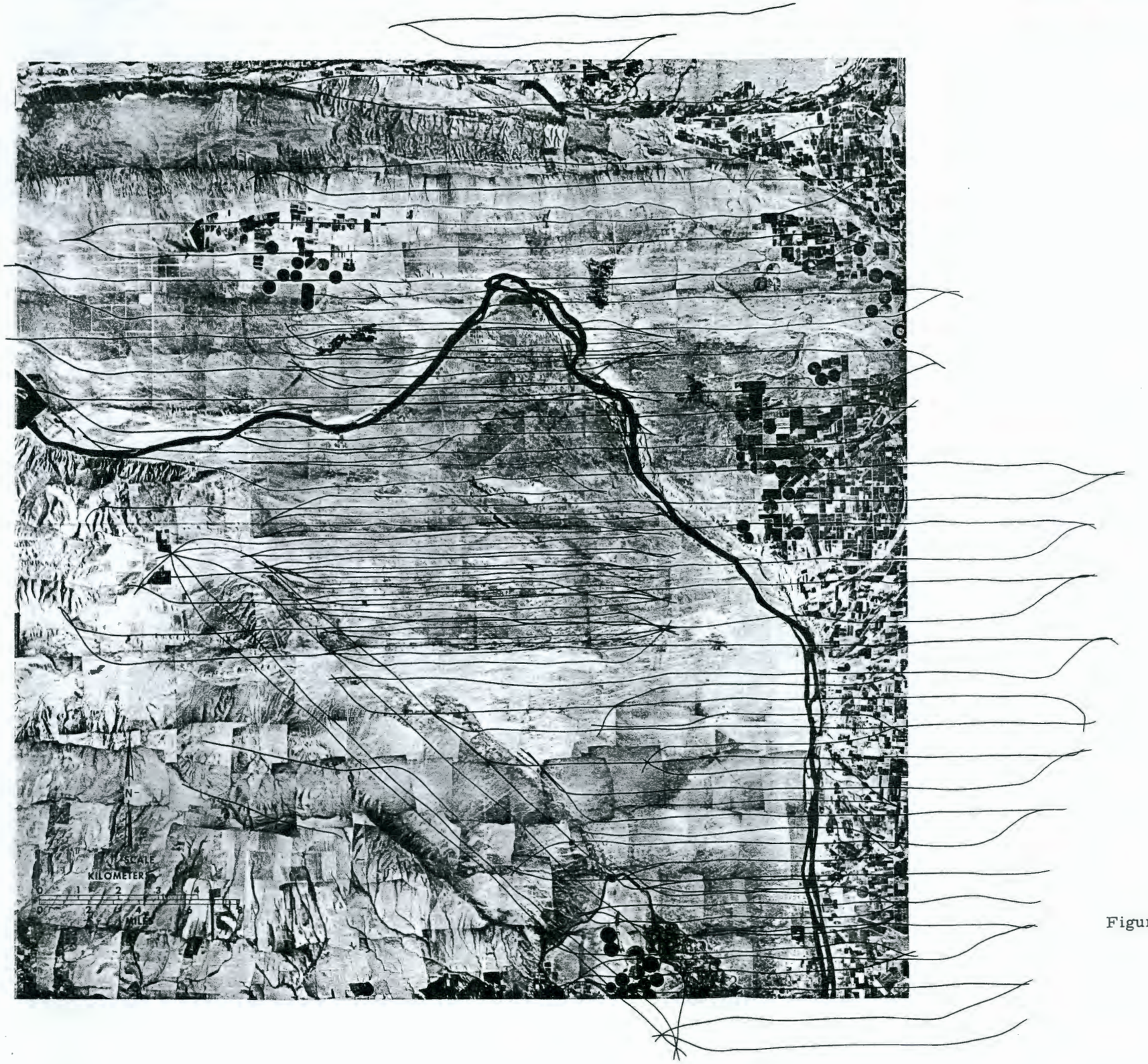

Figure 10. Flight lines flown during the fixed-wing (150-meter altitude) survey conducted over the Hanford Reservation during July 1973.

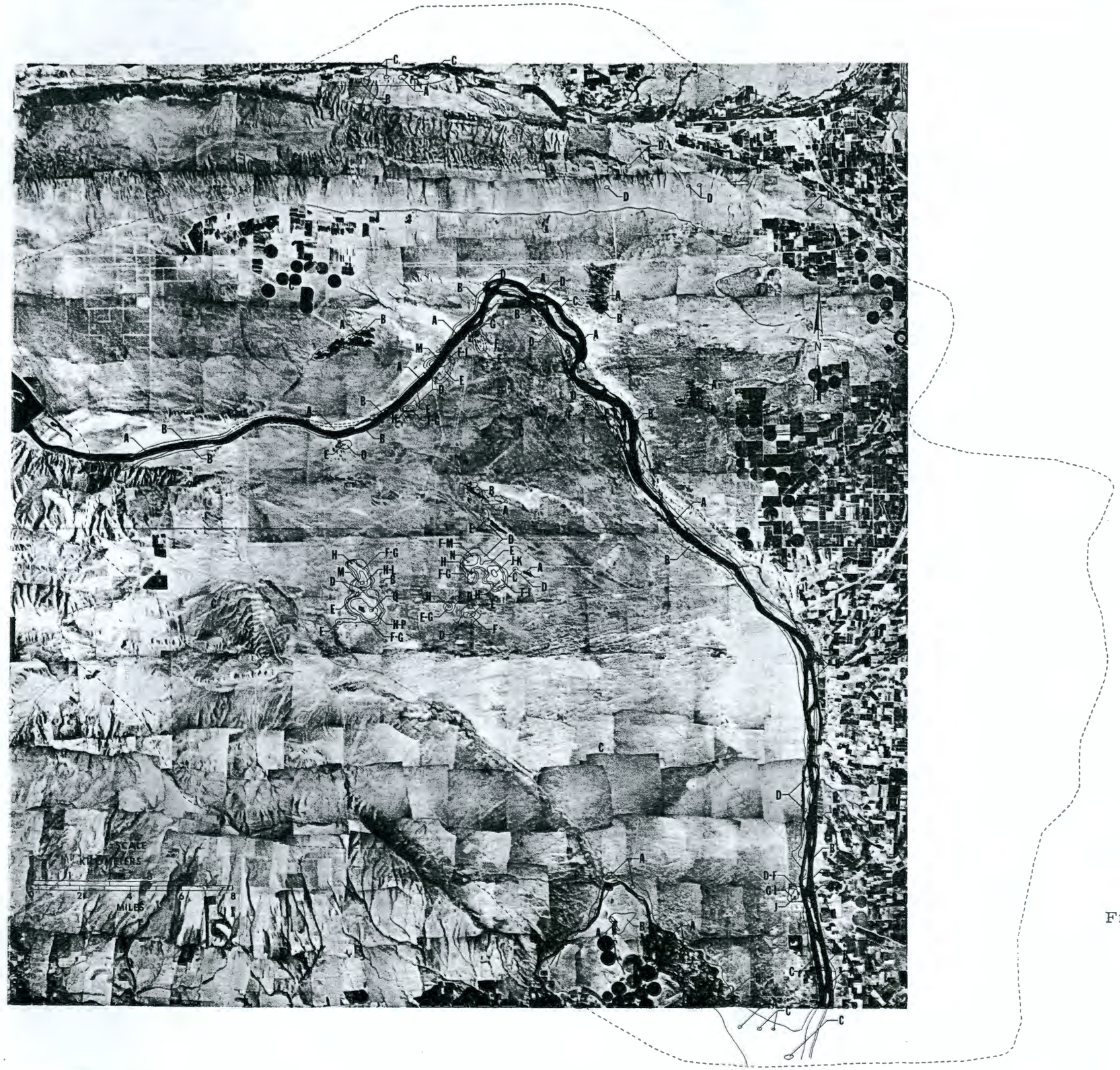

CONVERSION SCALE	
LETTER LABEL	GAMMA COUNT RATE 50keV — 3 MeV (cps at 150m altitude)
A	$< 3.0 \times 10^3$
B	$(3.0 - 3.8) \times 10^3$
C	$(3.8 - 6.0) \times 10^3$
D	$(6.0 - 9.0) \times 10^3$
E	$(9.0 - 13.) \times 10^3$
F	$(1.3 - 1.9) \times 10^4$
G	$(1.9 - 2.8) \times 10^4$
H	$(2.8 - 4.1) \times 10^4$
I	$(4.1 - 6.0) \times 10^4$
J	$(6.0 - 9.0) \times 10^4$
K	$(9.0 - 13.) \times 10^4$
L	$(1.3 - 1.9) \times 10^5$
M	$(1.9 - 2.8) \times 10^5$
N	$(2.8 - 4.1) \times 10^5$
O	$(4.1 - 6.0)$ & 10^5
P	$(6.0 - 9.0) \times 10^5$
Q	$(9.0 - 13.) \times 10^5$

Figure 11. Isopleth map of the total gamma ray count rate between 50 keV and 3 MeV (at 150-meter altitude) obtained during the fixed-wing portion of the Hanford survey flown during July 1973.

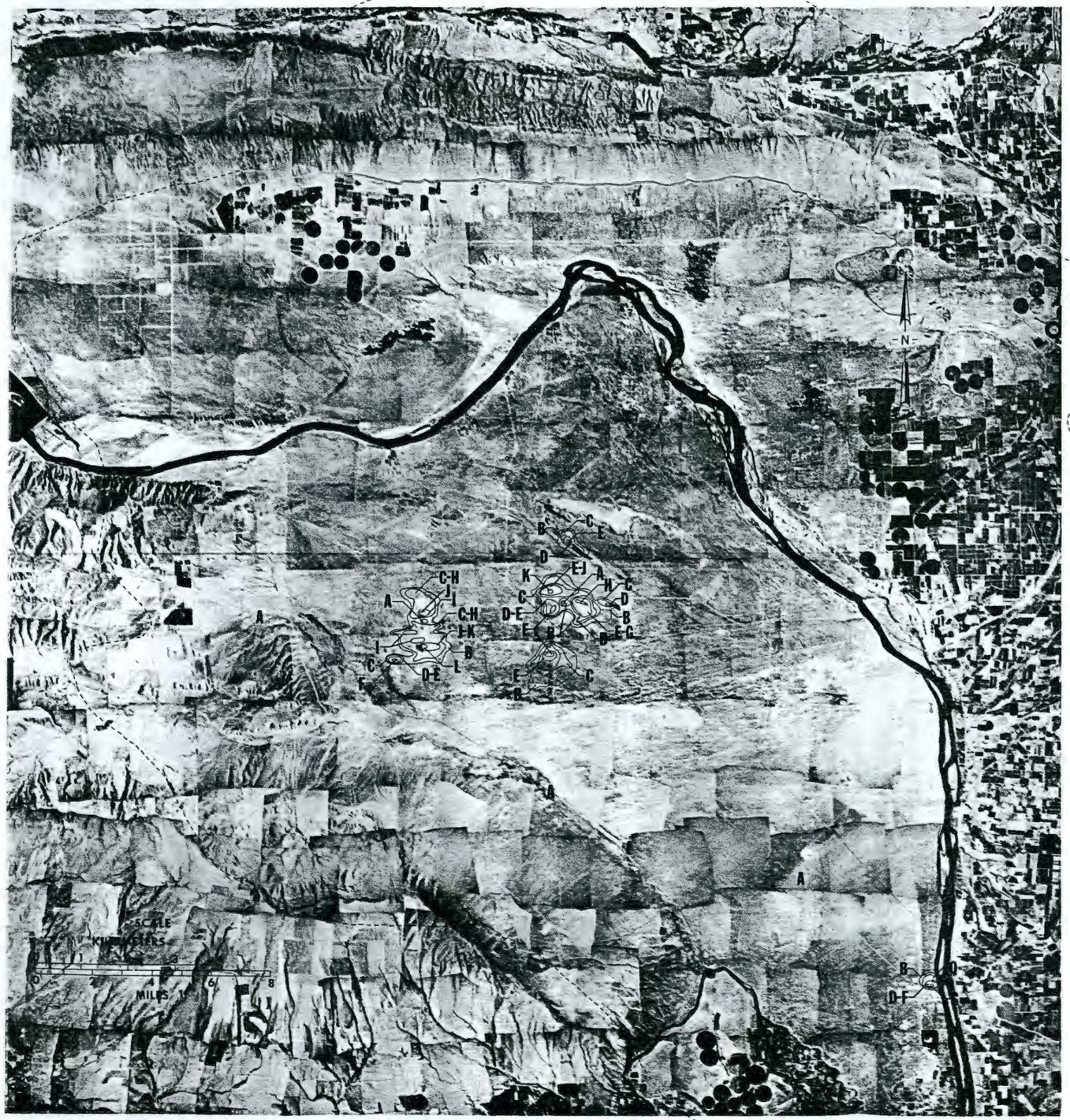

CONVERSION SCALE		
LETTER LABEL	^{137}Cs SURFACE CONCENTRATION (μC:/m^2)	^{137}Cs GAMMA EXPOSURE RATE AT 1 METER LEVEL (μR/h)
A	< 0.3	< 3
B	.3 — .6	3 — 6
C	.6 — 1.0	6 — 11
D	1.0 — 1.8	11 — 19
E	1.8 — 3.1	19 — 34
F	3.1 — 5.6	34 — 60
G	5.6 — 10	60 — 110
H	10 — 18	110 — 190
I	18 — 31	190 — 340
J	31 — 56	340 — 600
K	56 — 100	600 — 1100
L	100 — 180	1100 — 1900

Figure 12. Concentration and gamma exposure rate isopleths for ^{137}Cs obtained during the fixed-wing portion of the Hanford survey flown during July 1973.

CONVERSION SCALE		
LETTER LABEL	^{60}Co SURFACE CONCENTRATION (μCi/m^2)	^{60}Co GAMMA EXPOSURE RATE AT 1 METER LEVEL (μR/h)
A	< 0.1	< 4.6
B	.1 — .2	4.6 — 9.3
C	.2 — .4	9.3 — 17
D	.4 — .7	17 — 30
E	.7 — 1.2	30 — 52
F	1.2 — 2.1	52 — 93
G	2.1 — 3.8	93 — 170
H	3.8 — 6.7	170 — 300
I	6.7 — 12	300 — 520
J	12 — 21	520 — 930
K	21 — 38	930 — 1700
L	38 — 67	1700 — 3000

Figure 13. Concentration and gamma exposure rate isopleths for ^{60}Co obtained during the fixed-wing portion of the Hanford survey flown during July 1973.

than a D level were due to man-made isotopes. The A and B levels represent reduced count rates due to the presence of water. Even with the rather wide line spacings, the Columbia River could be followed quite well by drawing isopleths for these levels. Dotted lines were used in the isopleth map whenever an extrapolation was made across a large data gap.

The only prominent man-made isotopes observed in this survey were ^{137}Cs and ^{60}Co. Figures 12 and 13 give the results for each of these isotopes. All the activity observed around the 100 Areas was due to ^{60}Co. Although the detailed surveys over these areas showed several small areas of ^{137}Cs activity, none of these appeared in the whole site survey. The chemical separation areas contain both ^{137}Cs and ^{60}Co, with ^{137}Cs being dominant. ^{137}Cs is also observed in the Gable Mountain Pond and BC-Crib areas (both radiation controlled areas). Both ^{60}Co and ^{137}Cs are observed over the 300 Area (also a radiation controlled area).

Although exposure rate and concentration values are given in Figures 12 and 13 for ^{137}Cs and ^{60}Co, these should be used with extreme caution. Two facts should be kept in mind when comparing these results with ground measurements or with those obtained in the detailed surveys. First, flying at an altitude of 150 meters each one second data point represents the average count rate due to all sources within a circle having a diameter of roughly 300 to 400 meters. (This could actually be an advantage when trying to estimate the total integrated activity over a large area.) In addition, a large number of the sources observed in the survey are confined to rather small areas compared to the line spacings which were flown. These sources are more nearly representative of a localized "point" source than a distributed source, as assumed in the conversion table.

3.2 Reactor Areas

All of the plutonium production reactors operated at Hanford are located within the 100 Areas, which lie along the Columbia River in the northern part of the reservation. These areas were surveyed between October 15 and October 27, 1973. All the areas were flown with the Navy helicopter at an altitude of 45 meters, with 45 meter line spacings.

There are two primary sources of radiation in the reactor areas (excluding N Area). The first is that associated with the reactor building area. This generally comes from the reactor block, which contains unknown, but substantial, quantities of ^{14}C in the graphite and ^{60}Co in the thermal shield cast iron, and from small cribs and liquid waste disposal trenches which might exist in close proximity to the reactor building. The second major source of activity is connected with the cooling water effluent from each of the single-pass reactors. This effluent carried very low concentrations of long-lived radionuclides such as ^{60}Co, ^{137}Cs and ^{152}Eu. These were deposited in the soil surrounding the 107 retention basins, in the bottom of the retention basins and also in the soil at the bottom of the overflow trenches and the outfall structures. In some cases there were also some deposition in the soil along the effluent water lines where leaks occurred.

The retention basins were constructed of concrete along the bottom and sides for all reactors except for C and the two K reactors, where they were constructed of steel. Cooling water from the reactor was pumped into these basins and confined for a short period of time before being released back into the river. This allowed time for short-lived isotopes to decay before the water was released. If a fuel element failure occurred within the reactor, the fission product contaminated water could be diverted into trenches rather than released back into the river. These trenches were 3 to 6 meters deep and, for the most part, have been backfilled with earth. The retention basins have been filled with a minimum of one meter of earth. There is still, however, some activity observable in their vicinity.

In addition to the above, there also exists a number of solid waste burial grounds within the reactor areas. These, however, are sufficiently covered with earth that little or no activity can be observed, except in those cases where an open pit exists containing radioactive material.

The results of the gamma radiation survey are given in this section for each of the 100 Areas, starting with the 100-B Area and moving downstream to the 100-F Area. A map is given for each area which identifies the major facilities and also shows the locations of the various solid and liquid waste disposal areas. Two radiation isopleth maps are shown for each area. The first gives the total gamma count rate between 50 keV and 3 MeV, expressed as counts per second at 45 meter altitude. The second gives isoactivity and isodose isopleths for

^{60}Co, which was the dominant radioisotope observed in these areas. Spectral plots were taken over each area of activity identified in the gross count isopleth map. The presence of any isotope other than ^{60}Co is discussed in the text.

3.2.1 B and C Reactor Areas

This area contained two production reactors. The 100-B reactor was one of the three original reactors built at Hanford and the first to go into production. It started up in September, 1944 and was shut down permanently in February, 1968. The 100-C reactor started up in November, 1952 and was shut down in April, 1969. A map of the area is given in Figure 14. The radiation results are shown in Figures 15 and 16.

Five general areas of activity were observed. These were the 100-B Area solid waste burial ground, the 105-C reactor building area, the 105-B reactor building area, the 107-B and 107-C retention basins and the "C" trench. Spectral plots taken over each of these areas revealed the presence of ^{60}Co plus the naturally occurring radioisotopes of uranium, thorium, and potassium. No other isotopes due to man-made activity could be identified in the aerial results. The 105-C reactor building area had two distinct sources of activity, while the 105-B reactor building area had three separate sources of activity. All other activity shown in the contours is consistent with shine from the above sources and does not represent actual activity on the ground. At the time of the survey the 107-C trench had not been completely backfilled. Once this is done, the activity in this region should be greatly reduced. In July, 1974 an additional one meter of earth was placed over the 100-B Area solid waste burial ground.

3.2.2 KW and KE Reactor Areas

Two production reactors were operated in this area. The 100-KW reactor started operation in January, 1955 and was shut down in February, 1970. The 100-KE reactor started operation in April, 1955 and was shut down in January, 1971. A map of this area is given in Figure 17. Figures 18 and 19 give the aerial gamma radiation results.

Seven major areas of activity can be identified in the radiation isopleth maps. These are the 105-KW reactor building, the 107-KW retention basins, the 105-KE reactor building, the 107-KE retention

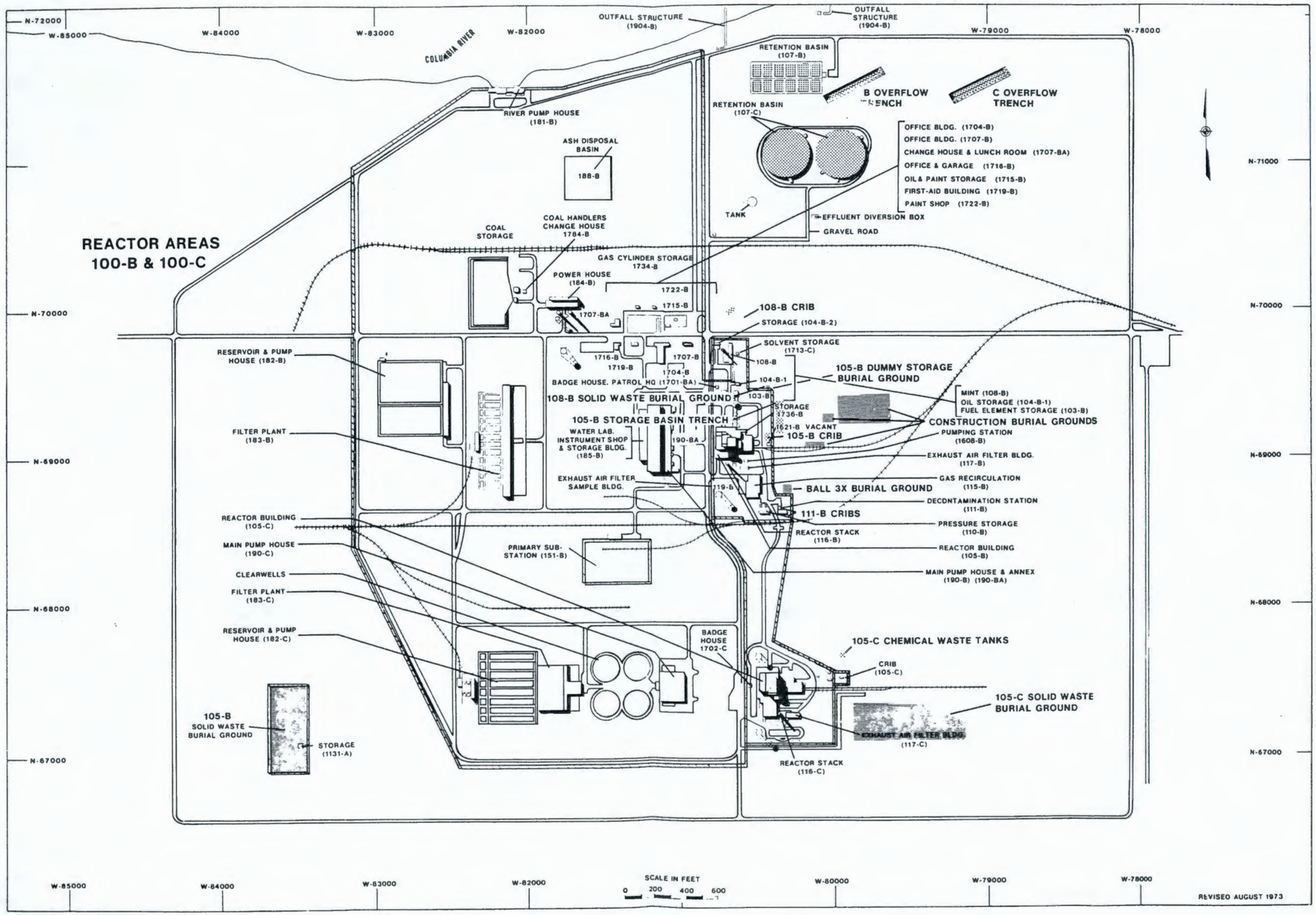

Figure 14. Facility map of the 100-B and 100-C reactor areas.

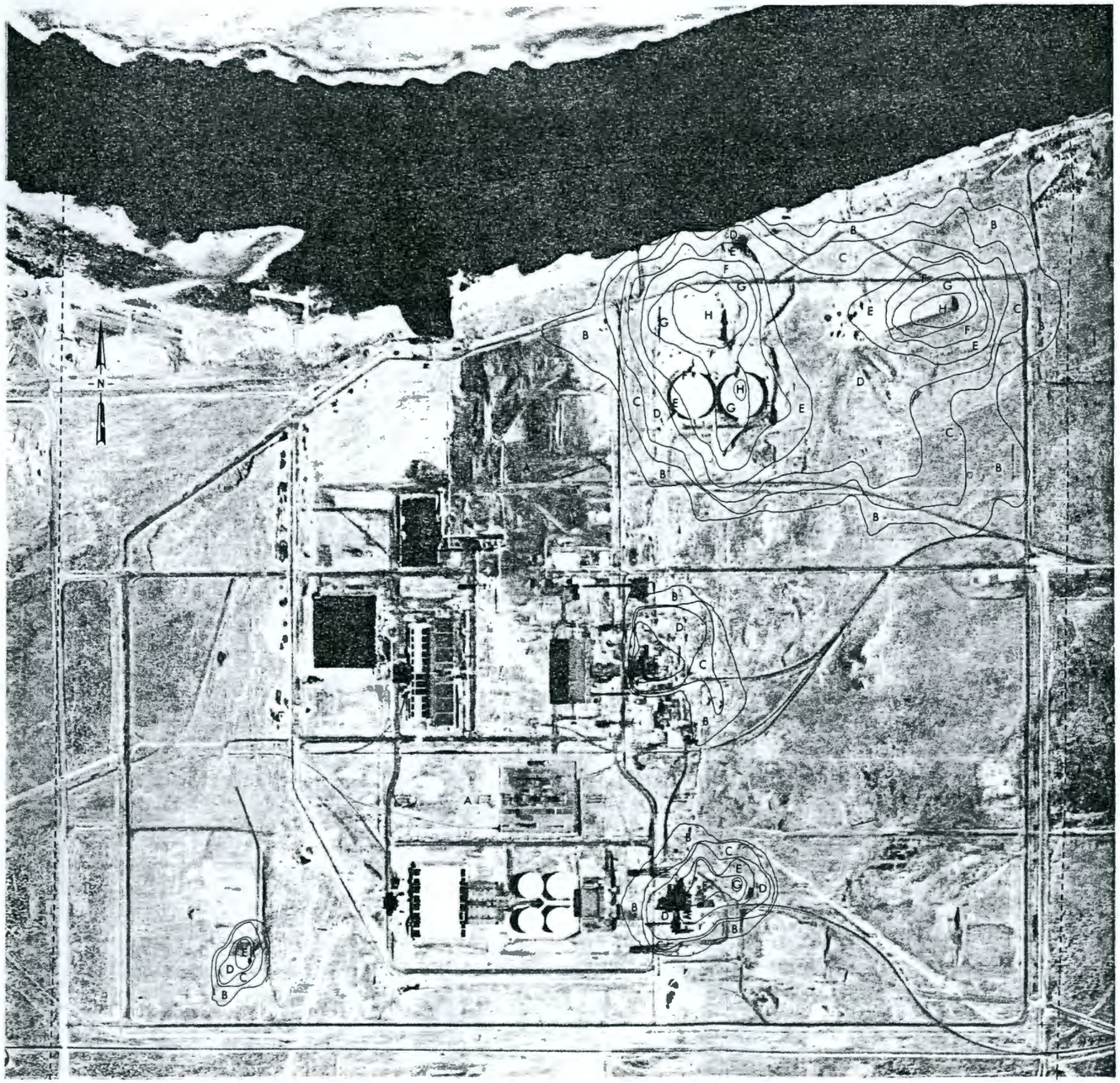

CONVERSION SCALE	
LETTER LABEL	GAMMA COUNT RATE* 50 keV — 3 MeV (cps at 45m altitude)
A	$< 1.4 \times 10^4$
B	$(1.4 - 1.7) \times 10^4$
C	$(1.7 - 2.1) \times 10^4$
D	$(2.1 - 3.2) \times 10^4$
E	$(3.2 - 4.7) \times 10^4$
F	$(4.7 - 7.1) \times 10^4$
G	$(7.1 - 11) \times 10^4$
H	$(1.1 - 1.6) \times 10^5$

*Without dead-time correction

SCALE
500 YARDS
500 METERS

Figure 15. Isopleth map of the total gamma ray count rate between 50 keV and 3 MeV (at 45-meter altitude) obtained during the October 1973 survey over the 100-B and 100-C reactor areas.

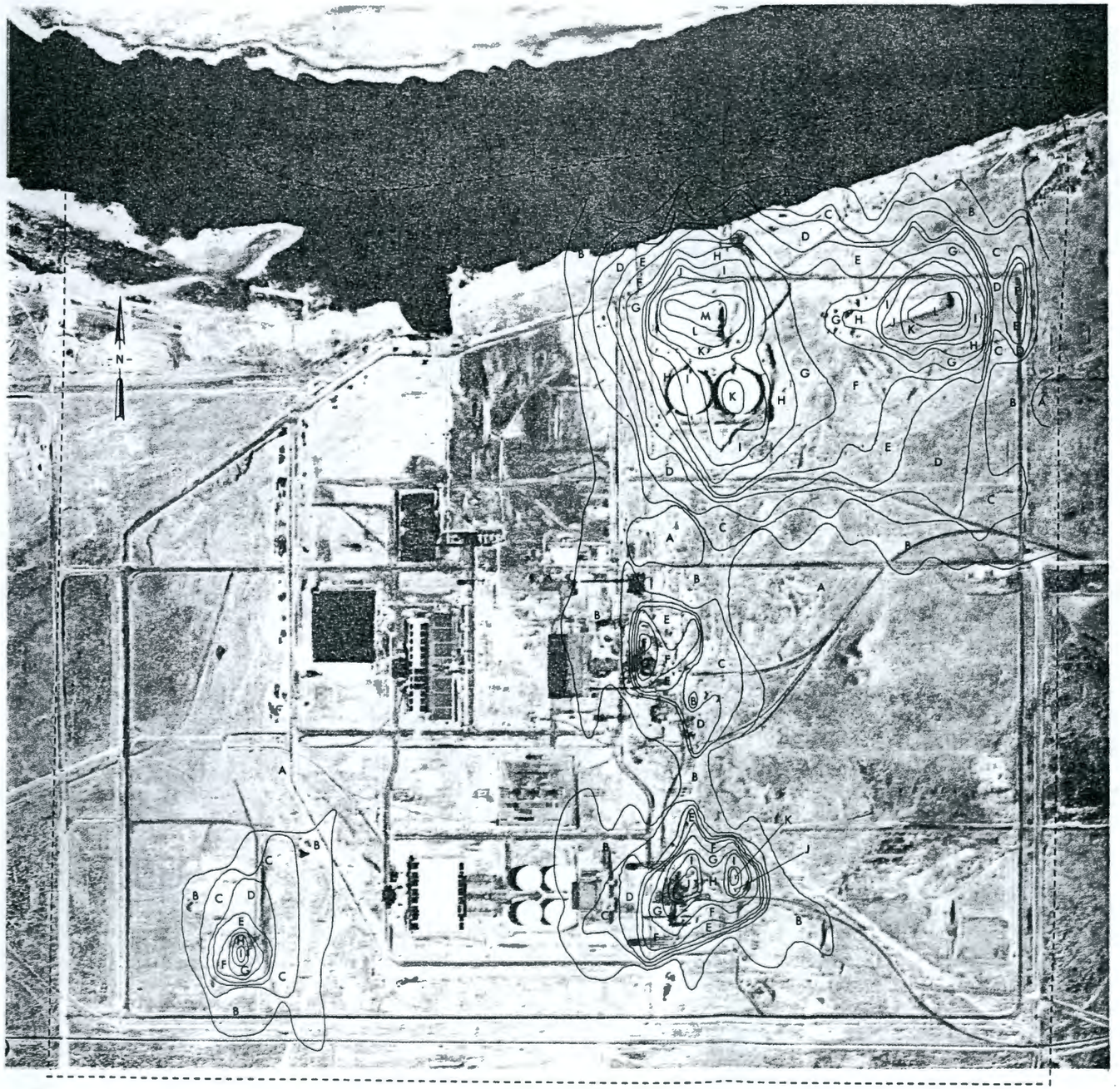

CONVERSION SCALE		
LETTER LABEL	^{60}Co SURFACE CONCENTRATION (μCi/m^2)	^{60}Co GAMMA EXPOSURE RATE AT 1 METER LEVEL (μR/h)
A	< .02	< 1.0
B	.02 – .05	1.0 – 2.2
C	.05 – .08	2.2 – 3.5
D	.08 – .13	3.5 – 5.6
E	.13 – .20	5.6 – 8.8
F	.20 – .32	8.8 – 14
G	.32 – .52	14 – 22
H	.52 – .80	22 – 35
I	.80 – 1.3	35 – 56
J	1.3 – 2.0	56 – 88
K	2.0 – 3.2	88 – 140
L	3.2 – 5.2	140 – 220
M	5.2 – 8.0	220 – 350

SCALE
500 YARDS
500 METERS

Figure 16. Concentration and gamma exposure rate isopleths for ^{60}Co derived from the aerial survey data obtained during October 1973 over the 100-B and 100-C reactor areas. The normal background exposure rate is approximately 10 μR/h in this area.

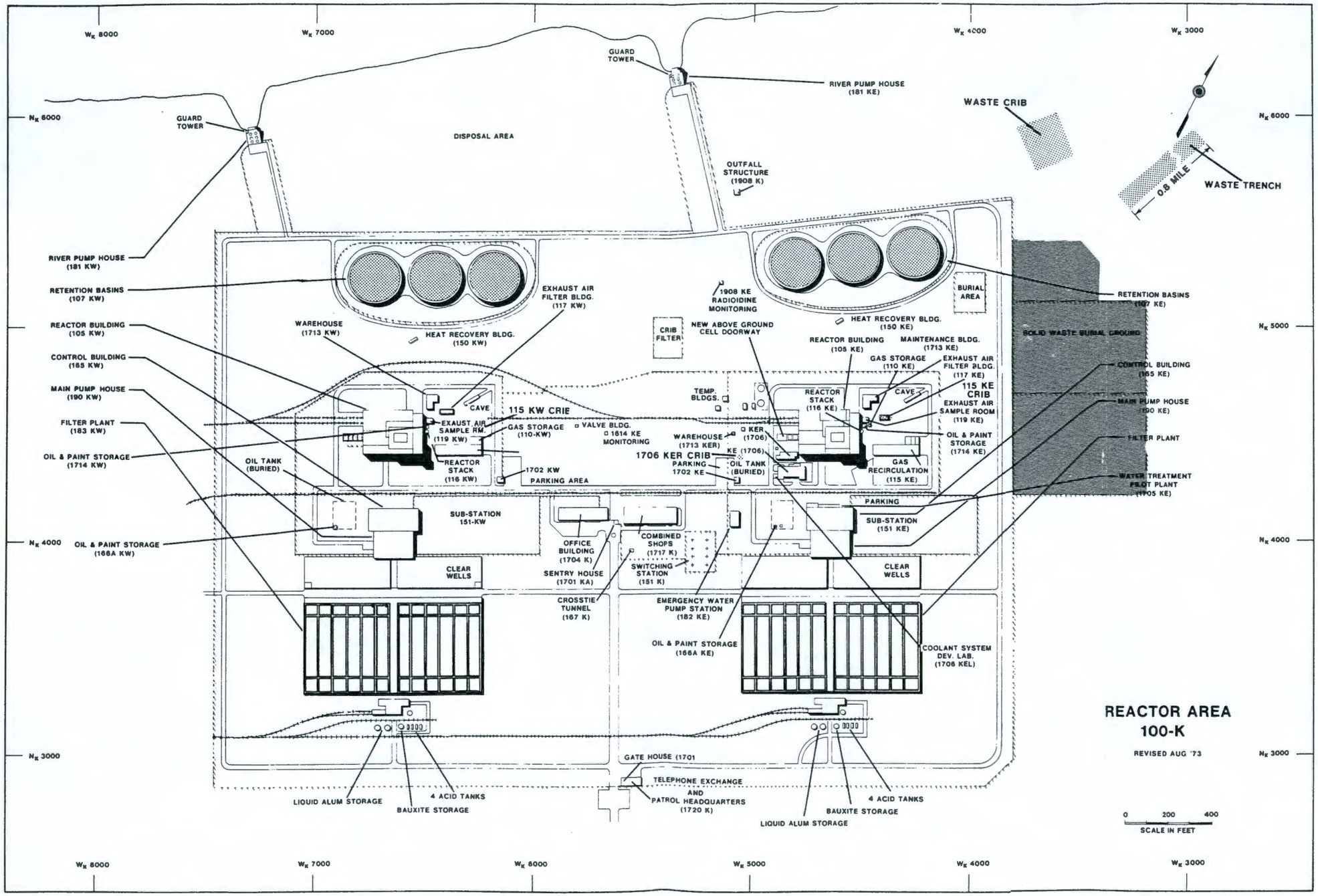

Figure 17. Facility map of the 100-KW and 100-KE reactor areas.

Figure 18. Isopleth map of the total gamma ray count rate between 50 keV and 3 MeV (at 45-meter altitude) obtained during the October 1973 survey over the 100-KW and 100-KE reactor areas.

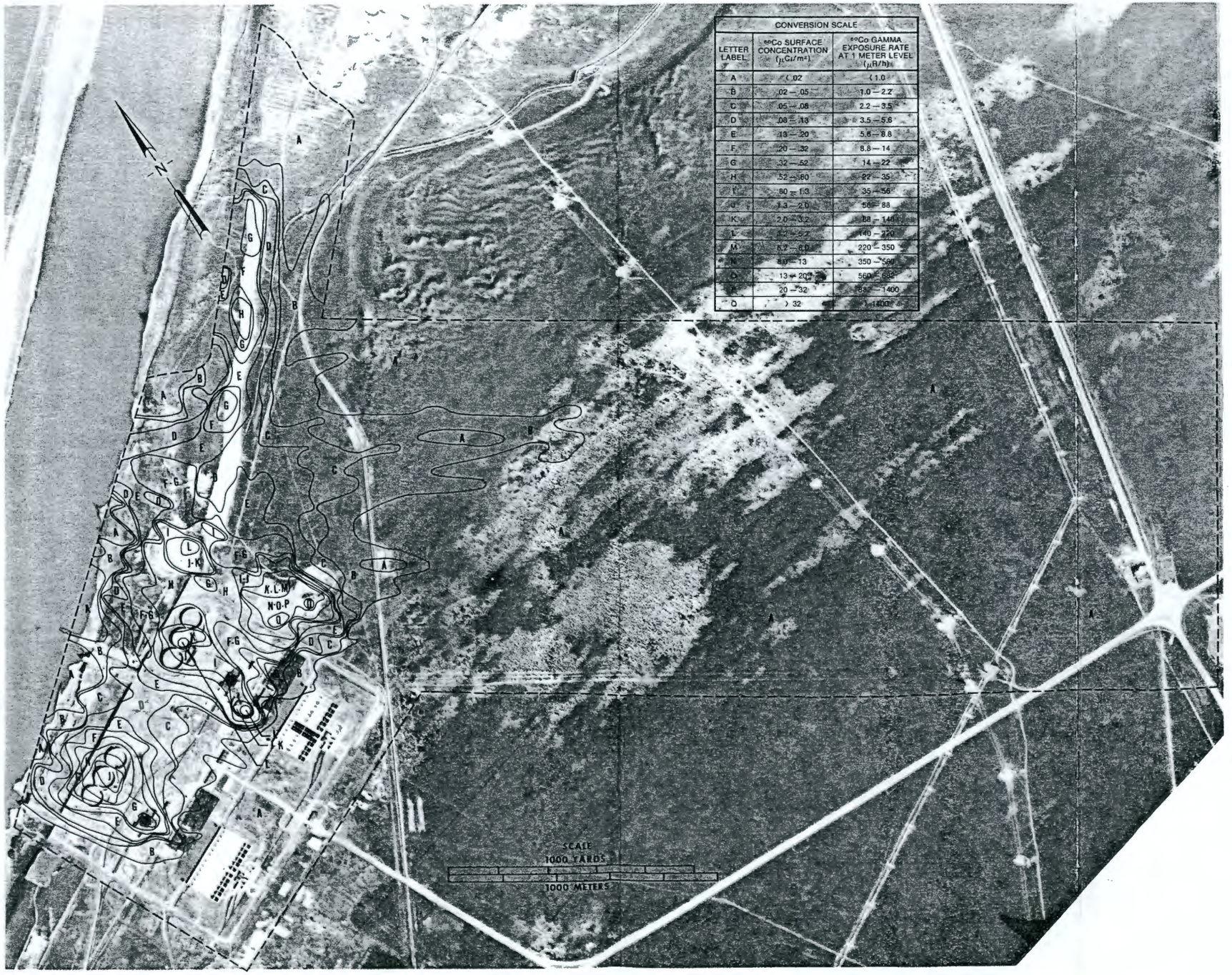

Figure 19. Concentration and gamma exposure rate isopleths for ^{60}Co derived from the aerial survey data obtained during October 1973 over the 100-KW and 100-KE reactor areas. The normal background exposure rate is approximately 10 μR/h in this area.

basins, the solid waste burial ground, the waste crib and the backfilled trench. These areas can all be identified in Figure 18. The 105-KE reactor building area had two distinct sources of activity. One was the reactor pile itself. The other was due to a ^{60}Co source within the 1706-KE Laboratory. A ground measurement gave a reading of 15 mR/h at the roof of this building. The roof area was roped off and clearly identified as a radiation area. Two distinct sources of activity were visible over the solid waste burial ground. These were due to two open burial pits containing radioactive material. All the activity observed appears well confined to the above areas. The activity indicated in the contours between these areas is consistent with what one would expect from shine at an altitude of 45 meters. Spectral plots taken over each of these areas identified ^{60}Co as the only man-made isotope identifiable in the aerial survey.

3.2.3 N Reactor Area

The 100-N reactor was activated in December, 1963 and is the only plutonium production reactor currently in operation at Hanford. In contrast to the other production reactors, which used a single-pass cooling system, the 100-N reactor has a closed cycle primary cooling system. River water is used in the secondary loop and is discharged directly back into the river.

For safety of N Reactor, the area itself was not surveyed. The survey was confined to the radioactive chemical waste treatment facility and associated trench area. A 90 meter tower, with guy wires, was located on the river side of the trench, prohibiting any low altitude flight lines being flown between the trench and the river. Figure 20 is a map of the area. The radiation results are presented in Figures 21 and 22.

All the activity observed appears to come from the 1301-N Crib and trench extension, associated with the radioactive waste disposal system. At the survey altitude of 45 meters, the radiation shine extends out for a distance of approximately 500 meters on all sides of the trench. Any low level activity on the ground within this area might well be masked by the shine from the trench itself.

3.2.4 D and DR Reactor Areas

Two plutonium production reactors were located in this area. The 100-D reactor, one of the three original reactors built at Hanford, was the second reactor to go into operation (in December, 1944). This

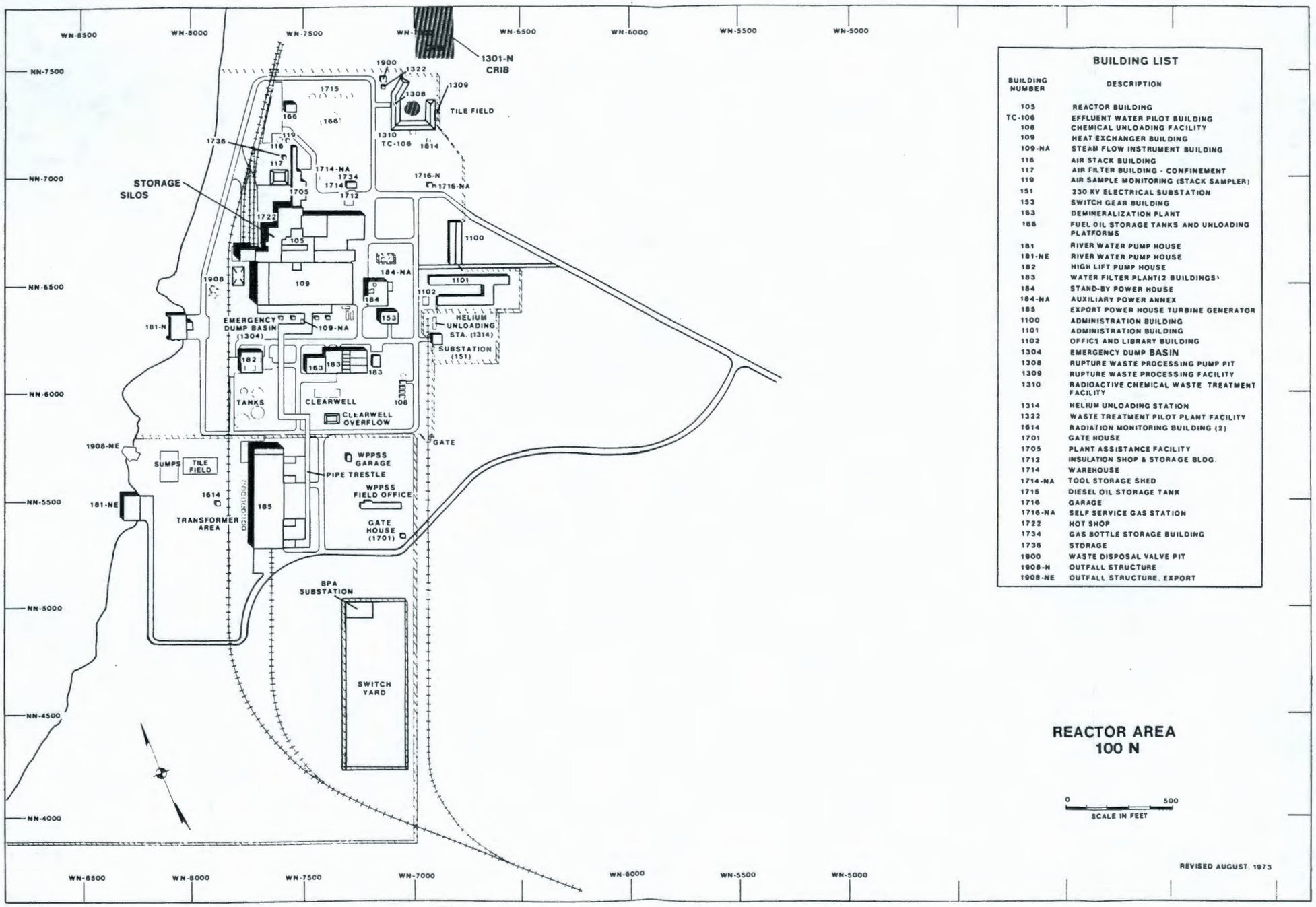

BUILDING LIST

BUILDING NUMBER	DESCRIPTION
105	REACTOR BUILDING
TC-106	EFFLUENT WATER PILOT BUILDING
108	CHEMICAL UNLOADING FACILITY
109	HEAT EXCHANGER BUILDING
109-NA	STEAM FLOW INSTRUMENT BUILDING
116	AIR STACK BUILDING
117	AIR FILTER BUILDING - CONFINEMENT
119	AIR SAMPLE MONITORING (STACK SAMPLER)
151	230 KV ELECTRICAL SUBSTATION
153	SWITCH GEAR BUILDING
163	DEMINERALIZATION PLANT
166	FUEL OIL STORAGE TANKS AND UNLOADING PLATFORMS
181	RIVER WATER PUMP HOUSE
181-NE	RIVER WATER PUMP HOUSE
182	HIGH LIFT PUMP HOUSE
183	WATER FILTER PLANT(2 BUILDINGS)
184	STAND-BY POWER HOUSE
184-NA	AUXILIARY POWER ANNEX
185	EXPORT POWER HOUSE TURBINE GENERATOR
1100	ADMINISTRATION BUILDING
1101	ADMINISTRATION BUILDING
1102	OFFICE AND LIBRARY BUILDING
1304	EMERGENCY DUMP BASIN
1308	RUPTURE WASTE PROCESSING PUMP PIT
1309	RUPTURE WASTE PROCESSING FACILITY
1310	RADIOACTIVE CHEMICAL WASTE TREATMENT FACILITY
1314	HELIUM UNLOADING STATION
1322	WASTE TREATMENT PILOT PLANT FACILITY
1614	RADIATION MONITORING BUILDING (2)
1701	GATE HOUSE
1705	PLANT ASSISTANCE FACILITY
1712	INSULATION SHOP & STORAGE BLDG.
1714	WAREHOUSE
1714-NA	TOOL STORAGE SHED
1715	DIESEL OIL STORAGE TANK
1716	GARAGE
1716-NA	SELF SERVICE GAS STATION
1722	HOT SHOP
1734	GAS BOTTLE STORAGE BUILDING
1736	STORAGE
1900	WASTE DISPOSAL VALVE PIT
1908-N	OUTFALL STRUCTURE
1908-NE	OUTFALL STRUCTURE, EXPORT

REACTOR AREA
100 N

0 500
SCALE IN FEET

Figure 20. Facility map of the 100-N reactor area.

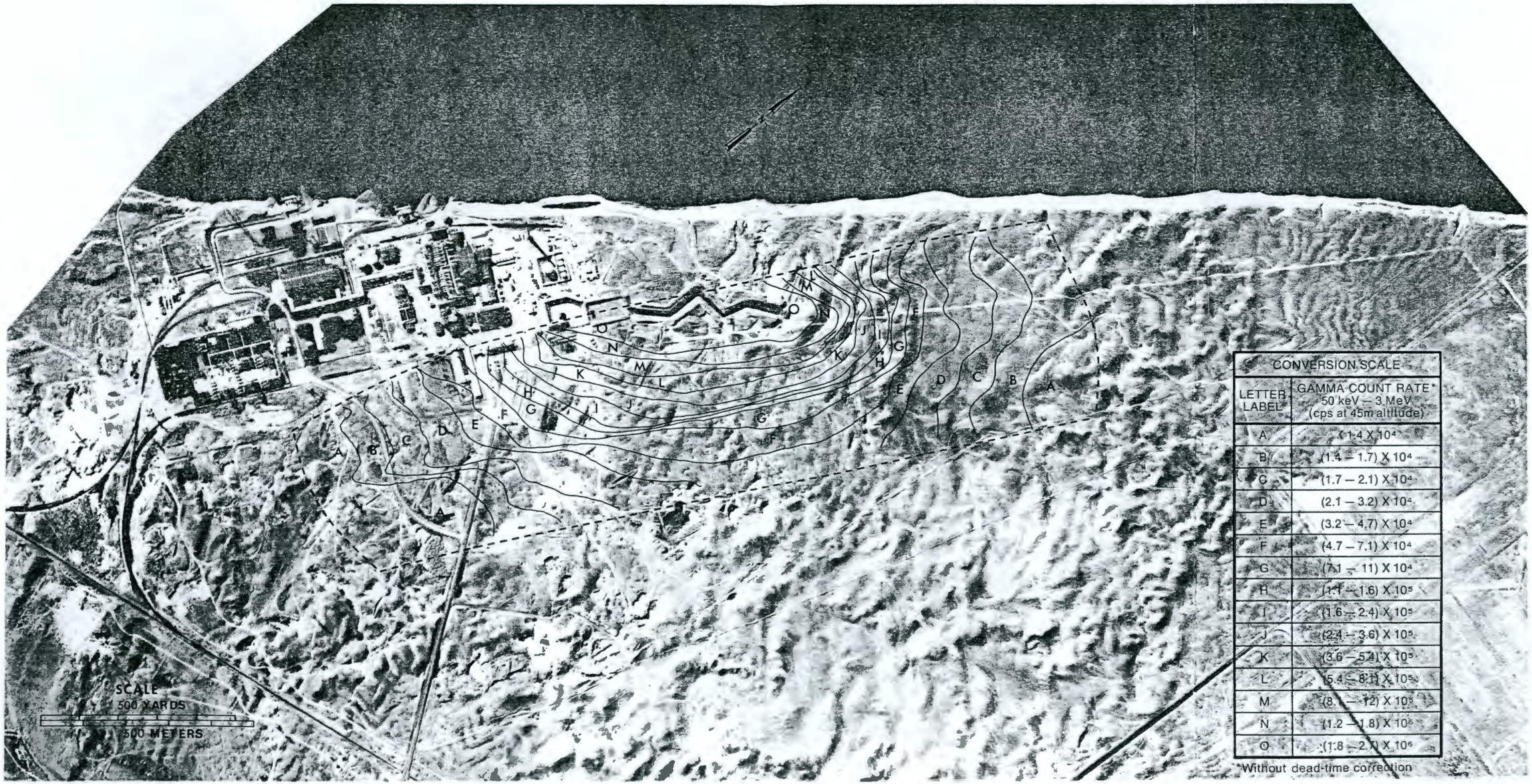

CONVERSION SCALE	
LETTER LABEL	GAMMA COUNT RATE* 50 keV — 3 MeV (cps at 45m altitude)
A	< 1.4 X 10^4
B	(1.4 – 1.7) X 10^4
C	(1.7 – 2.1) X 10^4
D	(2.1 – 3.2) X 10^4
E	(3.2 – 4.7) X 10^4
F	(4.7 – 7.1) X 10^4
G	(7.1 – 11) X 10^4
H	(1.1 – 1.6) X 10^5
I	(1.6 – 2.4) X 10^5
J	(2.4 – 3.6) X 10^5
K	(3.6 – 5.4) X 10^5
L	(5.4 – 8.1) X 10^5
M	(8.1 – 12) X 10^5
N	(1.2 – 1.8) X 10^6
O	(1.8 – 2.7) X 10^6

*Without dead-time correction

Figure 21. Isopleth map of the total gamma ray count rate between 50 keV and 3 MeV (at 45-meter altitude) obtained during the October 1973 survey over the 100-N reactor area.

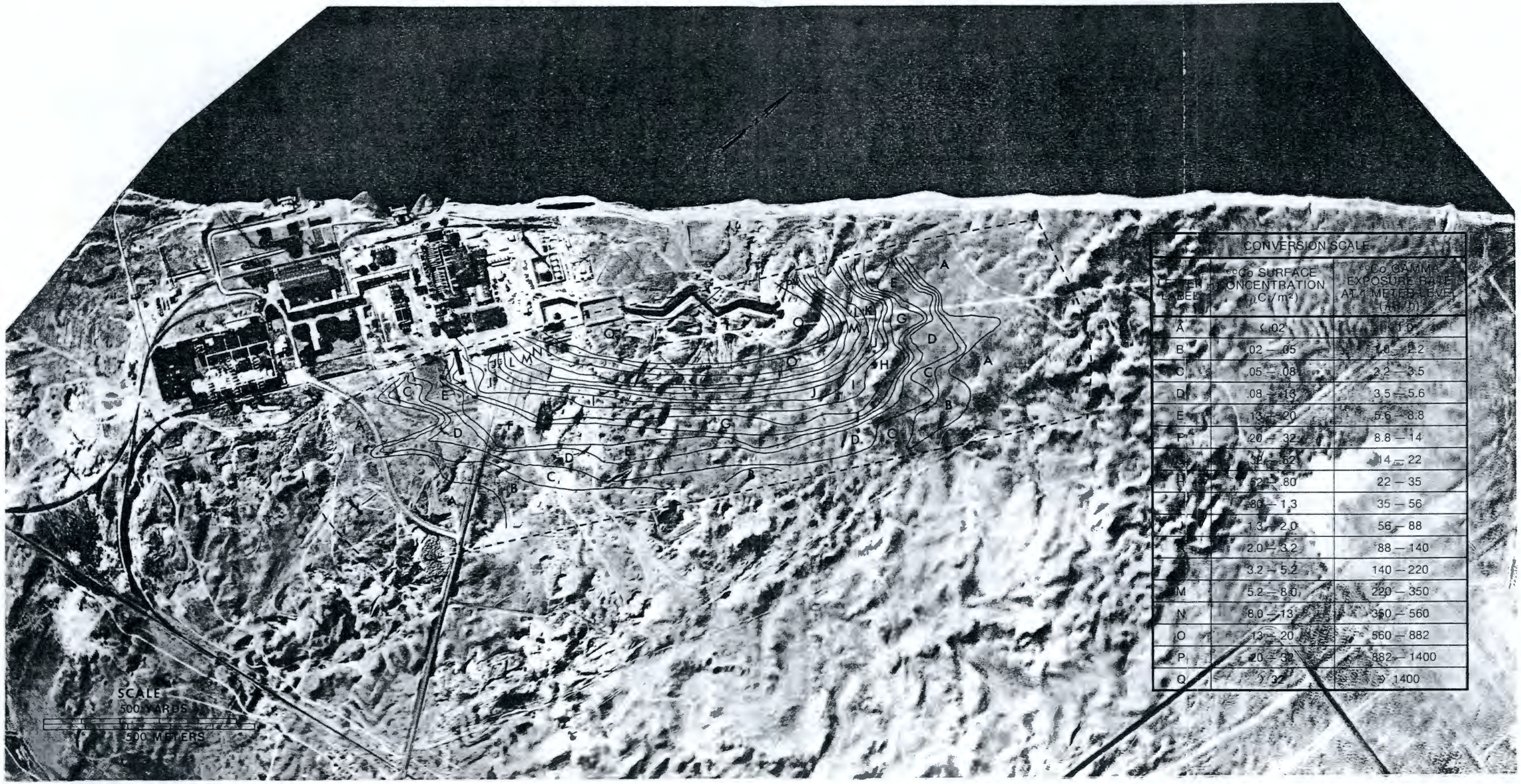

CONVERSION SCALE		
CONTOUR LABEL	^{60}Co SURFACE CONCENTRATION (μCi/m^2)	^{60}Co GAMMA EXPOSURE RATE AT 1 METER LEVEL (μR/h)
A	< .02	< 1.0
B	.02 — .05	1.0 — 2.2
C	.05 — .08	2.2 — 3.5
D	.08 — .13	3.5 — 5.6
E	.13 — .20	5.6 — 8.8
F	.20 — .32	8.8 — 14
G	.32 — .52	14 — 22
H	.52 — .80	22 — 35
I	.80 — 1.3	35 — 56
J	1.3 — 2.0	56 — 88
K	2.0 — 3.2	88 — 140
L	3.2 — 5.2	140 — 220
M	5.2 — 8.0	220 — 350
N	8.0 — 13	350 — 560
O	13 — 20	560 — 882
P	20 — 32	882 — 1400
Q	> 32	> 1400

Figure 22. Concentration and gamma exposure rate isopleths for ^{60}Co derived from the aerial survey data obtained during October 1973 over the 100-N reactor area. The normal background exposure rate is approximately 10 μR/h in this area.

reactor was permanently retired in June, 1967. The 100-DR reactor started operation in October, 1950 and was shut down in December, 1964. A map identifying the various facilities within this area is shown in Figure 23. Figures 24 and 25 give the radiation results.

Five general areas of activity were identified within the survey area. These are the 105-D reactor building area, the 105-DR reactor building area, an open burial trench within one of the solid waste burial grounds, the 107-D and 107-DR retention basins and a portion of the slough area which lies downstream of the 100-D Area. The activity in the slough area is the result of a gradual build-up from low level emissions into the river from past reactor operations. A C level is indicated on the gross count isopleth map over the cask storage pad, located just east of the 100-DR reactor building. The ^{60}Co isopleth map does not indicate any activity over this area. A spectral plot identified ^{137}Cs as the isotope present. Since the time of the survey, the open burial trench has been covered with earth. Additional earth cover has also been placed over the 107-DR retention basin.

3.2.5 H Reactor Area

The 100-H reactor started operation in October, 1949 and was shut down in April, 1965. A map of the area and the results of the aerial survey are given in Figures 26, 27 and 28.

Four regions of activity were identified in this area. These are the 105-H reactor building area, the 107-H retention basin and associated liquid waste disposal trench area, a small area along the river bank and an area within the 182-H reservoir. The activity in all the areas was due to ^{60}Co except for a small area just south of the 1608-H Crib, which was due to ^{137}Cs. An additional 50 cm of earth has been placed over this area since the time of the survey. The activity along the river and in the 182-H reservoir is the result of a gradual build-up from past operation of upstream reactors.

This will be the first of the reactor areas to be completely decommissioned. Since the survey some of the facilities have been torn down and the 182-H reservoir has been covered with earth.

3.2.6 F Reactor Area

The 100-F reactor, one of the three original plutonium production reactors, was activated in February, 1945 and permanently retired in June, 1965. Although the reactor facilities are shut down, Battelle Pacific Northwest Laboratories still operate some

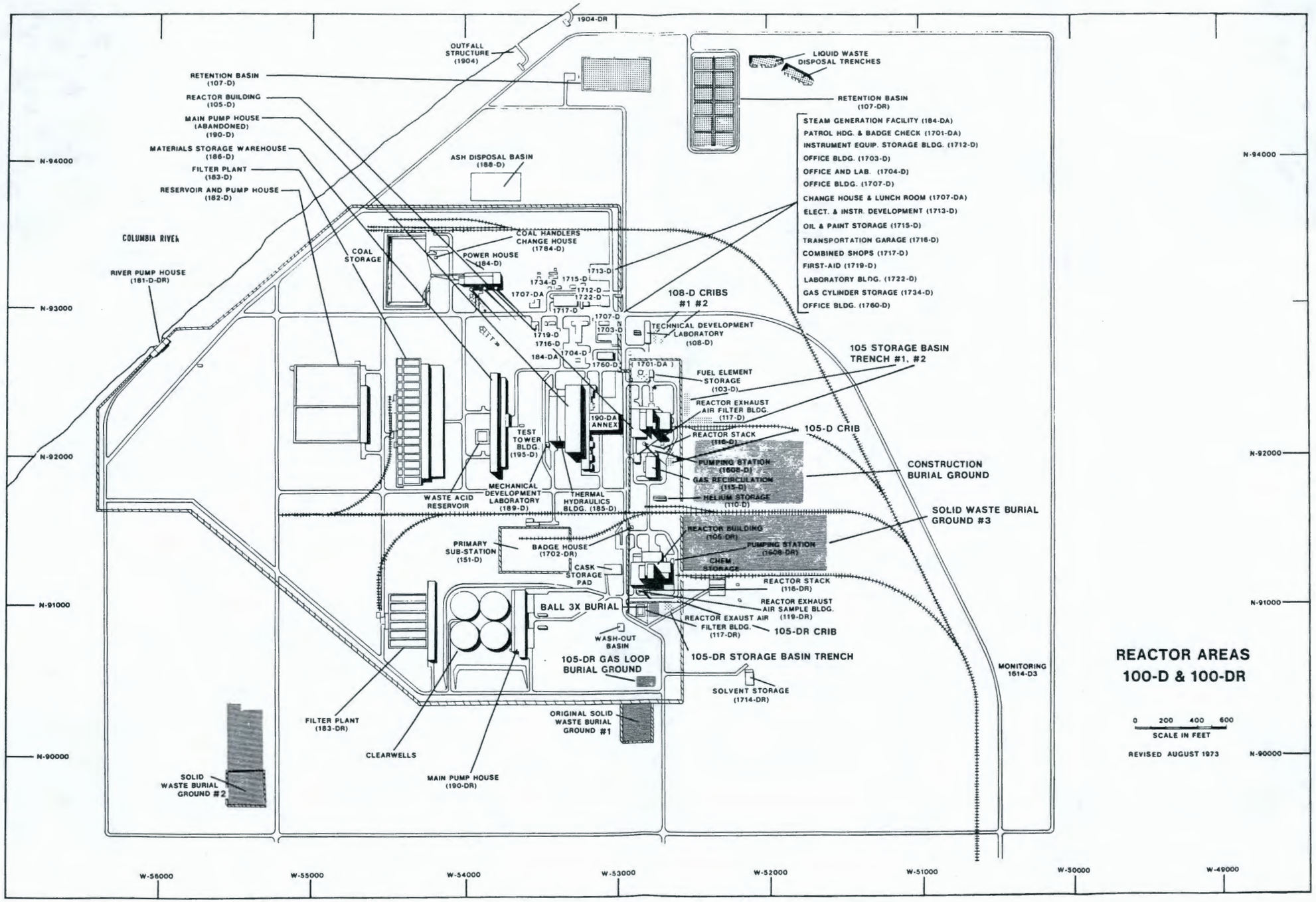

Figure 23. Facility map of the 100-D and 100-DR reactor areas.

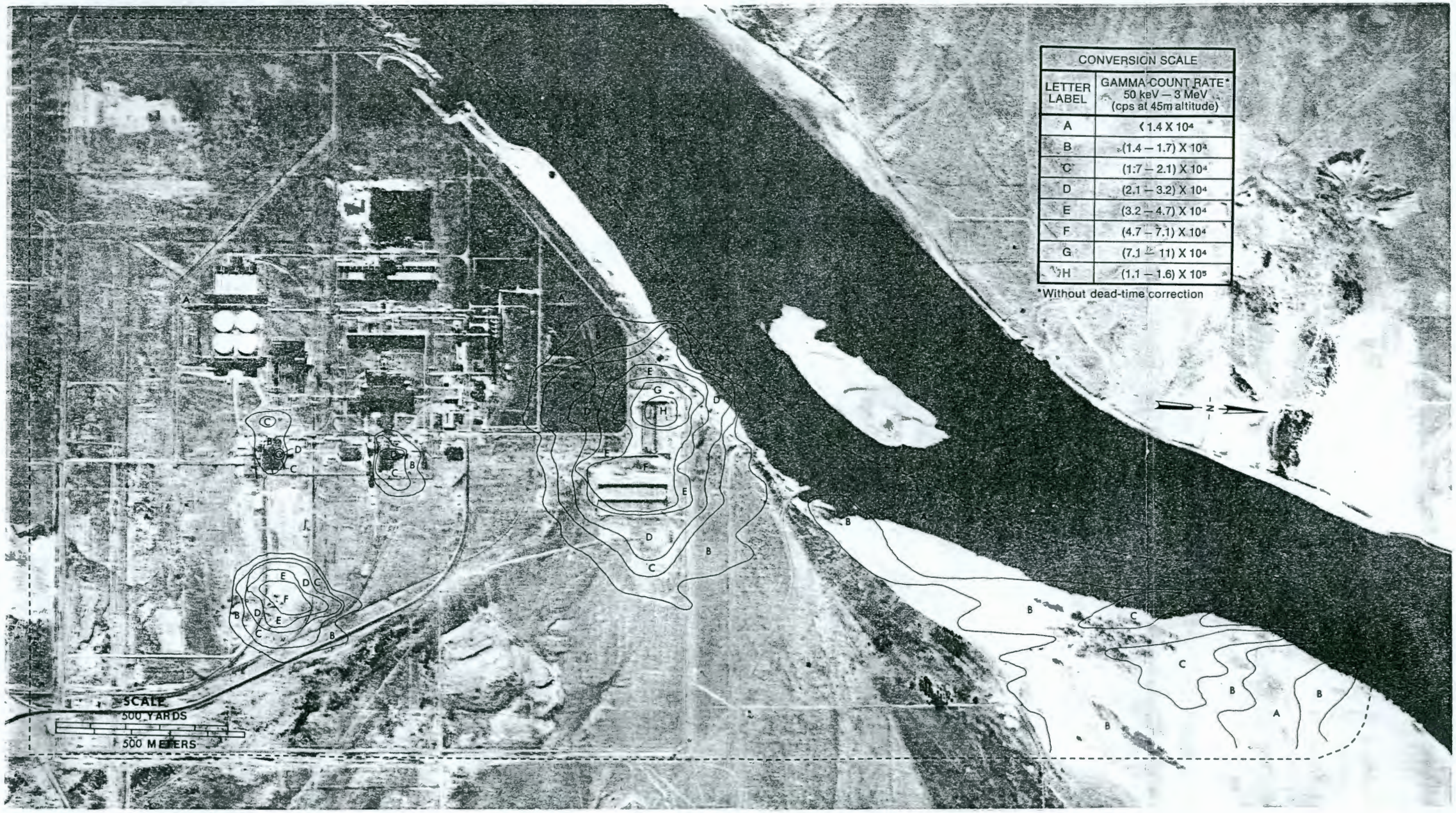

Figure 24. Isopleth map of the total gamma ray count rate between 50 keV and 3 MeV (at 45-meter altitude) obtained during the October 1973 survey over the 100-D and 100-DR reactor areas.

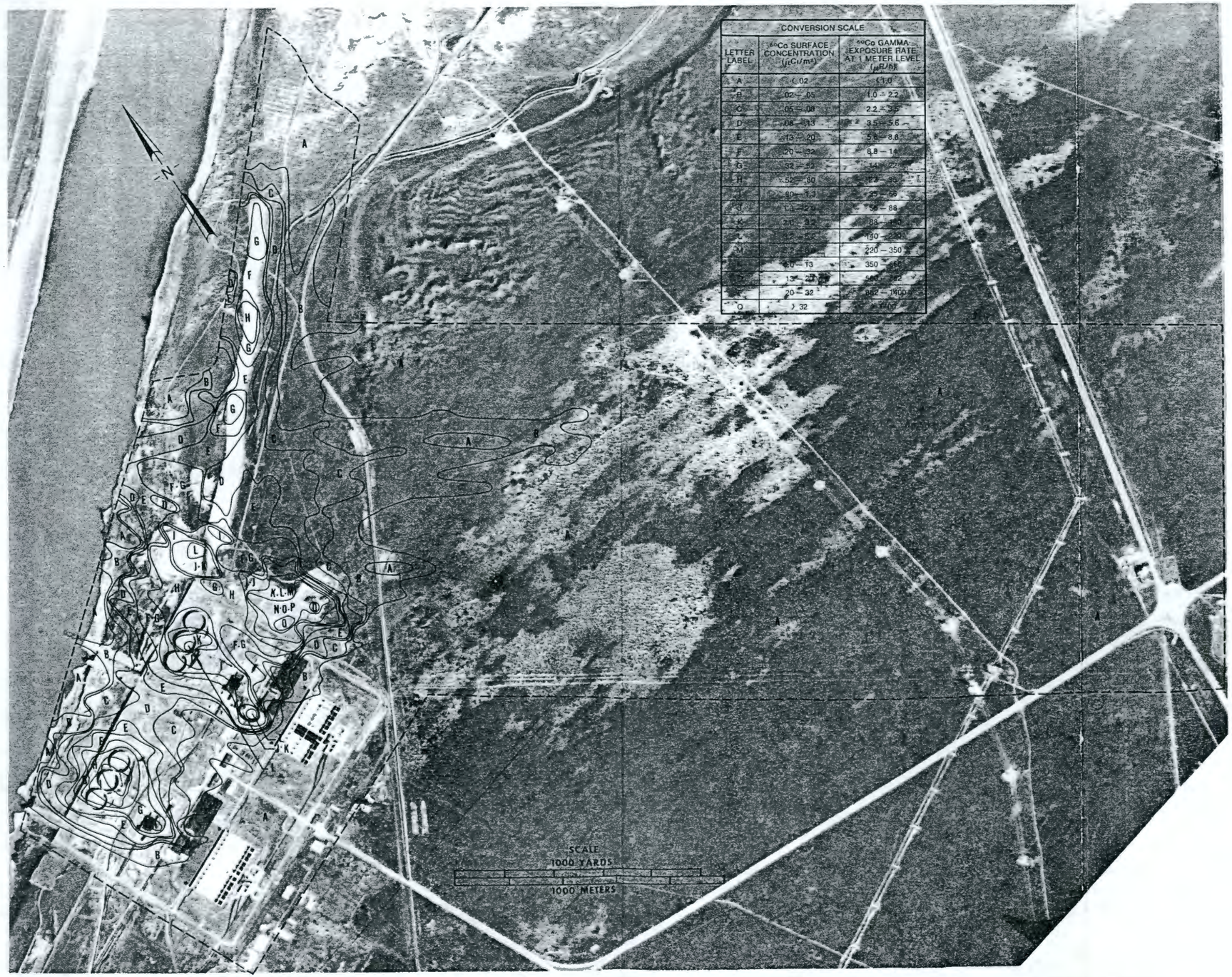

Figure 19. Concentration and gamma exposure rate isopleths for ^{60}Co derived from the aerial survey data obtained during October 1973 over the 100-KW and 100-KE reactor areas. The normal background exposure rate is approximately 10 μR/h in this area.

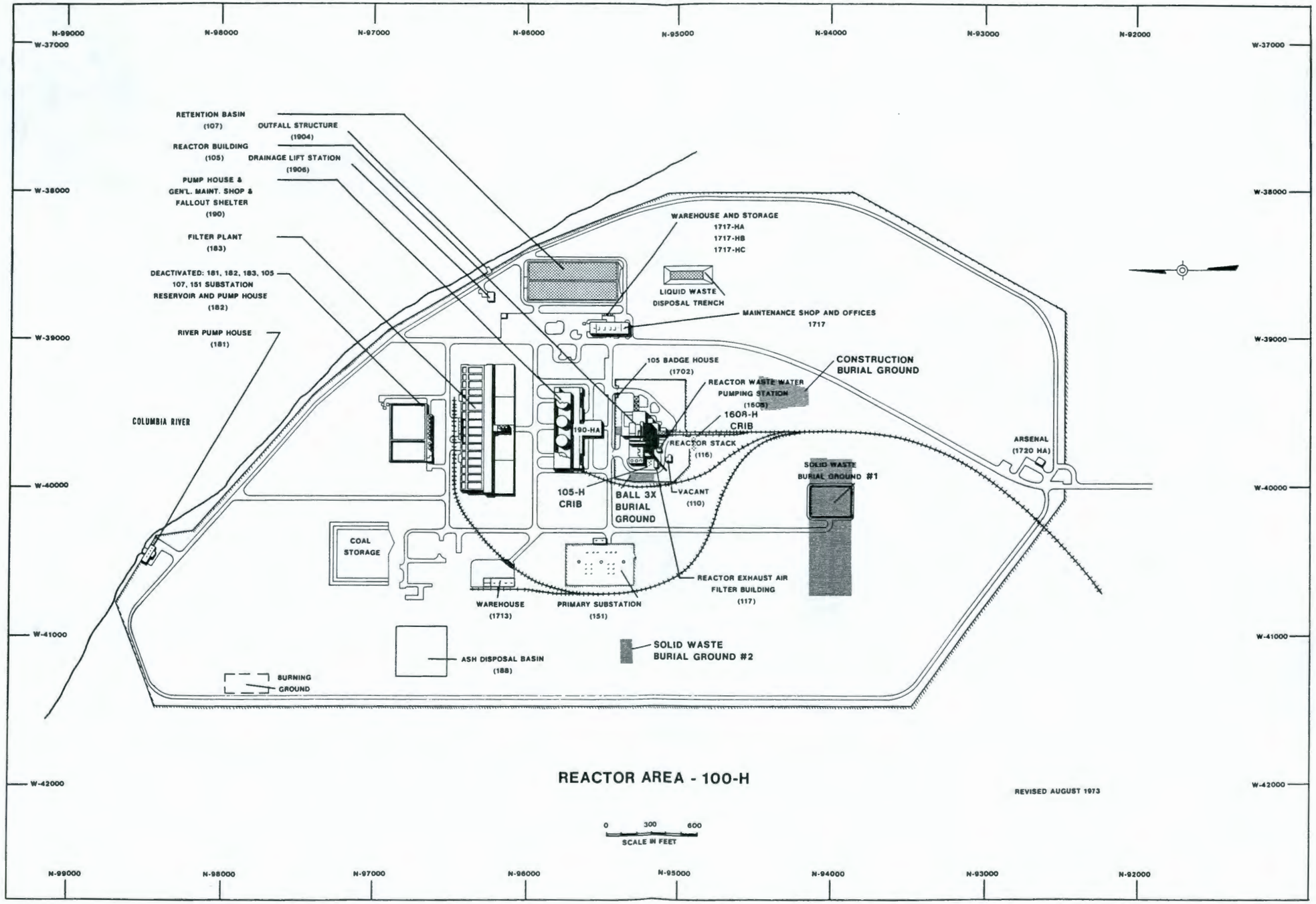

Figure 26. Facility map of the 100-H reactor area.

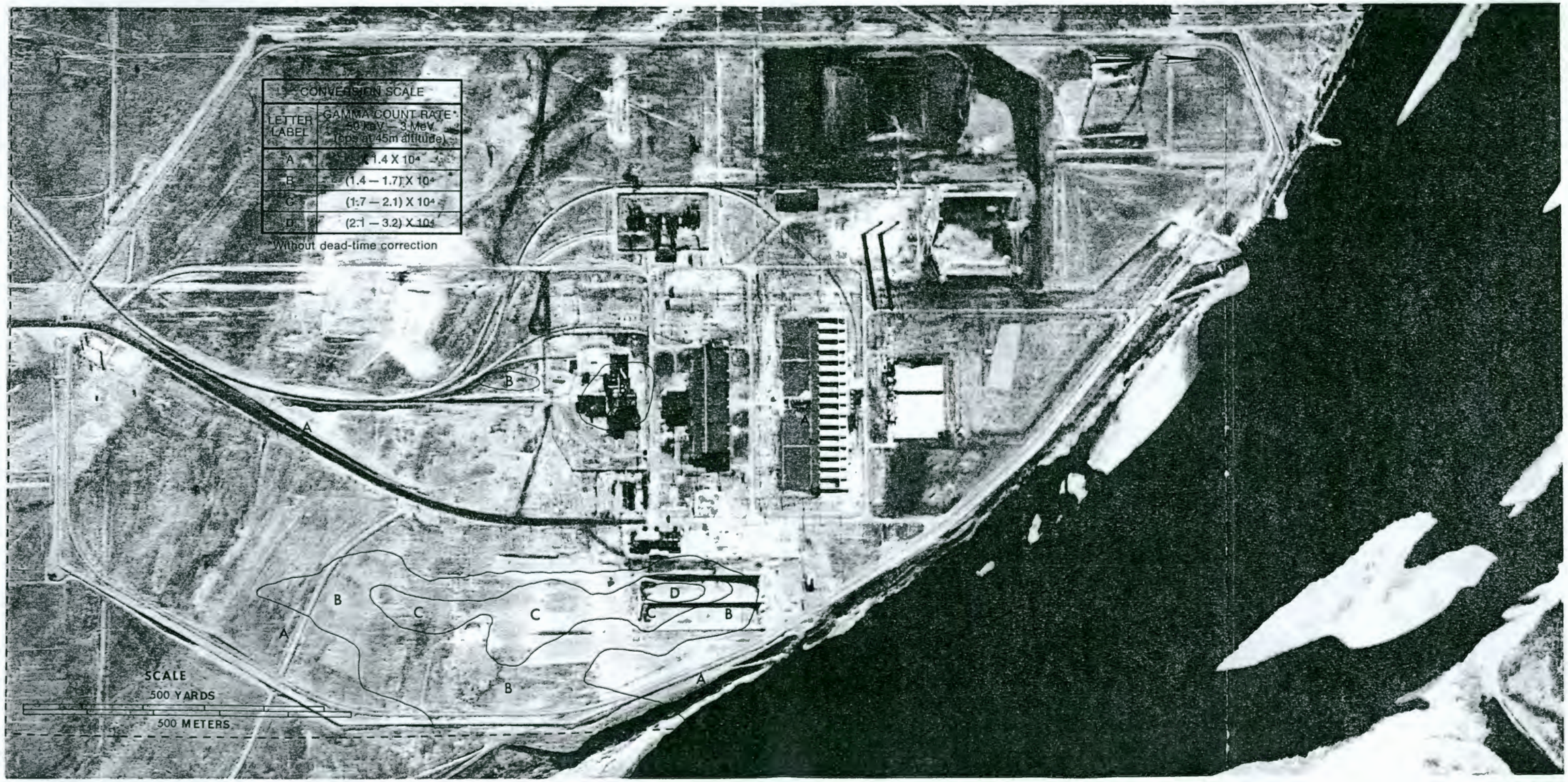

Figure 27. Isopleth map of the total gamma ray count rate between 50 keV and 3 MeV (at 45-meter altitude) obtained during the October 1973 survey over the 100-H reactor area.

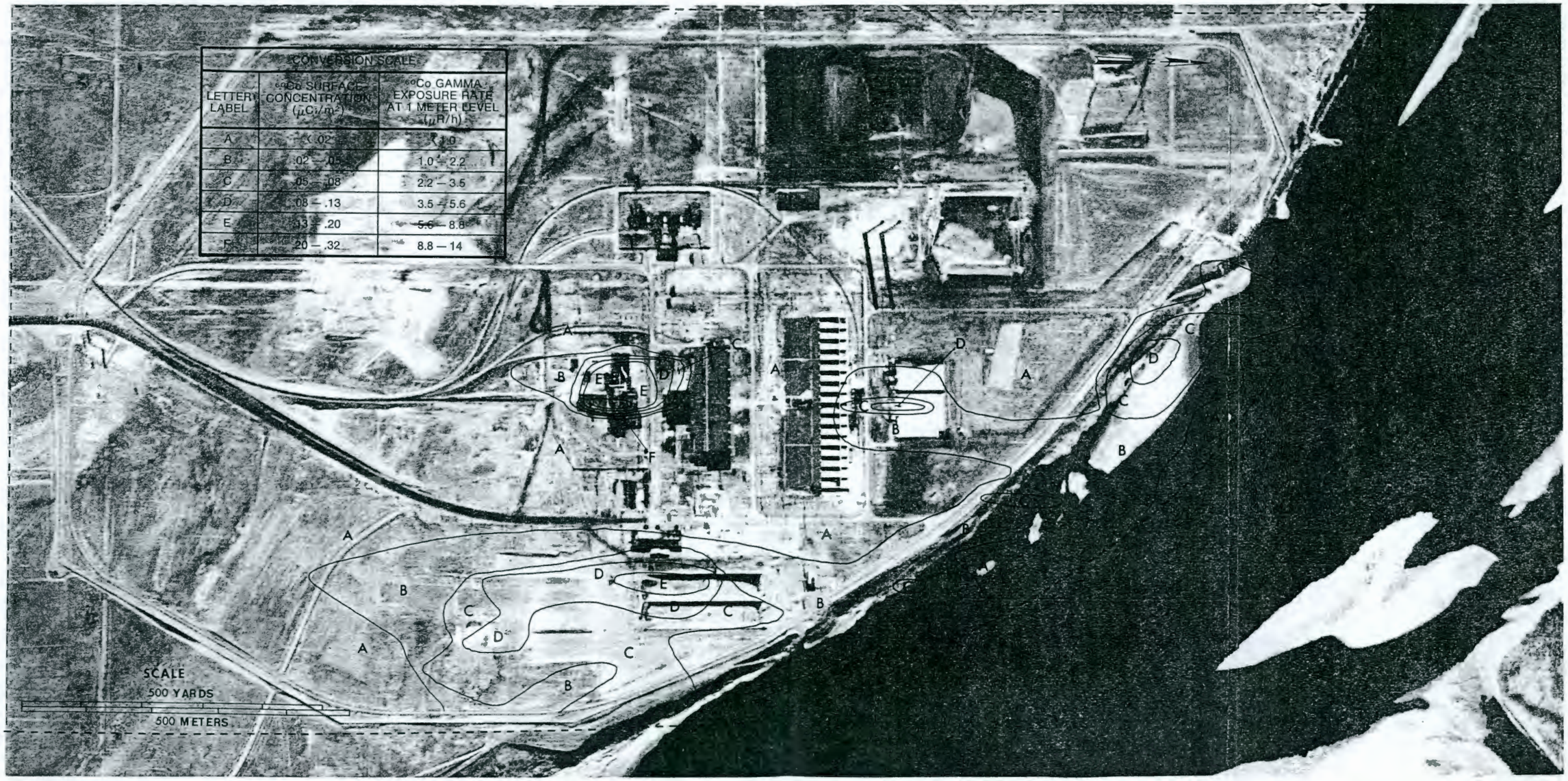

Figure 28. Concentration and gamma exposure rate isopleths for ^{60}Co derived from the aerial survey data obtained during October 1973 over the 100-H reactor area. The normal background exposure rate is approximately 10 $\mu R/h$ in this area.

limited biological laboratory facilities within the area. Figure 29 shows a map of the area identifying the major facilities and waste storage areas. The results of the aerial survey are given in Figures 30 and 31.

Eight areas of activity were identified in the aerial gamma radiation survey. These are the 141-L facility, a portion of the Lewis Canal, a region along the shoreline upstream from the Area, the 182-F reservoir, the 105-F reactor building, an old burial ground, the 1707-F, FA Inhalation Laboratories and the 107-F retention basin with its adjacent piping. Soil uptake experiments using ^{90}Sr and ^{137}Cs were carried out, at one time, within the 141-L facility. The aerial survey detected the low level residual ^{137}Cs activity within this area. A portion of the Lewis Canal showed some ^{60}Co activity visible at the surface. This was a natural ditch into which liquid wastes from the 105-F and 190-F buildings and decontamination wastes from the 189-F building were deposited. The activity observed along the upstream shoreline and over the 182-F reservoir is due to a long term build-up from the low level activity released into the Columbia River by past reactor operations. The burial area observed in the survey does not appear on the map given in Figure 29. This area is located due south of the 105-F storage basin trench, just outside the fence. A spectral plot taken over the area reveals the presence of some low level ^{137}Cs activity, as well as the ^{60}Co activity shown in Figure 31. Radon generators are in use in the 1707-F, FA Inhalation Laboratories. Figure 32 shows the result of subtracting a background spectrum, accumulated for the same length of time, from the spectrum obtained over this area. The characteristic ^{214}Bi daughter products of radon are clearly visible.

Some ^{60}Co activity can be seen along the effluent water line leading into the 107-F retention basin. All the activity in this part of the Area appears to come from the pipe line and the retention basin. A number of the active biological facilities and associated waste storage facilities are located in this region. These areas contain some ^{90}Sr. ^{90}Sr, however, decays via a beta decay, with no gamma emission. Thus, they do not appear in the gamma radiation isopleth maps.

A number of other waste storage areas, associated with the reactor operations, are also located within the 100-F Area. These, however, are sufficiently covered with earth that no gamma radiation could be detected at the surface in the aerial survey.

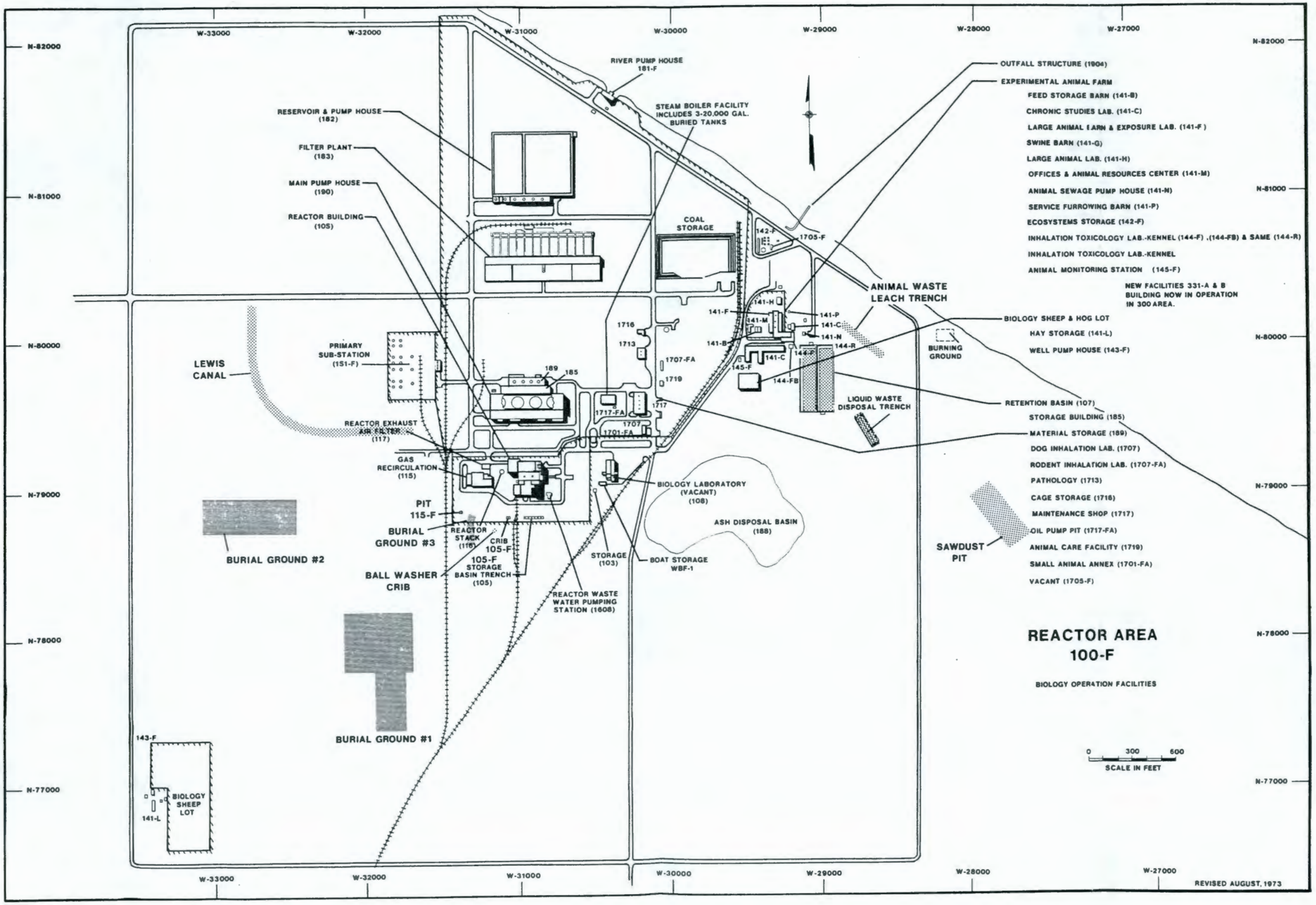

Figure 29. Facility map of the 100-F reactor area.

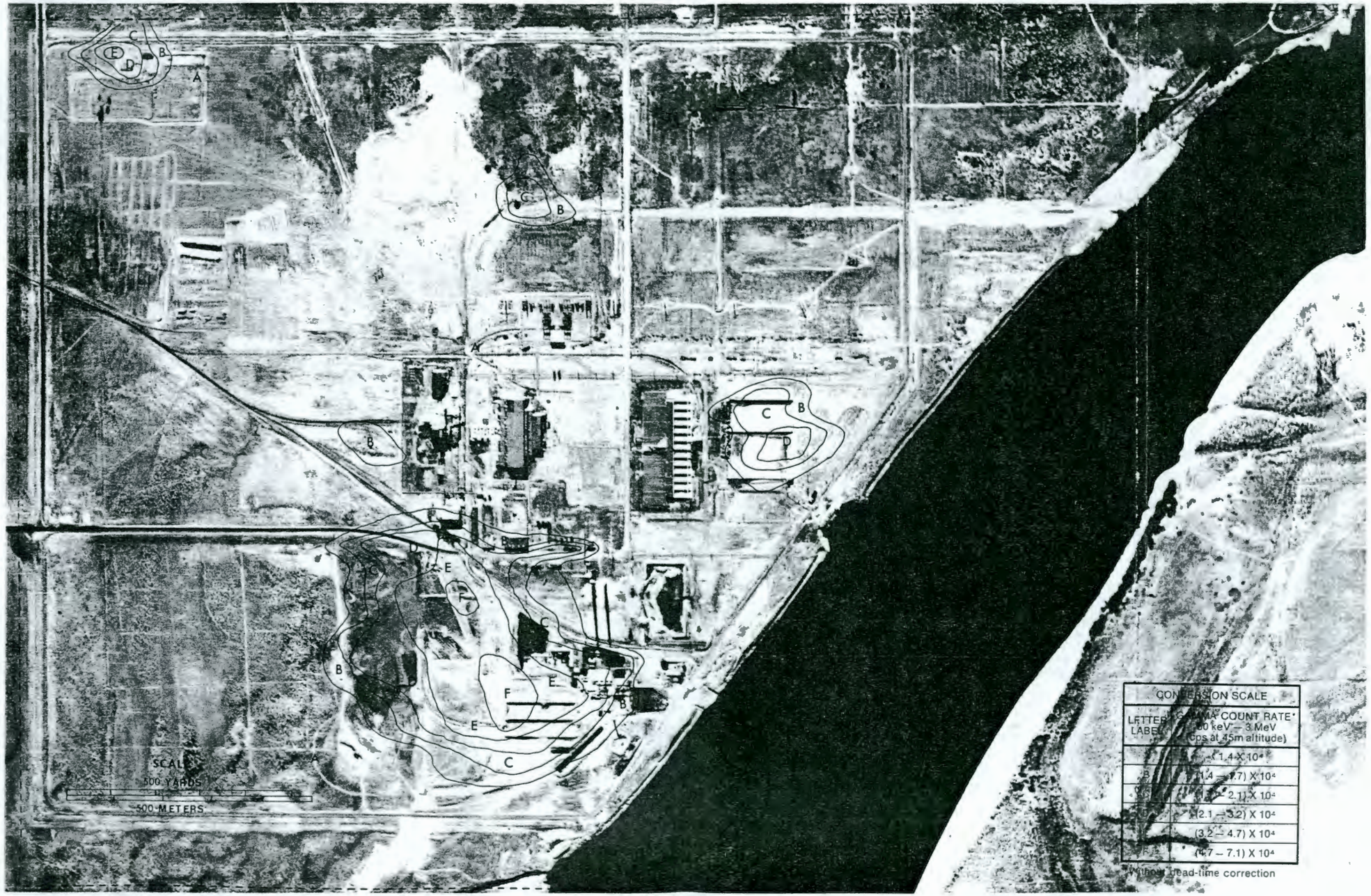

Figure 30. Isopleth map of the total gamma ray count rate between 50 keV and 3 MeV (at 45-meter altitude) obtained during the October 1973 survey over the 100-F reactor area.

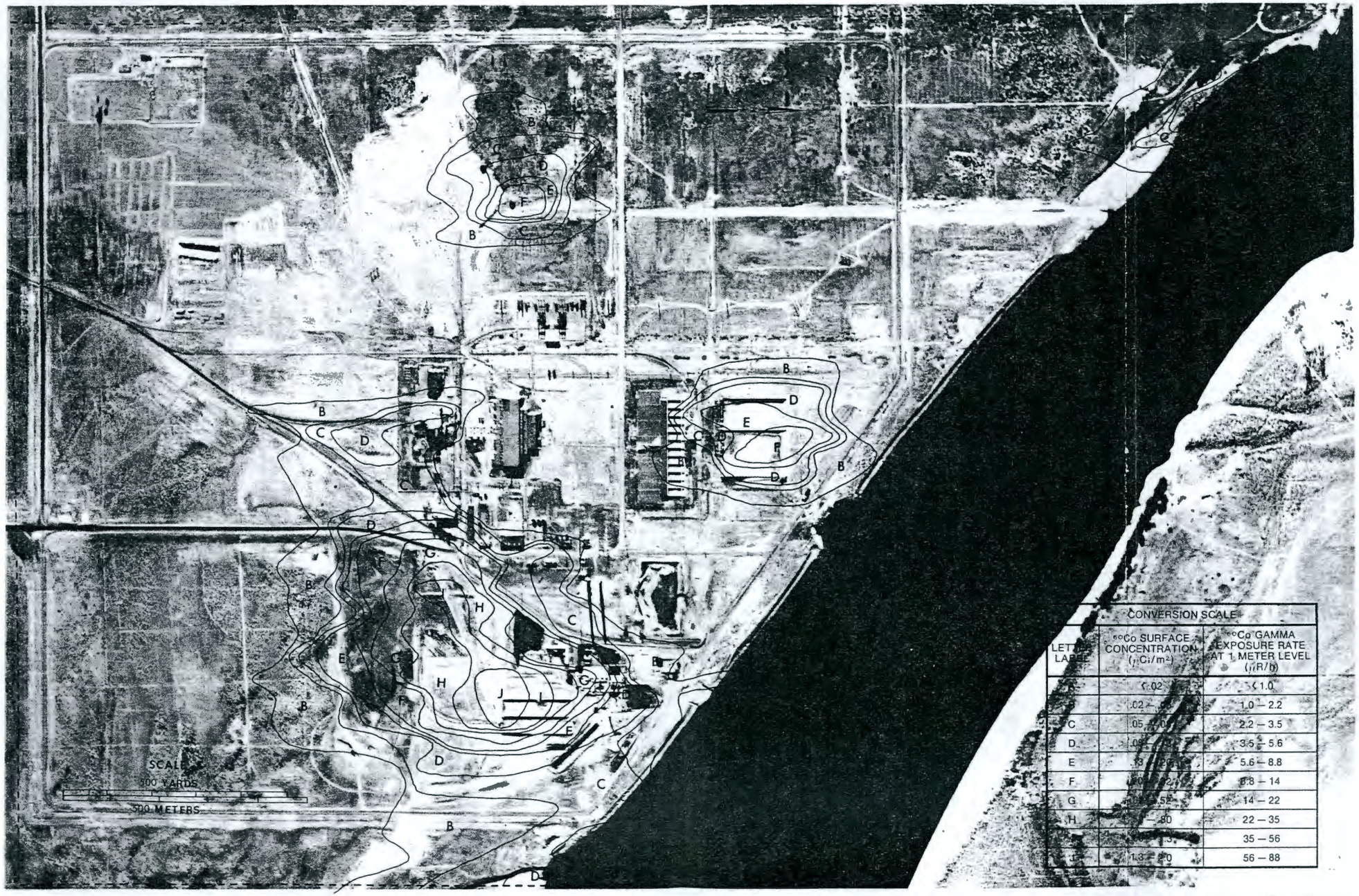

Figure 31. Concentration and gamma exposure rate isopleths for ^{60}Co derived from the aerial survey data obtained during October 1973 over the 100-F reactor area. The normal background exposure rate is approximately 10 μR/h in this area.

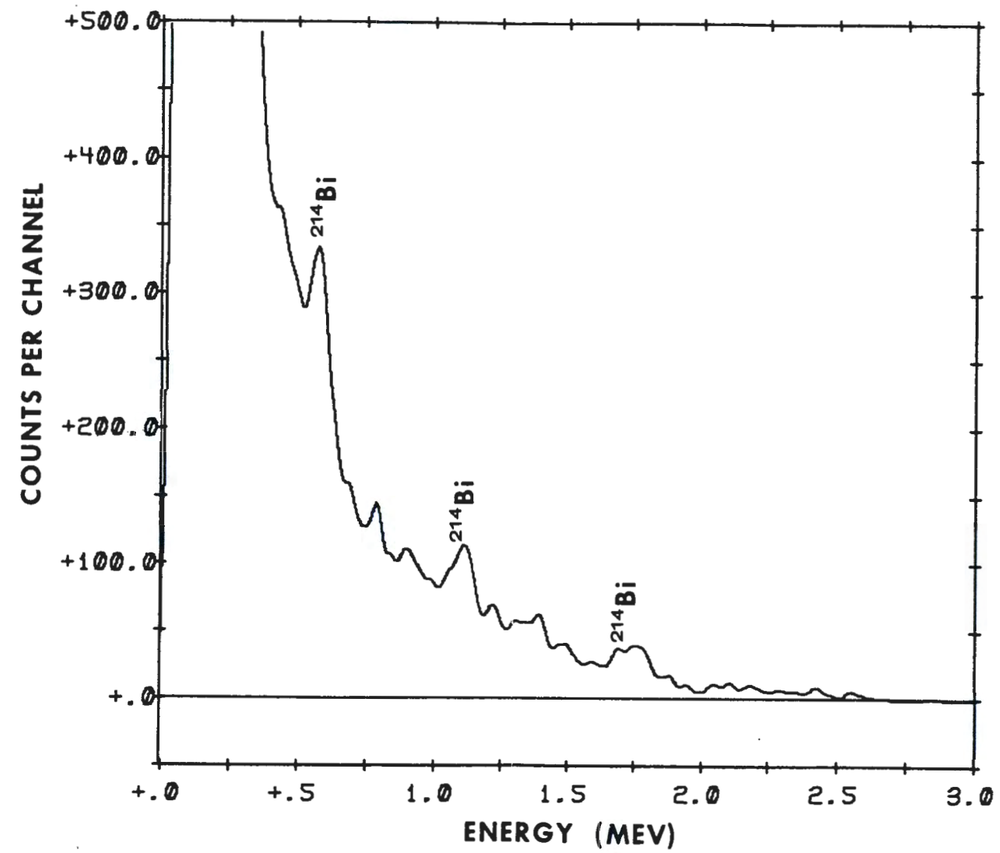

Figure 32. Gamma energy pulse height spectrum obtained over the 1707-F, FA Inhalation Laboratory after subtraction of the normal background components.

3.3 200 Area Plateau

The 200 Area Plateau is the site of the nuclear fuel chemical separation plants. These are located within the 200-East and 200-West Areas. Here the Bismuth Phosphate, Redox and the Purex chemical separation processes have been used to recover plutonium and uranium from irradiated uranium fuel elements. Due to its favorable geologic and hydrologic characteristics, a large number of high level fission product waste storage areas are also located in this region of the site.

Six areas were surveyed in detail within the 200 Area Plateau. These were the 200-West Area, the 200-East Area, the 200-North Area, the Gable Mountain Pond area, the BC-Crib area and an underground waste transfer line which runs between the 200-East and the 200-West Areas. All the surveys were conducted with the Navy helicopter at an altitude of 45 meters with 45 meter line spacings.

The activity observed in this region can be classified into three general catagories. First is the activity arising from the various handling, decontamination and storage facilities. Second is the activity associated with the solid and liquid waste burial grounds. Third is the low level activity associated with the contaminated cooling water ponds.

Four isotopes were identified in the aerial survey results: ^{60}Co, ^{137}Cs, ^{22}Na, and ^{241}Am, with ^{137}Cs and ^{60}Co being most prevalent. Only ^{137}Cs, however, was processed as an isopleth map. The location of the other isotopes is discussed in the text. All the radiation results are superimposed on photographs of the areas taken during July, 1973.

3.3.1 200-West Area

The 200-West Area, which was surveyed on October 23 and 25, 1973, has been in continuous use since 1944. In addition to the chemical separation plants, six high level fission product waste storage areas are located within this site. Figure 33 gives a map showing the location of the various facilities and storage areas. The radiation results are shown in Figures 34 and 35.

Twenty-seven distinct sources of activity were identified in the aerial survey. These areas, and the isotopes present, are identified as follows: 1) T-plant decontamination facility (^{137}Cs).

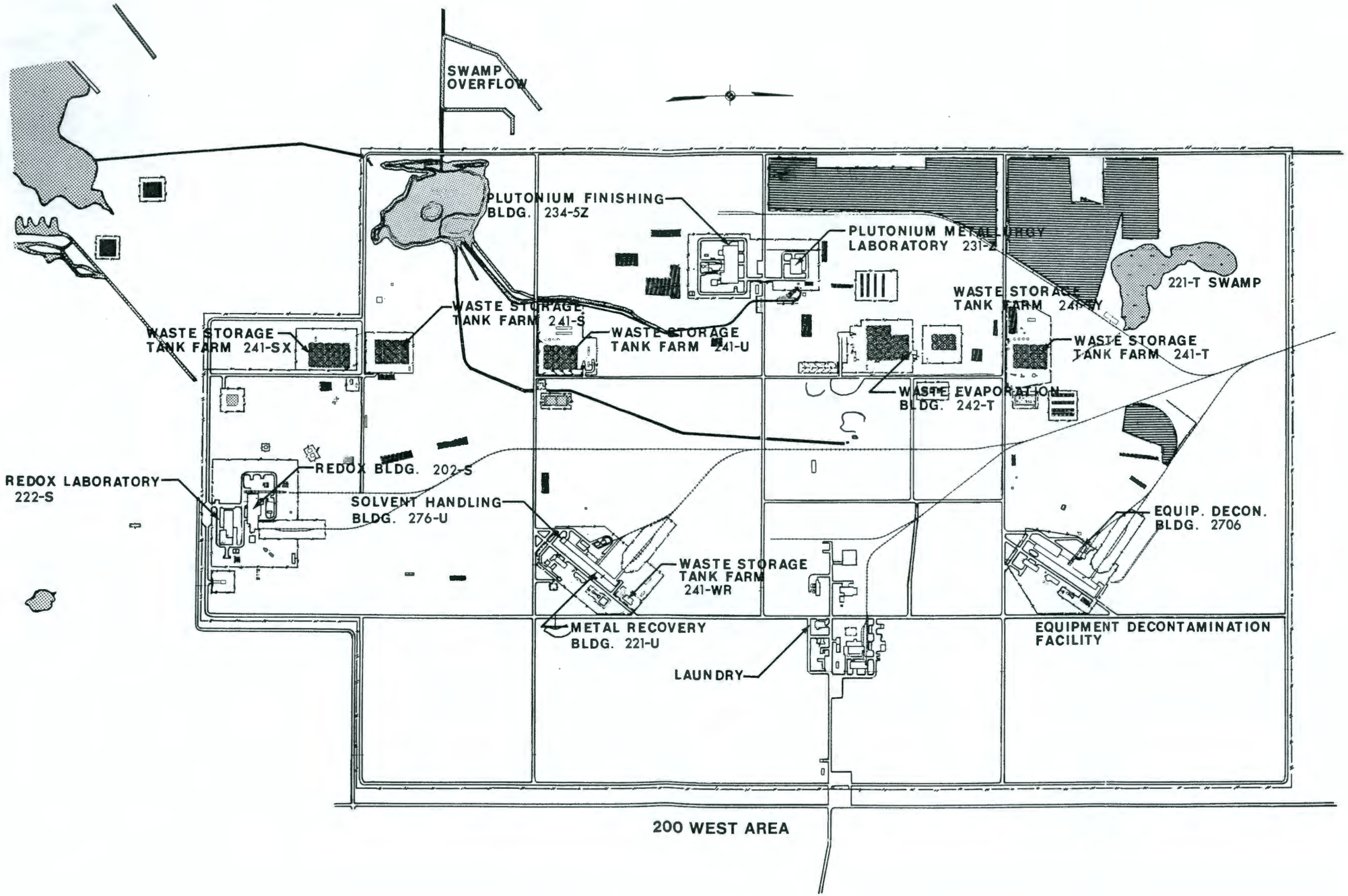

Figure 33. Facility map of the 200-West Area.

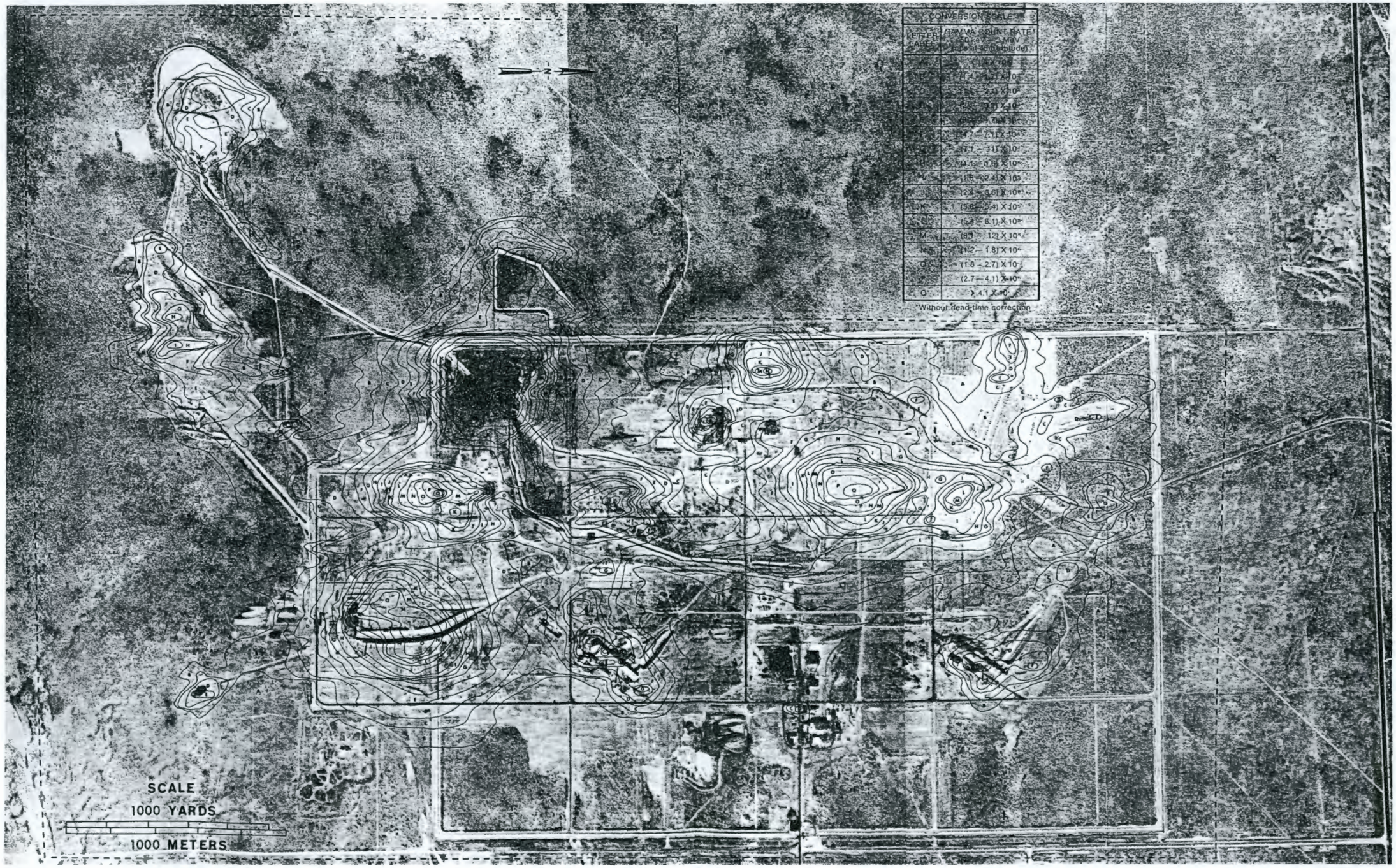

Figure 34. Isopleth map of the total gamma ray count rate between 50 keV and 3 MeV (at 45-meter altitude) obtained during the October 1973 survey over the 200-West Area.

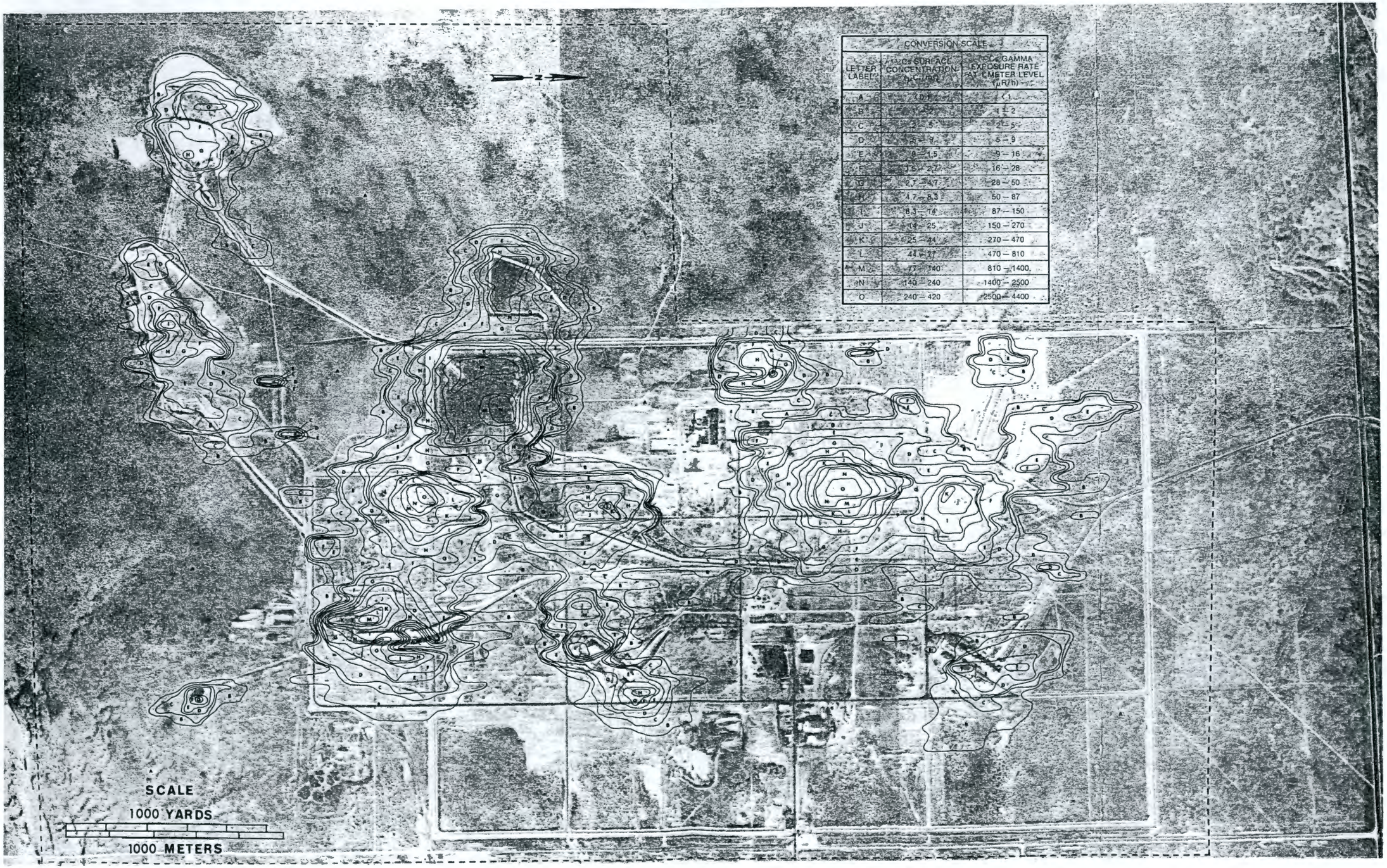

Figure 35. Concentration and gamma exposure rate isopleths for ^{137}Cs derived from the aerial survey data obtained during October 1973 over the 200-West Area. The normal background exposure rate is approximately 10 μR/h in this area.

2) A transient source within the area during the survey (^{137}Cs). 3) Another transient source within the area during the survey (^{60}Co). 4) T-plant cooling water pond (^{137}Cs). 5) Open solid waste burial pit (^{137}Cs). 6) High level fission product waste underground storage facility - "T" (^{137}Cs). 7) Protective clothing laundry (^{60}Co). 8) High level fission product waste evaporator facility (^{137}Cs). 9) Solid waste burial ground (^{137}Cs). 10) Open solid waste burial pit (^{60}Co and ^{137}Cs). 11) Plutonium Metallurgy Laboratory (^{137}Cs). 12) Laundry cooling pond (^{60}Co). 13) Plutonium handling facility (^{241}Am). 14) High level fission product waste underground storage facility - "U" (^{137}Cs). 15) Hallum reactor sodium storage facility (^{22}Na). 16) Intermediate level waste crib overflow (^{137}Cs). 17) U-plant organic treatment facility (^{137}Cs). 18) U-plant plutonium scrap storage facility (^{241}Am). 19) Waste metal recovery organic storage facility (^{137}Cs). 20) Redox plant rail car decontamination facility (^{60}Co). 21) Redox plant waste receiver tanks (^{137}Cs). 22) High level fission product waste underground storage facility - "SX" (^{137}Cs). 23) and 24) Contaminated U-plant cooling water ponds (^{137}Cs). 25) and 26) Contaminated Redox plant cooling water ponds (^{137}Cs). 27) Laboratory cooling water pond (^{137}Cs). The location of each of these areas is shown in Figure 36. Representative spectral plots taken over areas 15, 18, 21 and 24 are shown in Figure 37.

3.3.2 200-East Area

The 200-East Area is the second of two sites near the center of the Hanford Reservation set aside for the location of the chemical separation plants. This site has been in almost continuous use since 1945. Seven high level fission product waste storage areas are also located within the site. Figure 38 shows a map identifying the facilities located within the Area. The results of the aerial survey, conducted on October 26 and 27, 1973, are shown in Figures 39 and 40.

Sixteen sources of gamma radiation were located in the aerial survey. These are identified as follows: 1) Purex plant ventilation filter. 2) High level fission product waste underground storage facility - "A". 3) Intermediate level waste crib overflow. 4) Contaminated B-plant cooling water pond. 5) High level fission product waste underground storage facility - "C". 6) Above ground contaminated equipment storage area. 7) High level fission product waste underground storage facility - "B". 8) In-Tank-Solidification facility for

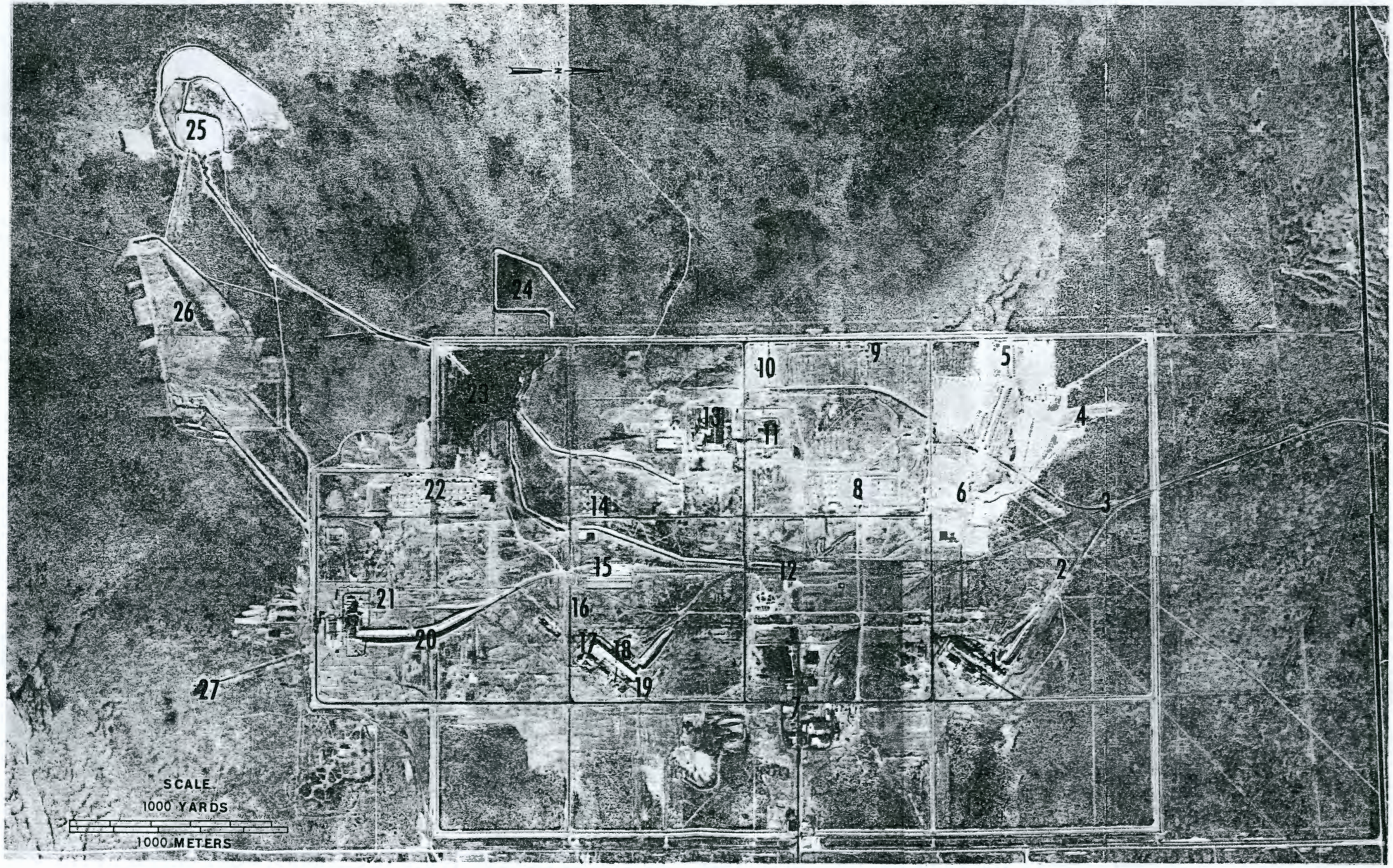

Figure 36. The location of each of the areas discussed in the text where elevated activity was observed during the October 1973 aerial survey over the 200-West Area.

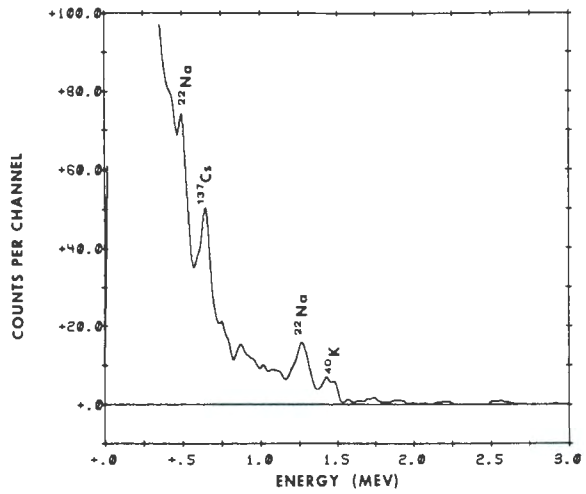

(a) Area 15

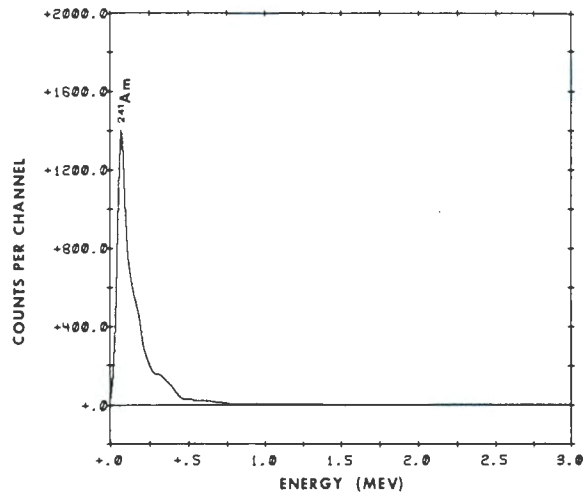

(b) Area 18

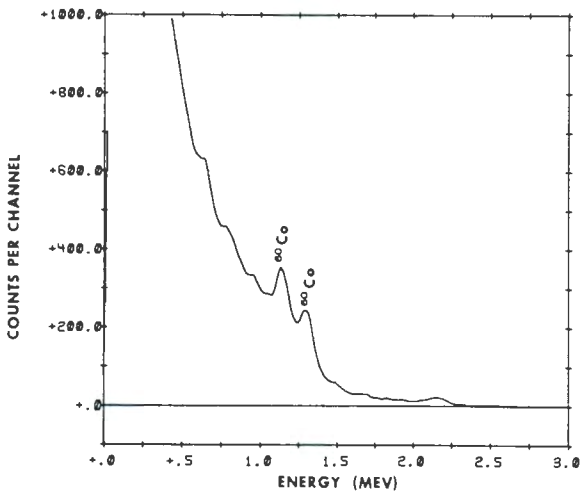

(c) Area 21

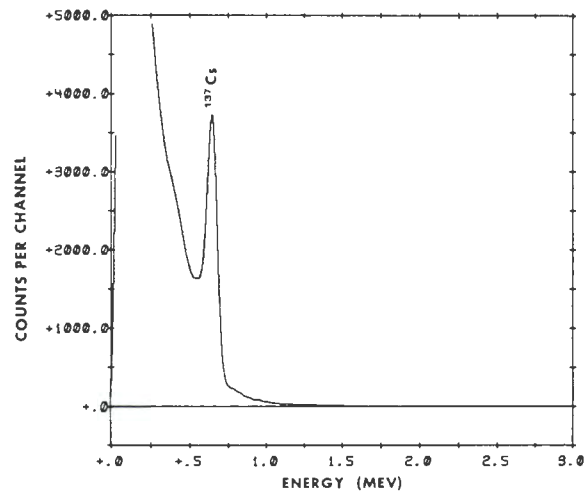

(d) Area 24

Figure 37. Gamma ray spectra obtained over four of the areas of elevated activity observed over the 200-West Area during the October 1973 aerial survey. The physical location of each area is shown in Fig. 36.

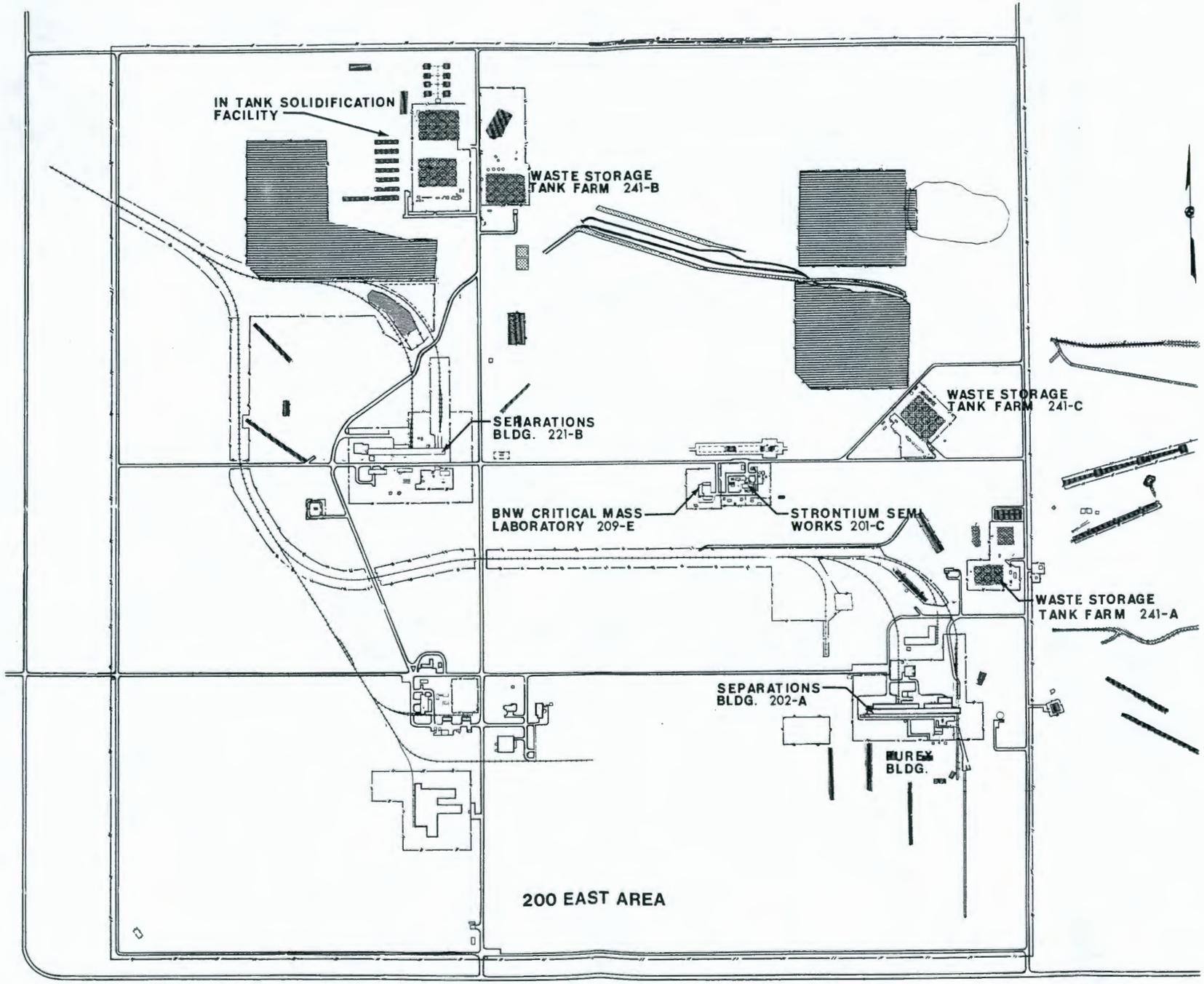

Figure 38. Facility map of the 200-East Area.

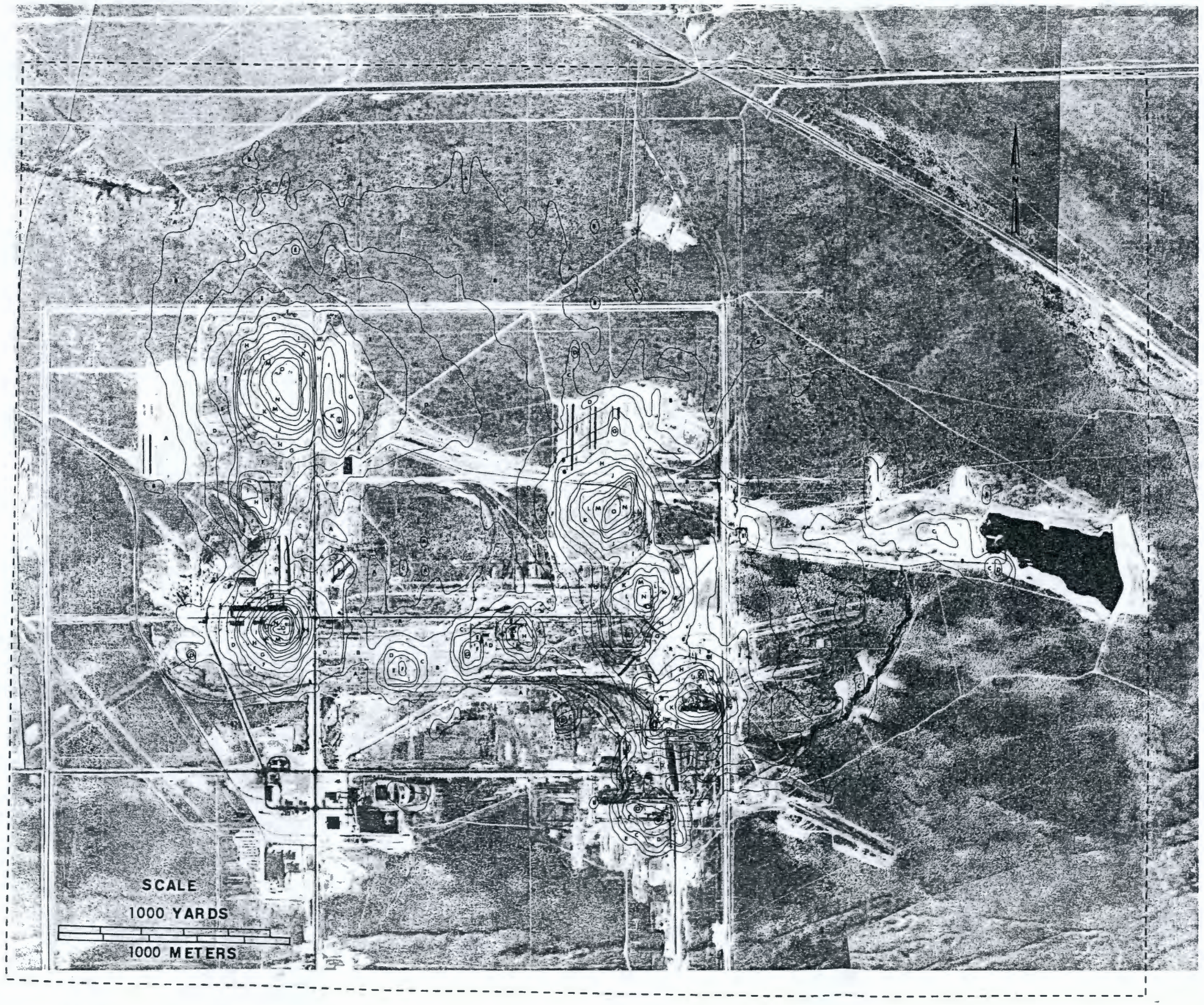

CONVERSION SCALE	
LETTER LABEL	GAMMA COUNT RATE* 50 keV — 3 MeV (cps at 45m altitude)
A	$< 1.4 \times 10^4$
B	$(1.4 - 1.7) \times 10^4$
C	$(1.7 - 2.1) \times 10^4$
D	$(2.1 - 3.2) \times 10^4$
E	$(3.2 - 4.7) \times 10^4$
F	$(4.7 - 7.1) \times 10^4$
G	$(7.1 - 11) \times 10^4$
H	$(1.1 - 1.6) \times 10^5$
I	$(1.6 - 2.4) \times 10^5$
J	$(2.4 - 3.6) \times 10^5$
K	$(3.6 - 5.4) \times 10^5$
L	$(5.4 - 8.1) \times 10^5$
M	$(8.1 - 12) \times 10^5$
N	$(1.2 - 1.8) \times 10^6$
O	$(1.8 - 2.7) \times 10^6$

*Without dead-time correction

Figure 39. Isopleth map of the total gamma ray count rate between 50 keV and 3 MeV (at 45-meter altitude) obtained during the October 1973 survey over the 200-East Area.

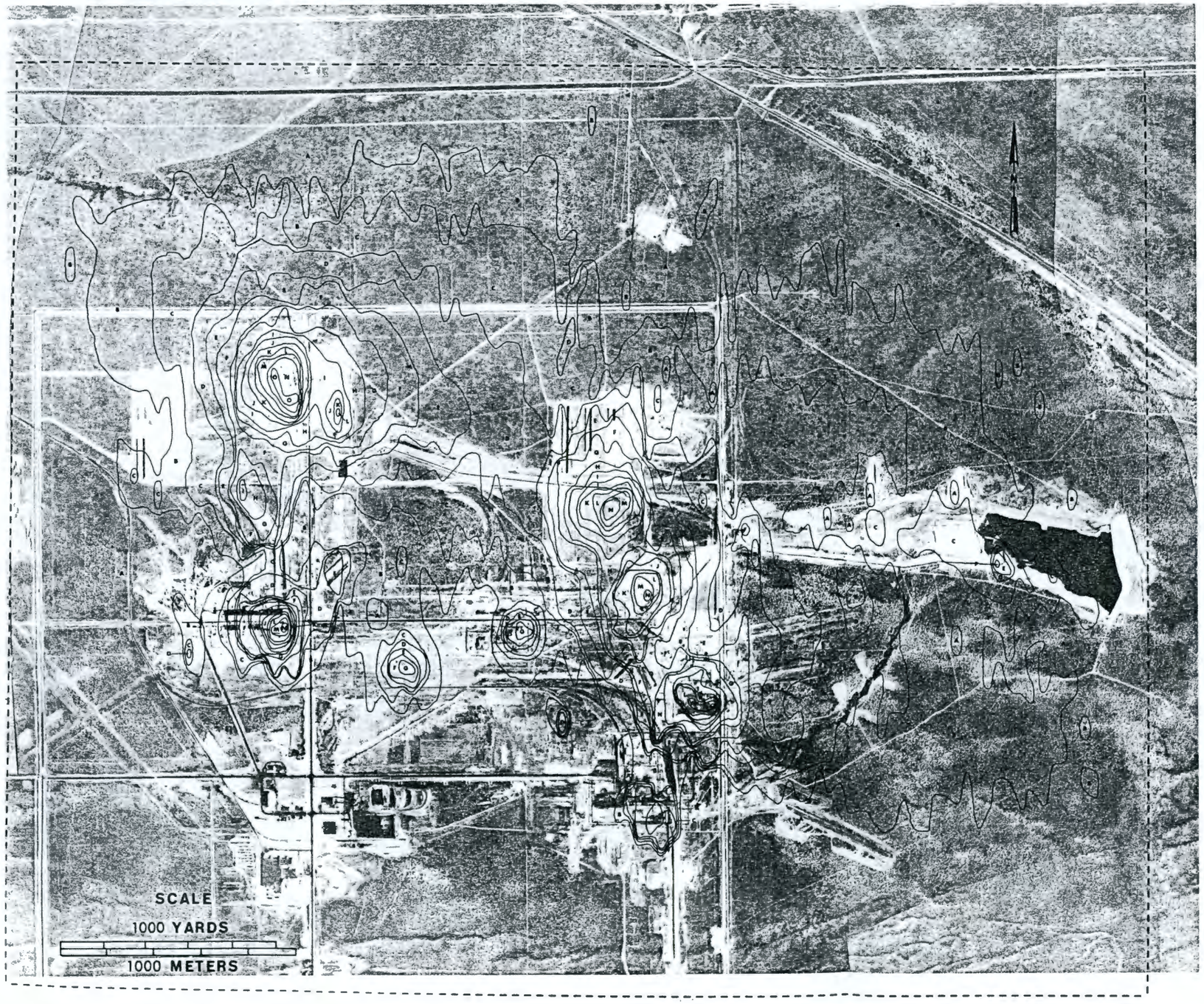

CONVERSION SCALE		
LETTER LABEL	^{137}Cs SURFACE CONCENTRATION ($\mu Ci/m^2$)	^{137}Cs GAMMA EXPOSURE RATE AT 1 METER LEVEL ($\mu R/h$)
A	< 0.1	< 1
B	.1 — .2	1 — 2
C	.2 — .5	2 — 5
D	.5 — .9	5 — 9
E	.9 — 1.5	9 — 16
F	1.5 — 2.7	16 — 28
G	2.7 — 4.7	28 — 50
H	4.7 — 8.3	50 — 87
I	8.3 — 14	87 — 150
J	14 — 25	150 — 270
K	25 — 44	270 — 470
L	44 — 77	470 — 810
M	77 — 140	810 — 1400
N	140 — 240	1400 — 2500
O	240 — 420	2500 — 4400

Figure 40. Concentration and gamma exposure rate isopleths for ^{137}Cs derived from the aerial survey data obtained during October 1973 over the 200-East Area. The normal background exposure rate is approximately 10 $\mu R/h$ in this area.

high level fission product waste. 9) Above ground contaminated equipment storage area. 10) Emergency diversion basin. 11) Open waste line diversion box. 12) B-plant ventilation filters. 13) Excavation exposing waste line. 14) Critical Mass Laboratory. 15) Semi-works ventilation filter. 16) Contaminated equipment storage area. The location of each of these areas is shown in Figure 41.

The ^{137}Cs activity shown in Figure 40 appears to account for all the areas of activity seen in the gross count isopleth map (Figure 39) except for area 14. A spectral plot over this region identified ^{241}Am as the gamma source. An excavation exposing a waste line (area 13) was made after the aerial photographs were taken, but before the radiation survey. This area has now been backfilled with earth.

3.3.3 Waste Transfer Line

A waste transfer pipeline running between the 200-West and 200-East Areas was surveyed on March 29, 1974. As expected, the only activity visible at the surface was a small area of low level ^{137}Cs activity in the vicinity of the pumping station. Figure 42 shows the results of the survey.

3.3.4 Gable Mountain Pond

Gable Mountain Pond is located to the north of the 200-East Area. Accidently contaminated cooling water from the Purex building was transported via an underground pipe line into this area in 1964. The area was originally surveyed in June, 1973. This survey was repeated on March 28, 1974 and extended out to include the West Lake area. The results of the March, 1974 survey are given in Figures 43 and 44.

All the activity observed in the aerial survey was confined to the Gable Mountain Pond area. No evidence of man-made gamma activity could be found in the West Lake area.

3.3.5 BC-Crib Area

The BC-Crib area was surveyed during the initial 45 meter aerial survey requested by ARHCO and conducted between May 22 and June 6, 1973. This is the only one of the eight areas covered during that survey which was not reflown in the later surveys. The area is a radiation controlled area located directly south of the 200-East Area.

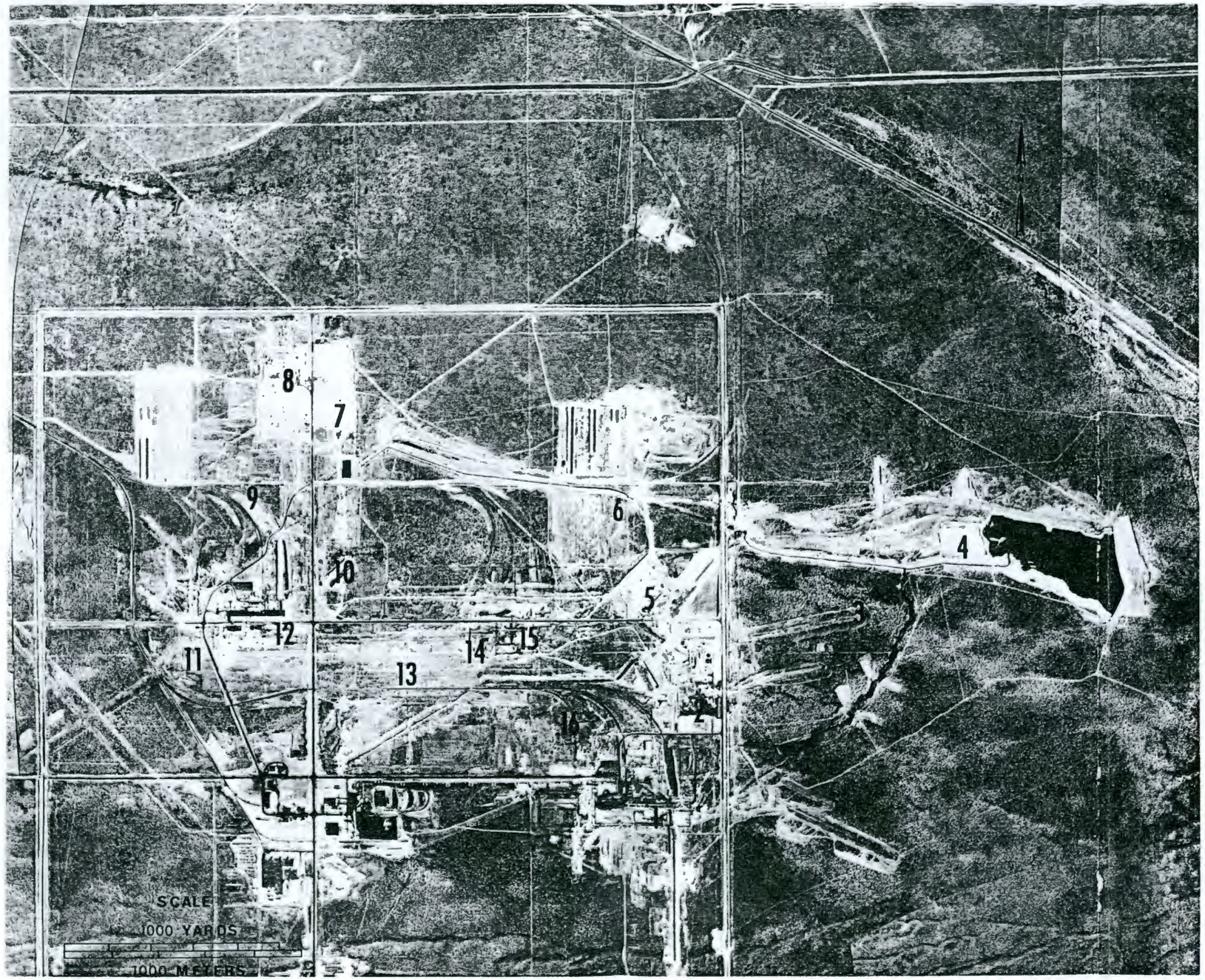

Figure 41. The location of each of the areas discussed in the text where elevated activity was observed during the October 1973 aerial survey over the 200-East Area.

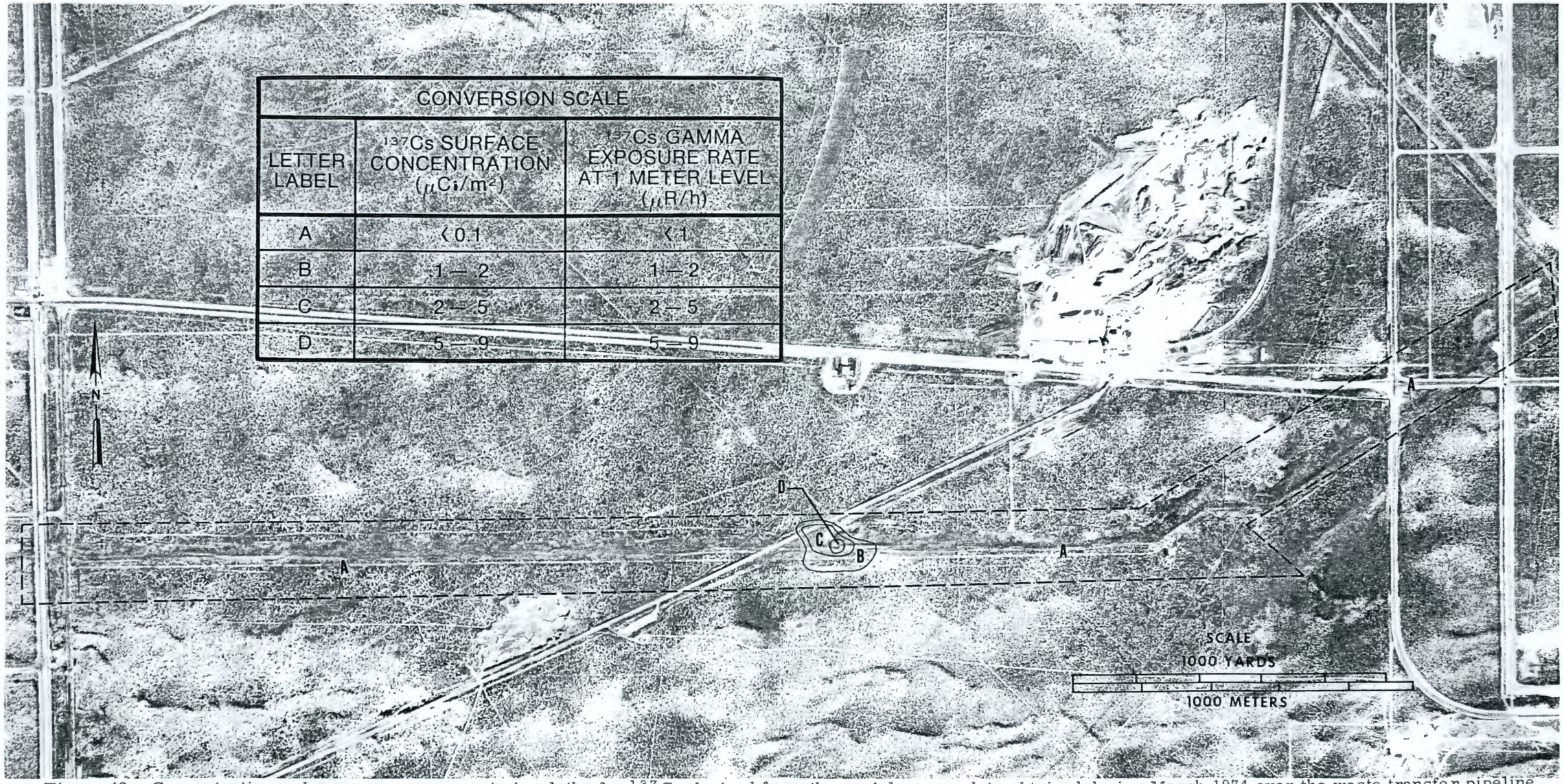

CONVERSION SCALE		
LETTER LABEL	^{137}Cs SURFACE CONCENTRATION ($\mu Ci/m^2$)	^{137}Cs GAMMA EXPOSURE RATE AT 1 METER LEVEL ($\mu R/h$)
A	< 0.1	< 1
B	1 – 2	1 – 2
C	2 – 5	2 – 5
D	5 – 9	5 – 9

Figure 42. Concentration and gamma exposure rate isopleths for ^{137}Cs derived from the aerial survey data obtained during March 1974 over the waste transfer pipeline running between the 200-West and 200-East Areas. The normal background exposure rate is approximately 10 $\mu R/h$ over this area.

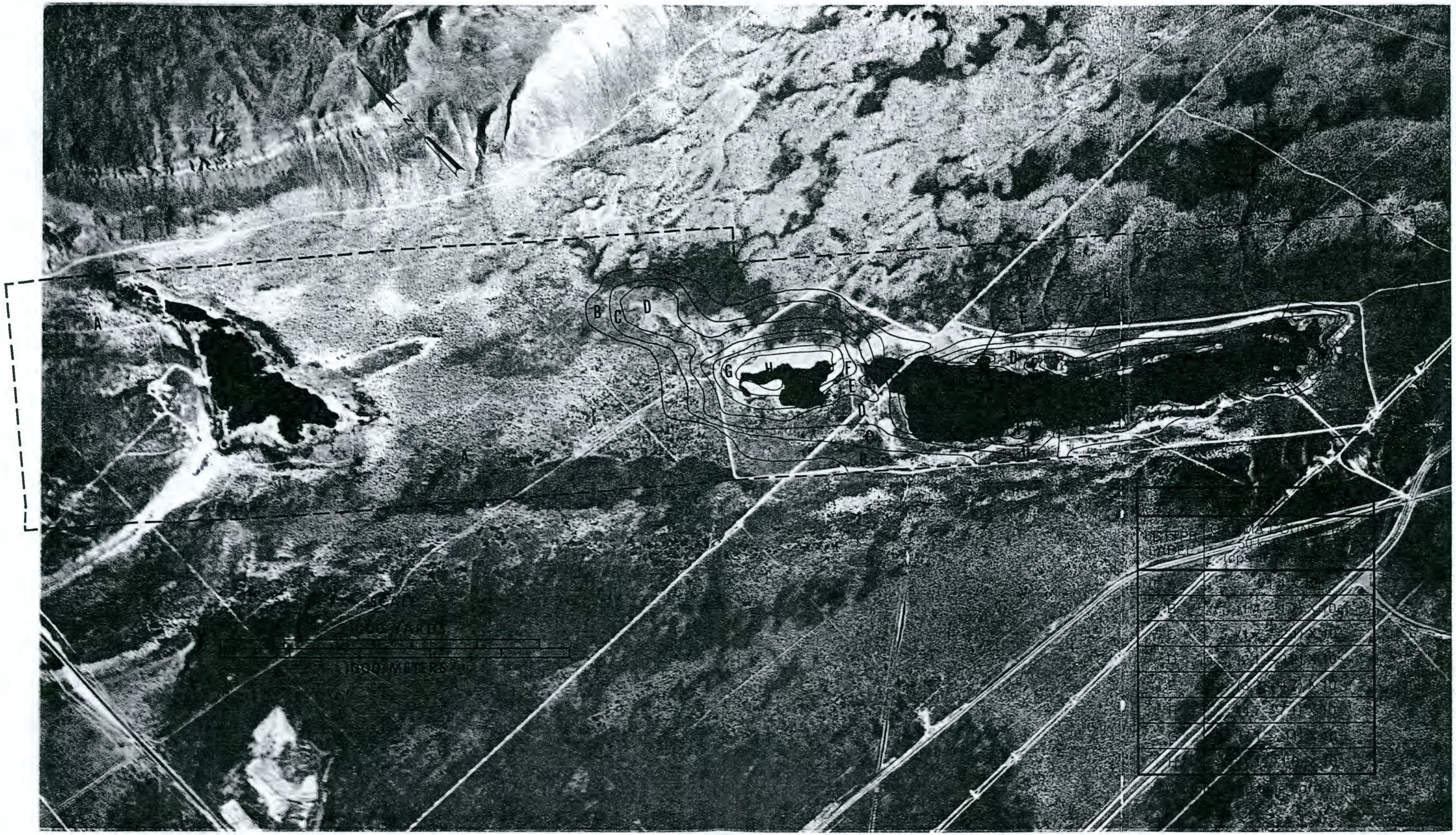

Figure 43. Isopleth map of the total gamma ray count rate between 50 keV and 3 MeV (at 45-meter altitude) obtained during the March 1974 survey over the Gable Mountain Pond Area.

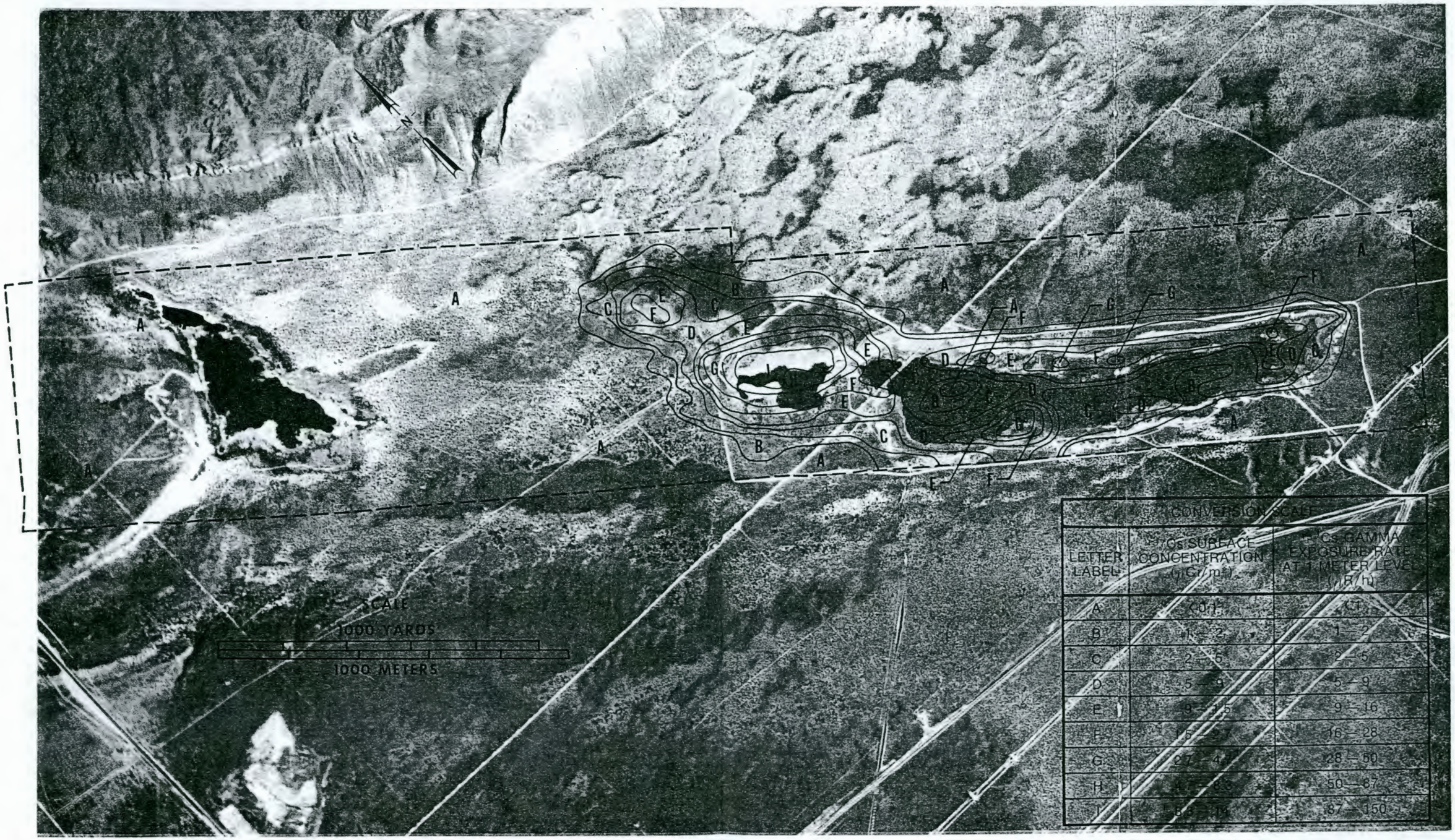

Figure 44. Concentration and gamma exposure rate isopleths for ^{137}Cs derived from the aerial survey data obtained during March 1974 over the Gable Mountain Pond area. The normal background exposure rate is approximately 10 $\mu R/h$ in this area.

In order to minimize the volume of waste resulting from the uranium recovery process, a nickel ferrocyanide process was used to precipitate out the bulk of the ^{90}Sr and ^{137}Cs. The precipitate was stored in the high level waste tanks and the supernate was placed in trenches, about 4 meters deep, located within the BC-Crib area and then covered with 3 meters of soil.

An animal, probably a badger, managed to burrow into the crib area exposing a salt cake. The salt cake was discovered by rabbits, resulting in contamination being spread out over about four square miles from rabbit and coyote (coyotes ate the rabbits) excrement. This contamination was discovered in 1964 and the trenches, initially covered with earth, were covered over with gravel and asphalt to prevent further subsurface entry by animals.

An extensive number of ground measurements and laboratory soil sample analyses have been made in this area. The results of these measurements and the aerial survey results (shown in Figures 45 and 46) are discussed in detail in reference 5. Based on the aerial survey results and laboratory analyses, a total ^{137}Cs activity of 14.5 curies was found within the contaminated area. The bulk of this activity lies within 10 cm of the surface.

Excellent correlation was obtained between the aerial survey results and the ground measurements. In one of the higher areas of concentration six composite samples were taken of the surface (top 5 cm), ranging from 10 to 100 individual samples per composite. An average of this composite sampling indicated an activity of 11.5 $\mu Ci/m^2$ compared with 10 $\mu Ci/m^2$ obtained from the aerial survey.

A privately - owned radioactive waste burial site is located in the northwest corner of the area surveyed. The activity observed in Figure 45 over this site is due to ^{60}Co.

3.3.6 200-North Area

The 200-North Area lies to the northeast of the 200-West Area. Several storage facilities were located within this site. The aerial survey, conducted on March 28, 1974, did not detect the presence of any man-made activity within this Area.

3.4 Burial Grounds

Two small burial grounds, 318-11 and 318-10, were surveyed on October 22, 1973 at an altitude of 45 meters. The 318-11

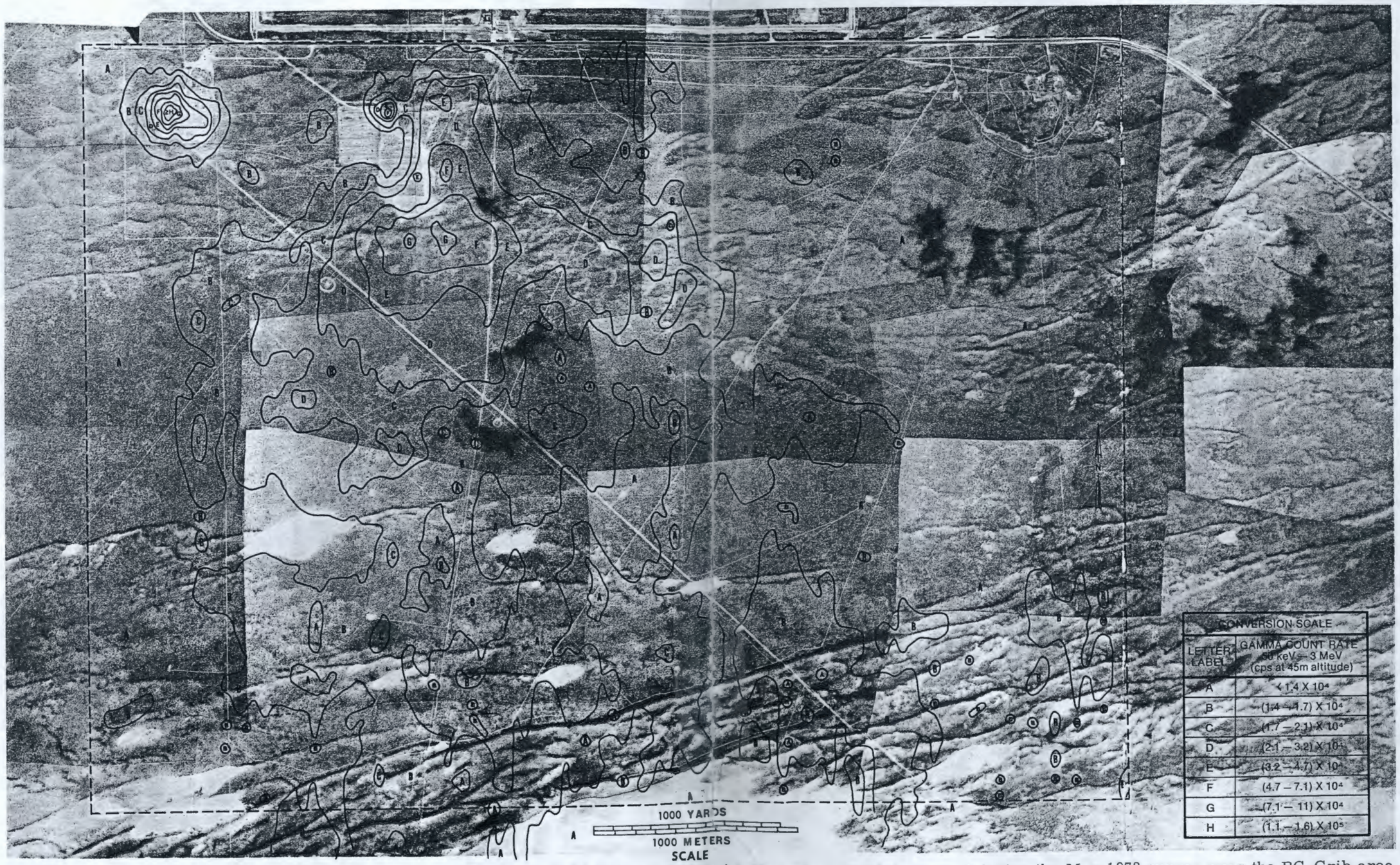

Figure 45. Isopleth map of the total gamma ray count rate between 50 keV and 3 MeV (at 45-meter altitude) obtained during the May 1973 survey over the BC-Crib area.

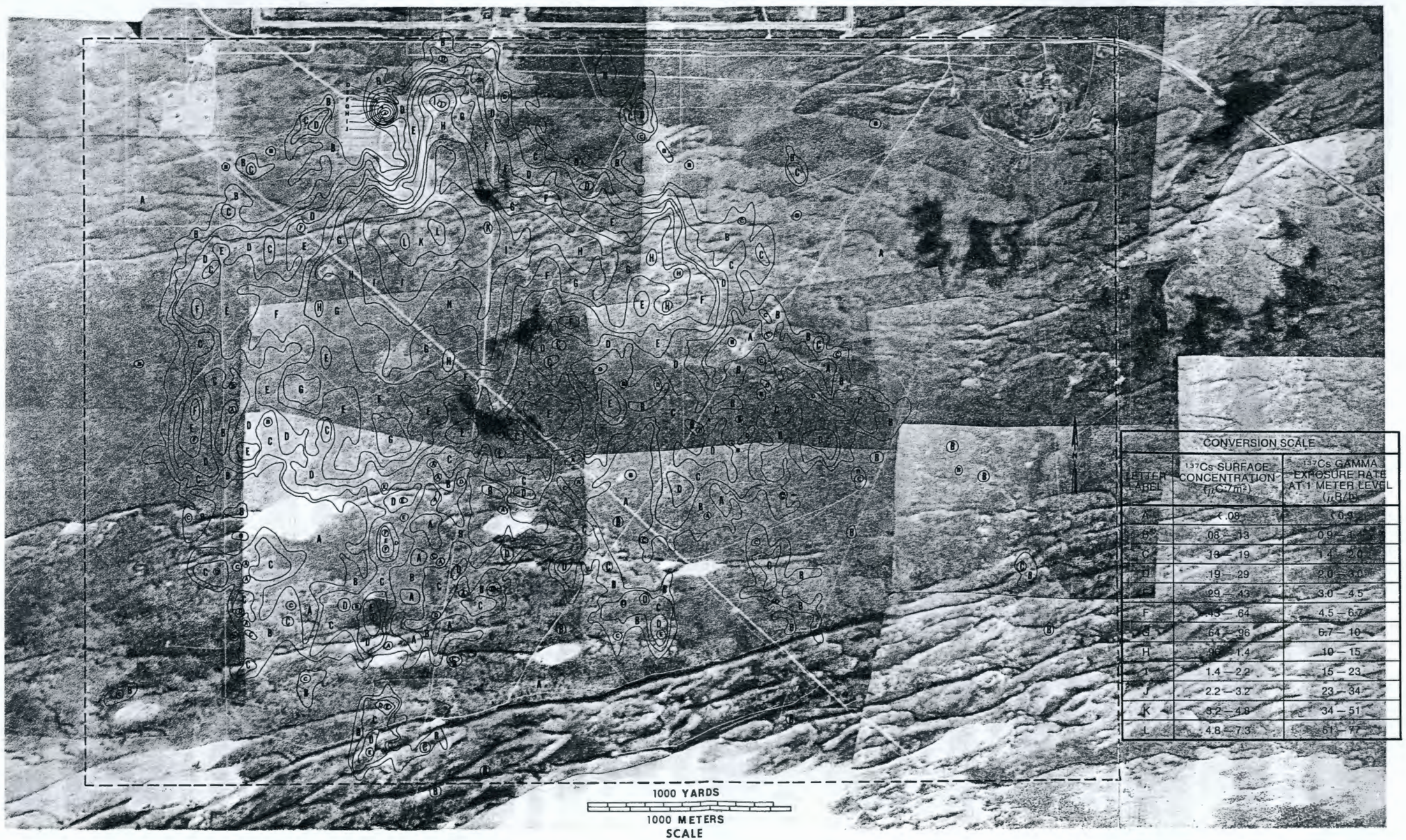

CONVERSION SCALE		
LETTER LABEL	^{137}Cs SURFACE CONCENTRATION (μC/m^2)	^{137}Cs GAMMA EXPOSURE RATE AT 1 METER LEVEL (μR/h)
A	< .08	< 0.9
B	.08 – .13	0.9 – 1.4
C	.13 – .19	1.4 – 2.0
D	.19 – .29	2.0 – 3.0
E	.29 – .43	3.0 – 4.5
F	.43 – .64	4.5 – 6.7
G	.64 – .96	6.7 – 10
H	.96 – 1.4	10 – 15
I	1.4 – 2.2	15 – 23
J	2.2 – 3.2	23 – 34
K	3.2 – 4.8	34 – 51
L	4.8 – 7.3	51 – 77

Figure 46. Concentration and gamma exposure rate isopleths for ^{137}Cs derived from the aerial survey data obtained during May 1973 over the BC-Crib area. The normal background exposure rate is approximately 10 μR/h in this area.

burial ground is located approximately 3.5 kilometers southeast of the wye barricade and the 318-10 burial ground is located approximately 4 kilometers north of the 300 Area (see Figure 1). No evidence of any man-made gamma ray activity could be detected during the aerial survey over either of these areas.

3.5 300 Area

The 300 Area is located in the extreme southeast corner of the Hanford reservation, just north of the Richland city limits. A variety of activities are carried on in this area. These include uranium reactor fuel manufacturing, radiochemical and radiometallurgical laboratories, laboratories and test facilities in support of plutonium reactor fuels development, liquid metal technology and fast flux test reactor support. A large life sciences laboratory occupies the extreme southeast corner. Some facilities are no longer used for their original purpose, such as the retired Plutonium Recycle Test Reactor (309 Building). Two large leaching ponds for process waste water are located in the northeast corner of the area. A map of the area is given in Figure 47.

Portions of the area were surveyed in October, 1973 and in April, 1974. The mid section of the area, where a number of small laboratories are located, was not surveyed as a safety precaution. The radiation results for both surveys were combined and are given in Figures 48 and 49.

Three isotopes (^{60}Co, ^{137}Cs and ^{234m}Pa) were identified within this area. ^{234m}Pa is a daughter of ^{238}U and was observed in areas where large amounts of depleted uranium were stored. In particular, ^{234m}Pa was identified along the eastern edge of the North Process Pond, over the 313 Building and in the vicinity of the 311 Building. ^{60}Co, due to an accumulation from low level releases over many years, was found in the South Process Pond. A large ^{60}Co source, stored under water, is located in the 3730 Building. Gamma rays from this source, emitted through test channels in the gamma pit, were observed. Both ^{60}Co and ^{137}Cs were identified in the above ground liquid waste handling facilities located near the 309 Building and at the 340 facility.

3.6 Columbia River Survey

A detailed survey was conducted along the shore line and over the slough areas and islands of the Columbia River between March 26 and April 8, 1974. The survey covered an area from

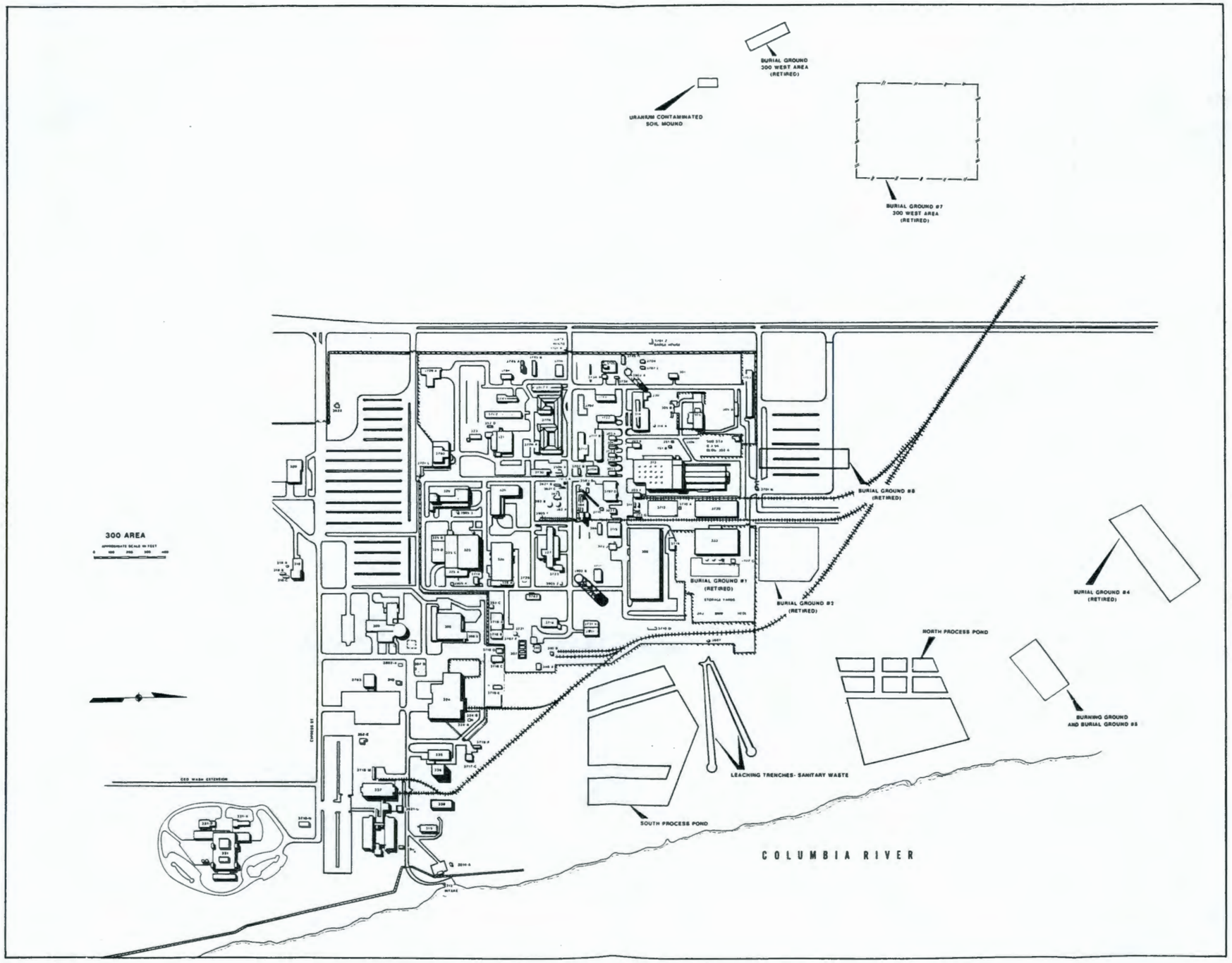

Figure 47. Facility map of the 300 Area.

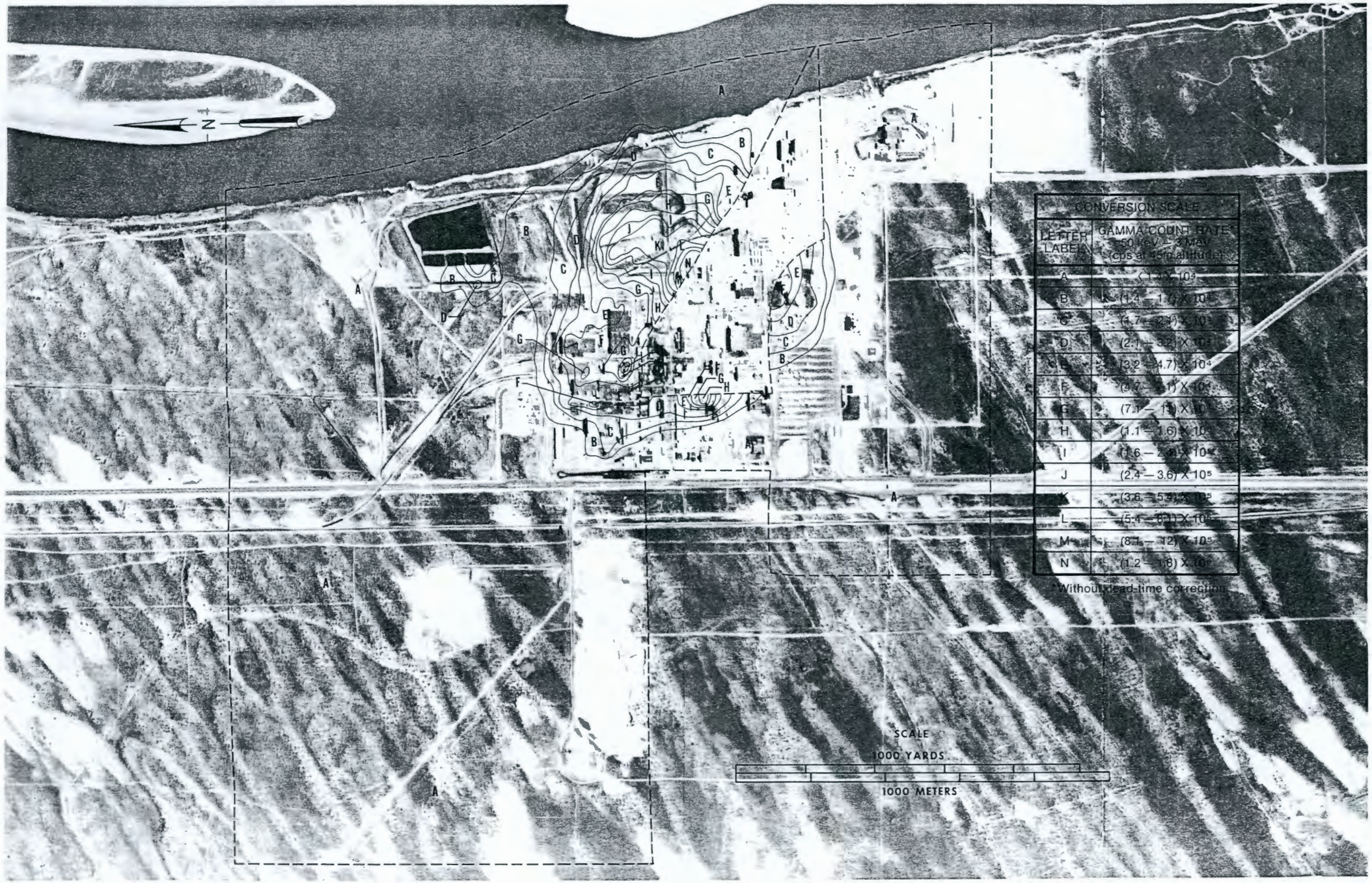

Figure 48. Isopleth map of the total gamma ray count rate between 50 keV and 3 MeV (at 45-meter altitude) obtained during the October 1973 and April 1974 surveys over the 300 Area.

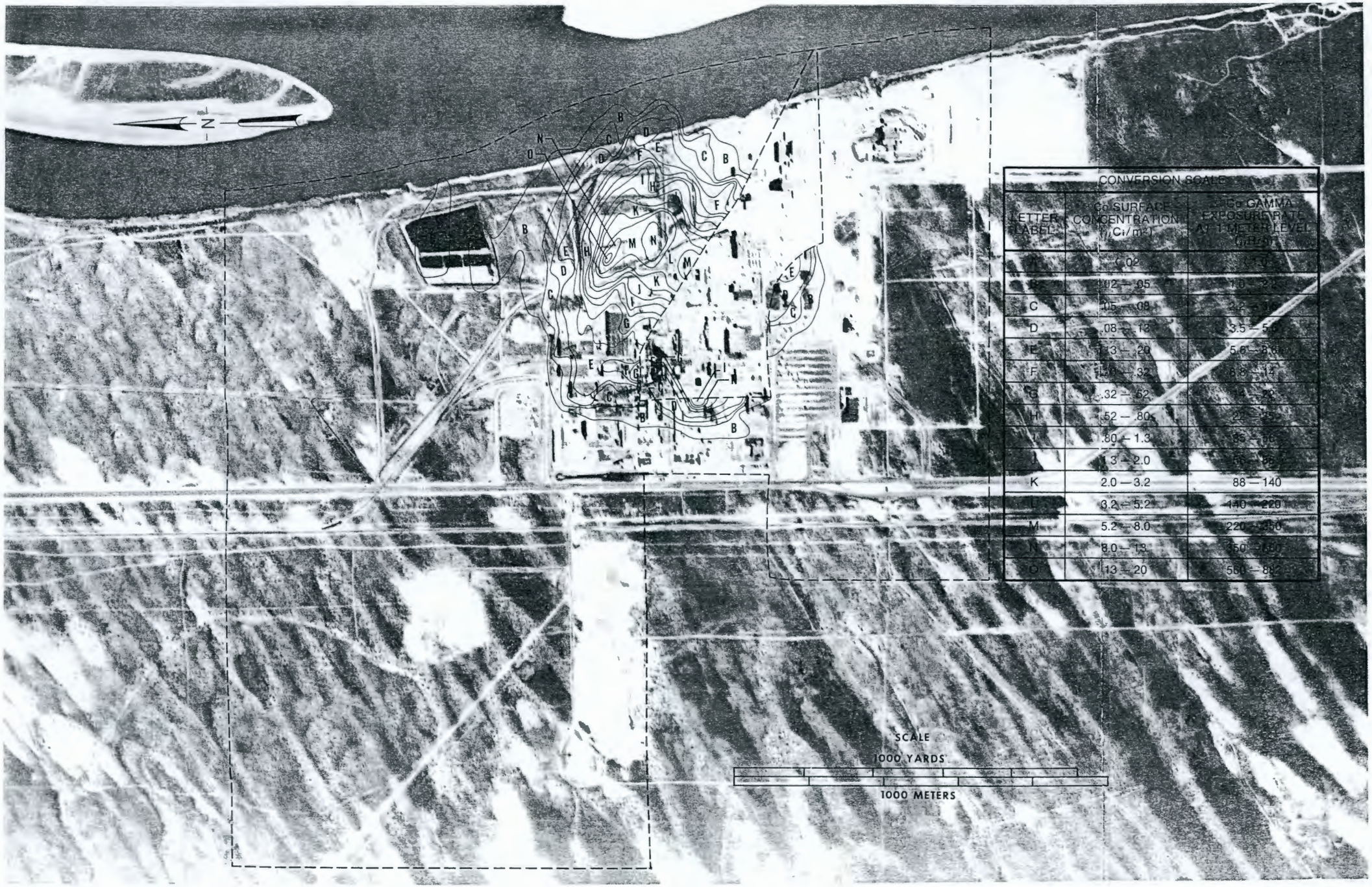

CONVERSION SCALE

LETTER LABEL	^{60}Co SURFACE CONCENTRATION (μCi/m²)	^{60}Co GAMMA EXPOSURE RATE AT 1 METER LEVEL (μR/h)
A	< .02	< 1.0
B	.02 — .05	1.0 — 2.2
C	.05 — .08	2.2 — 3.5
D	.08 — .13	3.5 — 5.6
E	.13 — .20	5.6 — 8.8
F	.20 — .32	8.8 — 14
G	.32 — .52	14 — 22
H	.52 — .80	22 — 35
I	.80 — 1.3	35 — 56
J	1.3 — 2.0	56 — 88
K	2.0 — 3.2	88 — 140
L	3.2 — 5.2	140 — 220
M	5.2 — 8.0	220 — 350
N	8.0 — 13	350 — 560
O	13 — 20	560 — 882

Figure 49. Concentration and gamma exposure rate isopleths for ^{60}Co derived from the aerial survey data obtained during October 1973 and April 1974 over the 300 Area. The normal background exposure rate is approximately 10 μR/h in this area.

approximately four kilometers above the Vernita Bridge to approximately 10 kilometers below the intersection of the Snake River with the Columbia River. An additional 20 kilometers downstream from McNary Dam was also surveyed. The total area covered was arbitrarily divided into twelve sections, each of which were surveyed separately.

The survey was conducted at an altitude of 45 meters using the Navy helicopter. A minimum of three lines, spaced roughly 60 meters apart, were flown along each bank of the river, starting at the shoreline and moving inland. Additional lines were flown inland if any man-made activity was still visible on the third line. Straight lines, spaced approximately 60 meters apart, were flown over the slough areas and the river islands. All these lines were flown with the aid of aerial photographs taken just prior to the radiation survey.

A photo mosaic of the river, identifying each of the twelve sections surveyed, is given in Figure 50. The radiation results are shown in Figures 51 to 64. Because of the presence of water, which caused large fluctuations in the natural terrestrial background count rate, the gross count information was not very useful for this particular survey. For this reason, only the ^{60}Co isopleth maps are shown. In two of the regions surveyed ^{137}Cs could also be observed. These results are also shown.

The highest activity observed within the site boundary occurred along the slough area between the 100-H and 100-D Areas and along the slough area just north of the old Hanford townsite. Both ^{60}Co and ^{137}Cs were observed in these areas. Radiation levels up to 14 $\mu R/h$ from ^{60}Co and 3 $\mu R/h$ from ^{137}Cs were seen in the slough area between 100-H and 100-D. Levels up to 22 $\mu R/h$ from ^{60}Co and 1 $\mu R/h$ from ^{137}Cs were seen in the other slough area. The highest radiation levels observed in areas accessible to the public occurred on the islands between the old Hanford townsite and Pasco, where a maximum reading in the range of 9 to 14 $\mu R/h$ due to ^{60}Co was obtained. No ^{137}Cs activity could be seen in these areas. (The average background exposure rate around the Hanford reservation is approximately 10 $\mu R/h$.)

The activity seen along the Columbia River is the result of a long term build-up from the low level activity released into the river during past reactor operations. Since the shut down of the single-pass reactors between 1965 and 1971, the activity observed along the river has significantly decreased [6]. Soil sample measurements taken along the river by Battelle Northwest (the Environmental Monitoring

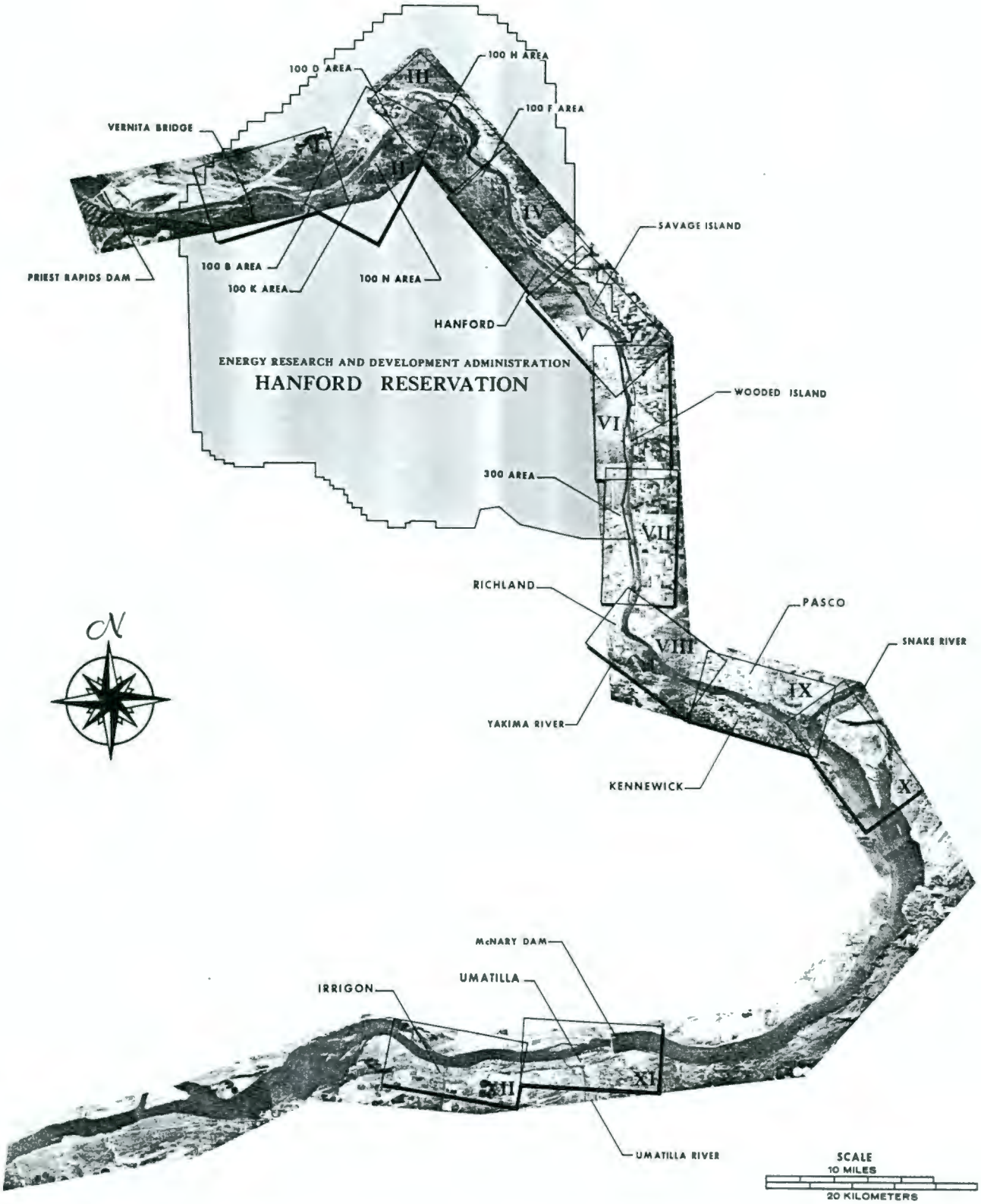

Figure 50. A photo mosaic of the Columbia River showing the twelve areas surveyed during March and April 1974.

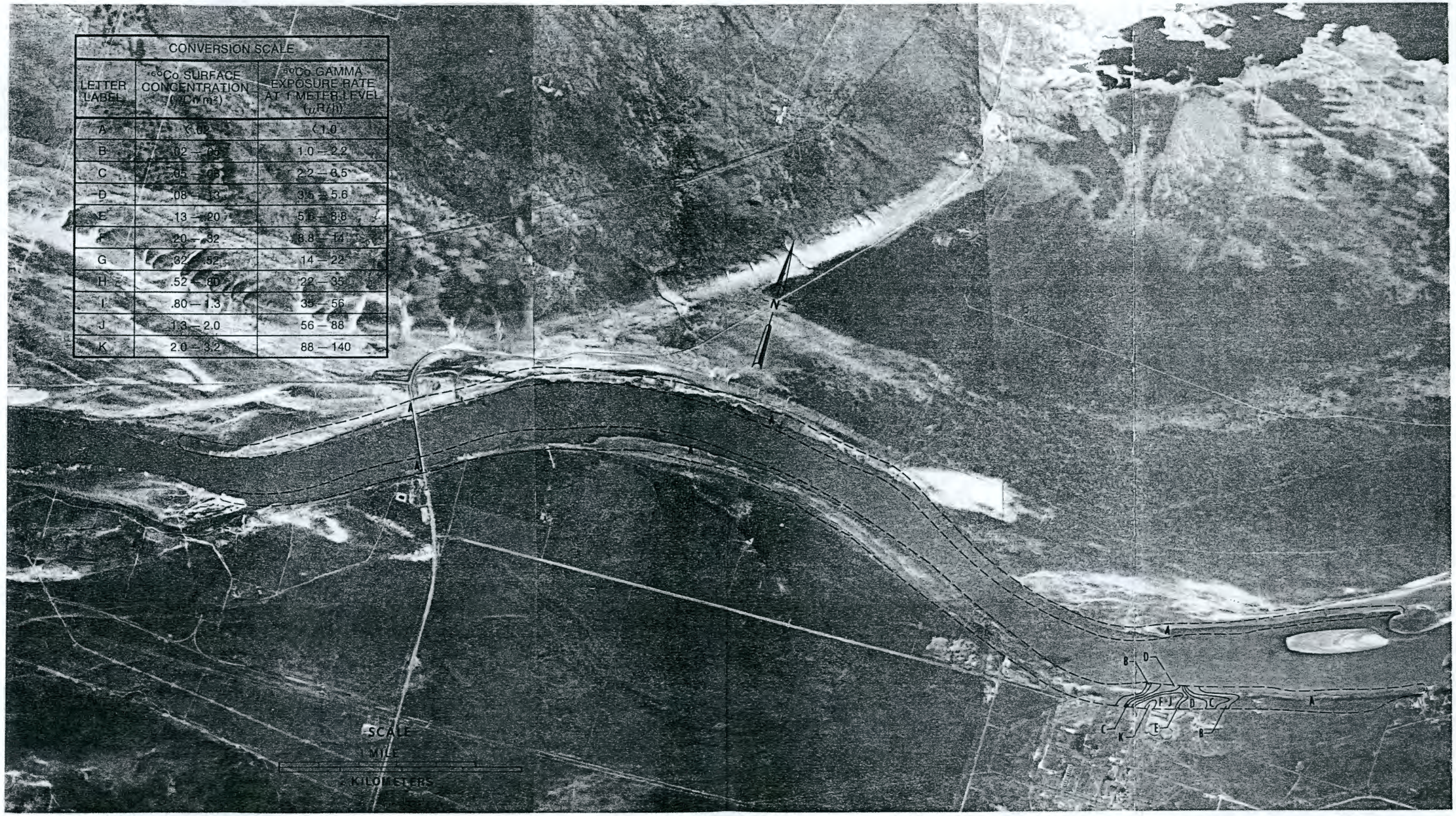

CONVERSION SCALE		
LETTER LABEL	^{60}Co SURFACE CONCENTRATION (μCi/m²)	^{60}Co GAMMA EXPOSURE RATE AT 1 METER LEVEL (μR/h)
A	< .02	< 1.0
B	.02 — .05	1.0 — 2.2
C	.05 — .08	2.2 — 3.5
D	.08 — .13	3.5 — 5.6
E	.13 — .20	5.6 — 8.8
F	.20 — .32	8.8 — 14
G	.32 — .52	14 — 22
H	.52 — .80	22 — 35
I	.80 — 1.3	35 — 56
J	1.3 — 2.0	56 — 88
K	2.0 — 3.2	88 — 140

Figure 51. Concentration and gamma exposure rate isopleths for ^{60}Co derived from the aerial survey data obtained during March and April 1974 along the Columbia River between the Vernita Bridge and the 100-B Area. The normal background exposure rate is approximately 10 μR/h in this area.

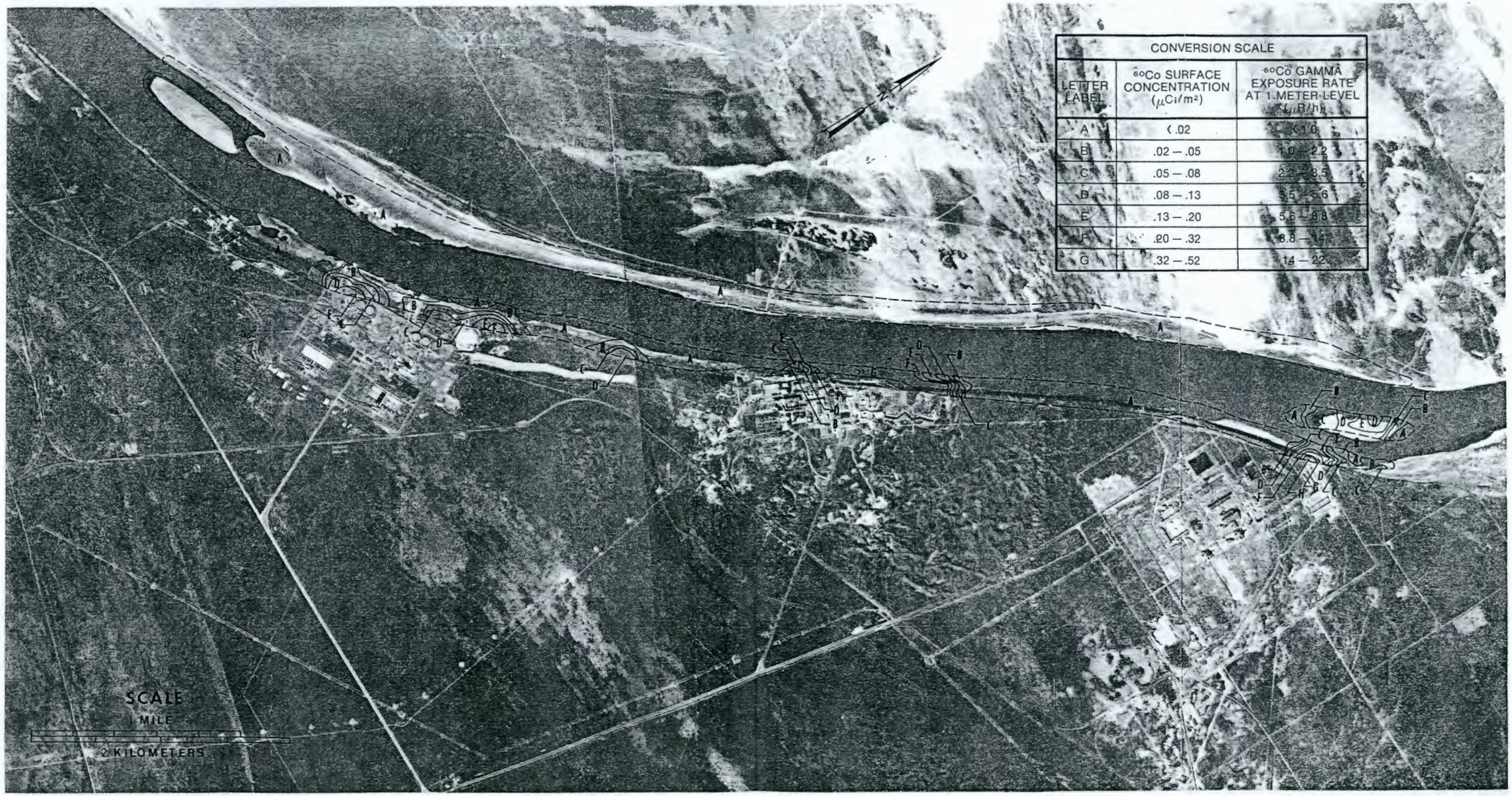

Figure 52. Concentration and gamma exposure rate isopleths for ^{60}Co derived from the aerial survey data obtained during March and April 1974 along the Columbia River between the 100-B and 100-D reactor areas. The normal background exposure rate is approximately 10 $\mu R/h$ in this area.

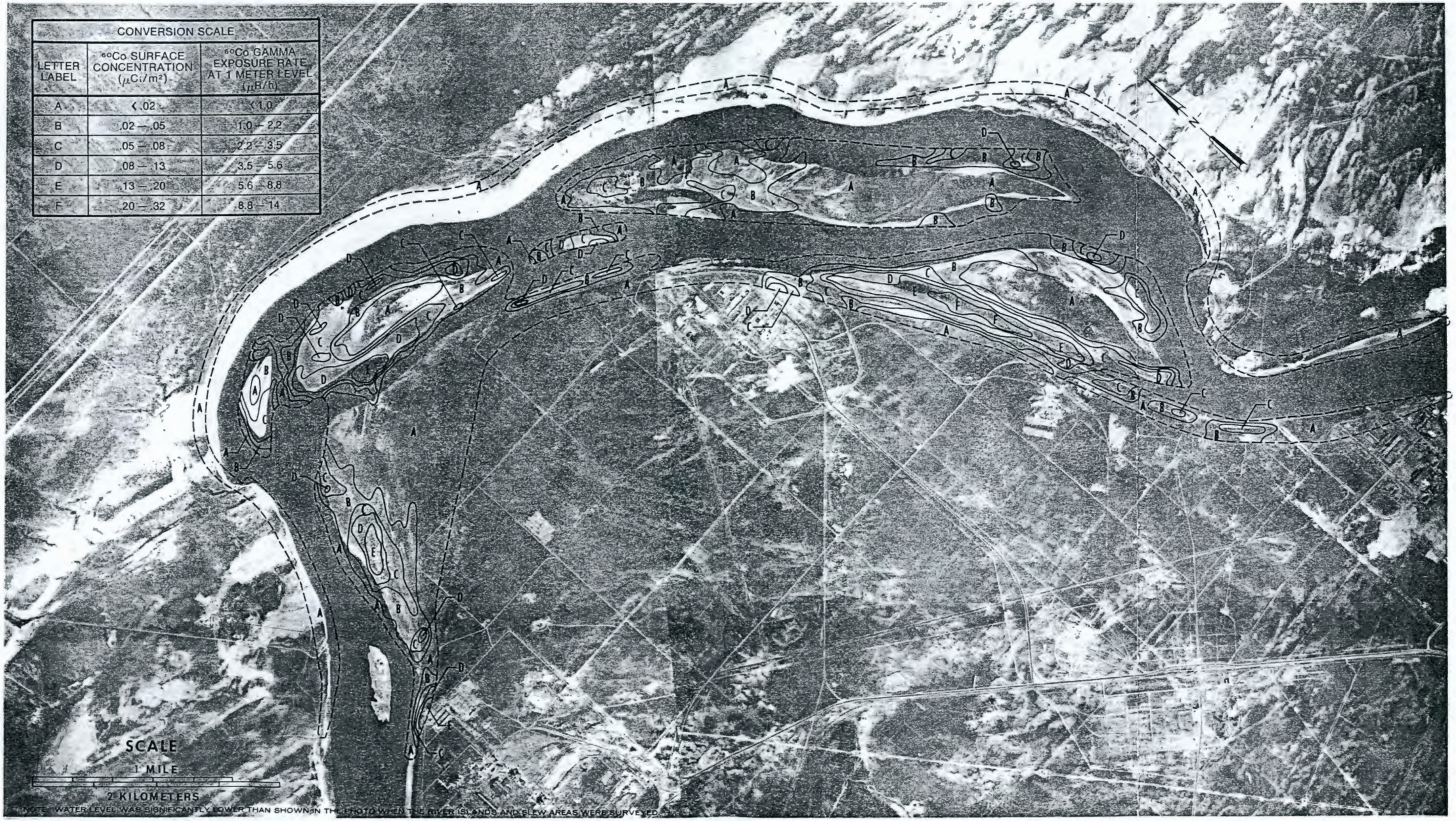

Figure 53. Concentration and gamma exposure rate isopleths for ^{60}Co derived from the aerial survey data obtained during March and April 1974 along the Columbia River between the 100-D and 100-F reactor areas. The normal background exposure rate is approximately 10 μR/h in this area.

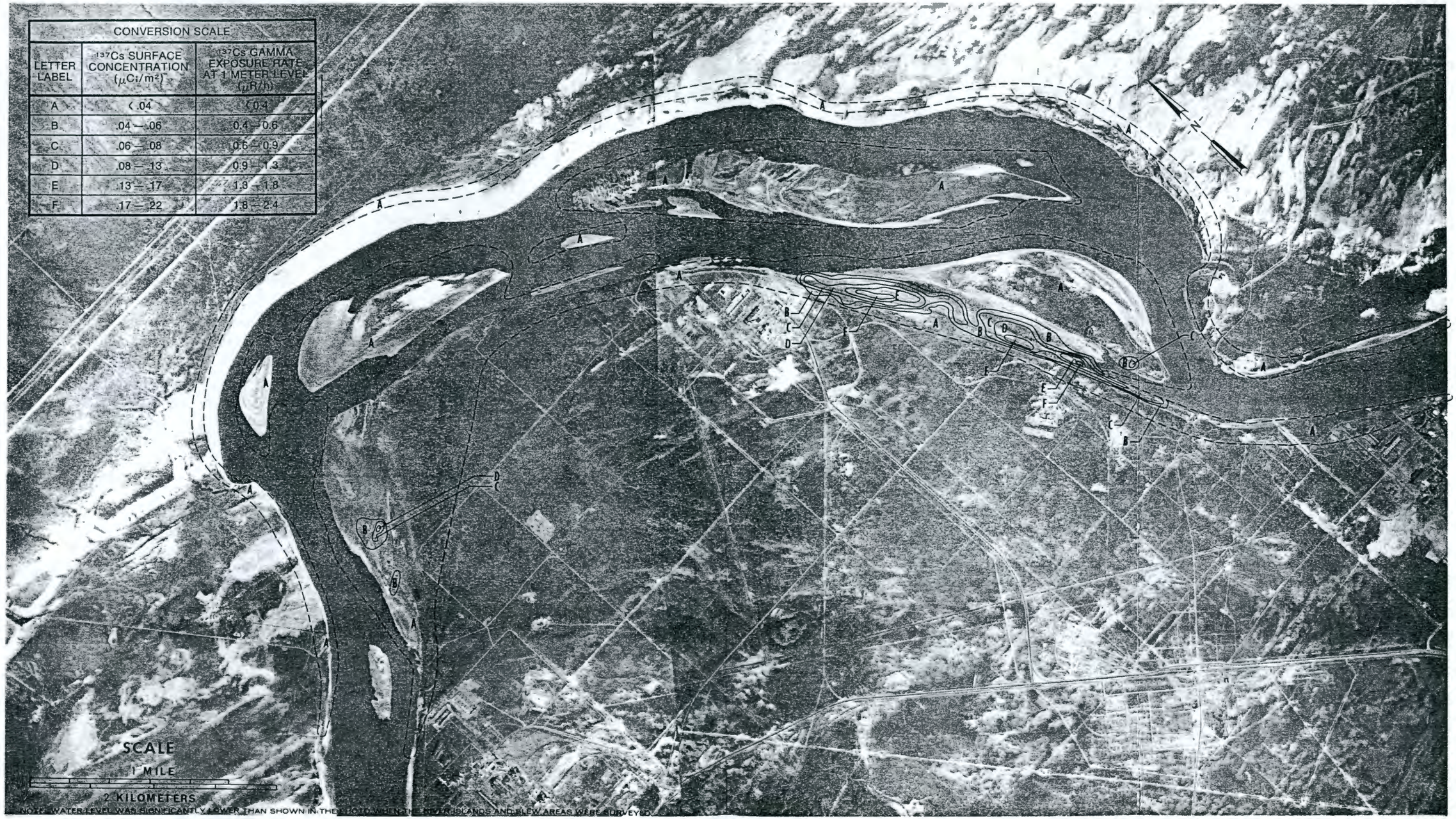

Figure 54. Concentration and gamma exposure rate isopleths for ^{137}Cs derived from the aerial survey data obtained during March and April 1974 along the Columbia River between the 100-D and 100-F reactor areas. The normal background exposure rate is approximately 10 μR/h in this area.

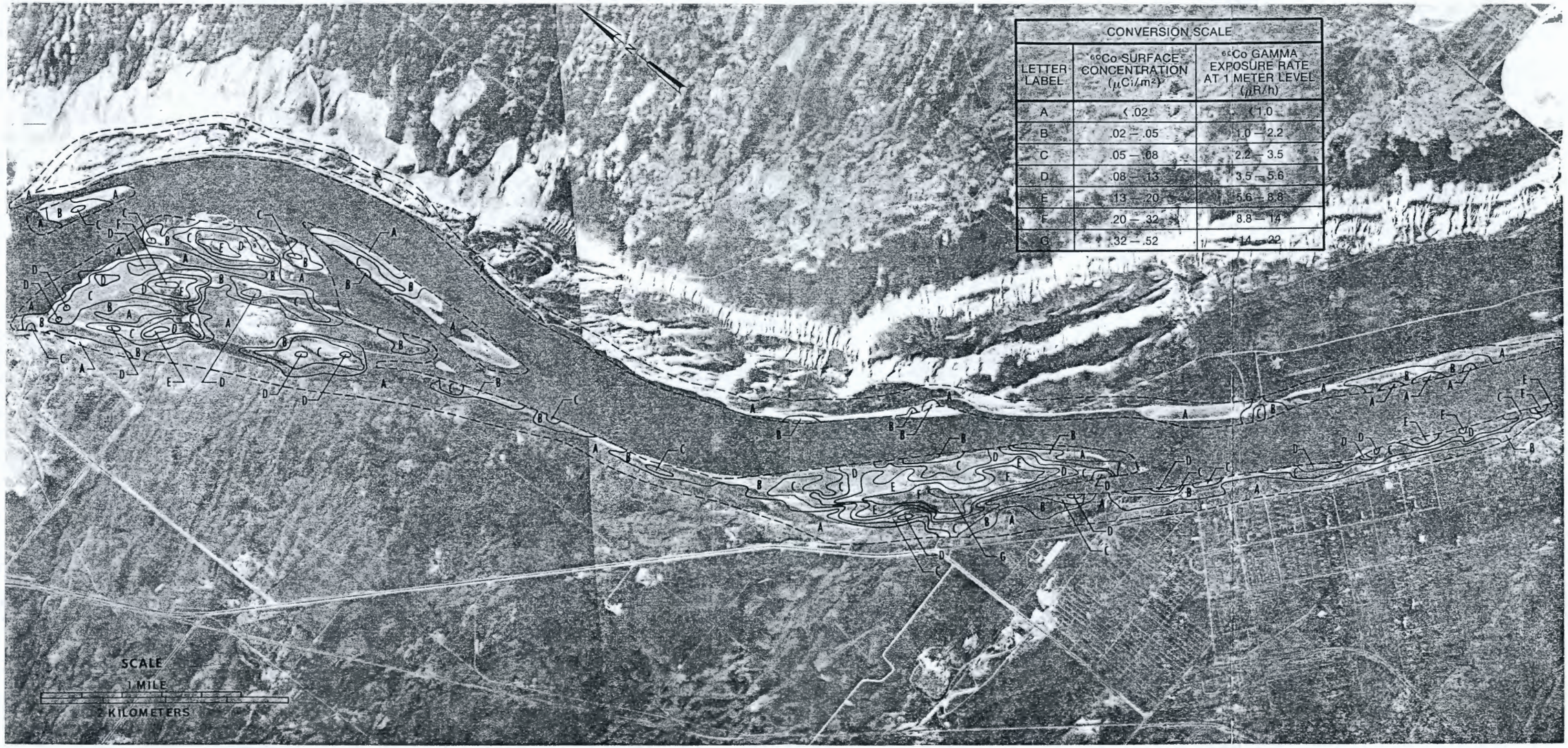

Figure 55. Concentration and gamma exposure rate isopleths for ^{60}Co derived from the aerial survey data obtained during March and April 1974 along the Columbia River from the 100-F reactor area to the old Hanford townsite. The normal background exposure rate is approximately 10 μR/h in this area.

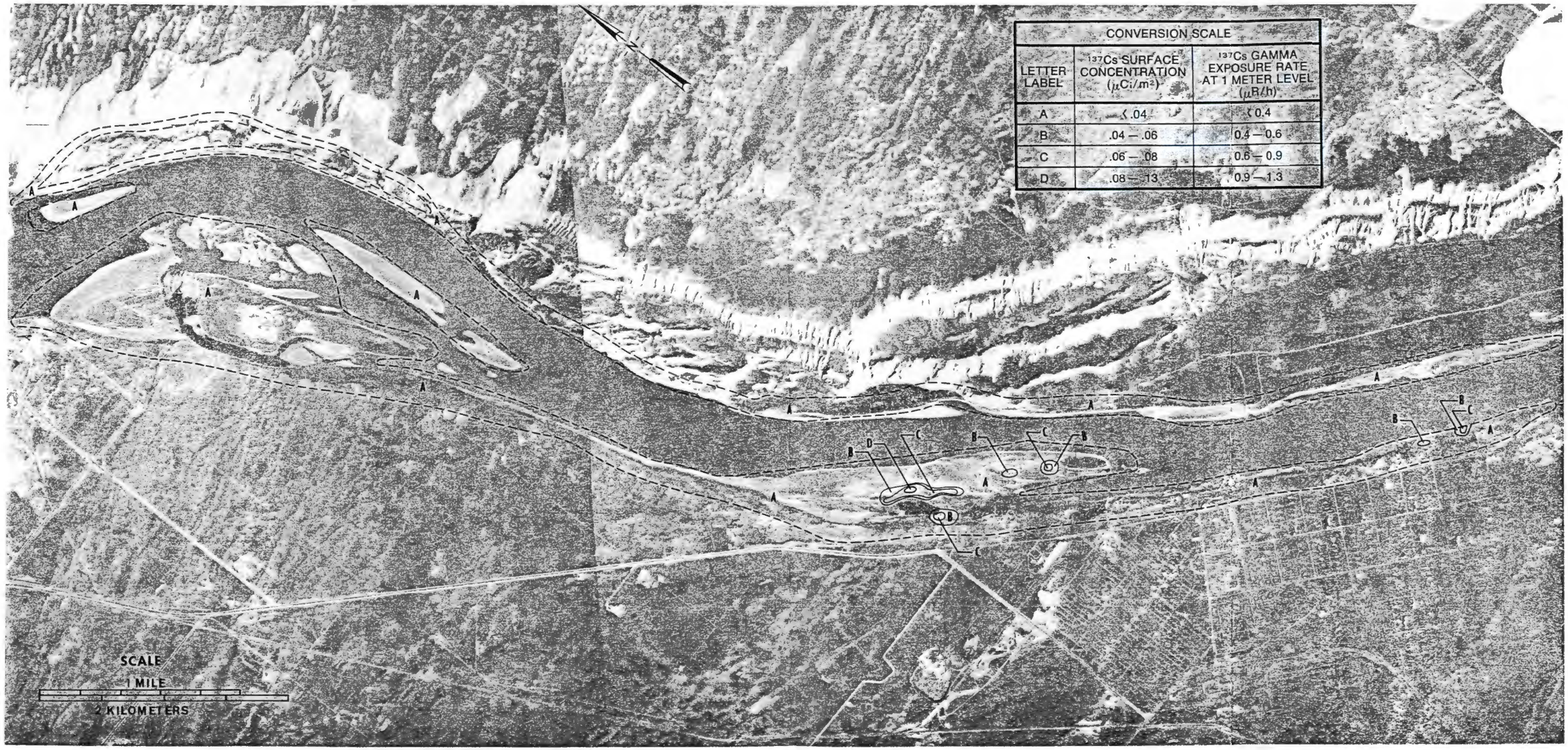

Figure 56. Concentration and gamma exposure rate isopleths for ^{137}Cs derived from the aerial survey data obtained during March and April 1974 along the Columbia River from the 100-F reactor area to the old Hanford townsite. The normal background exposure rate is approximately 10 μR/h in this area.

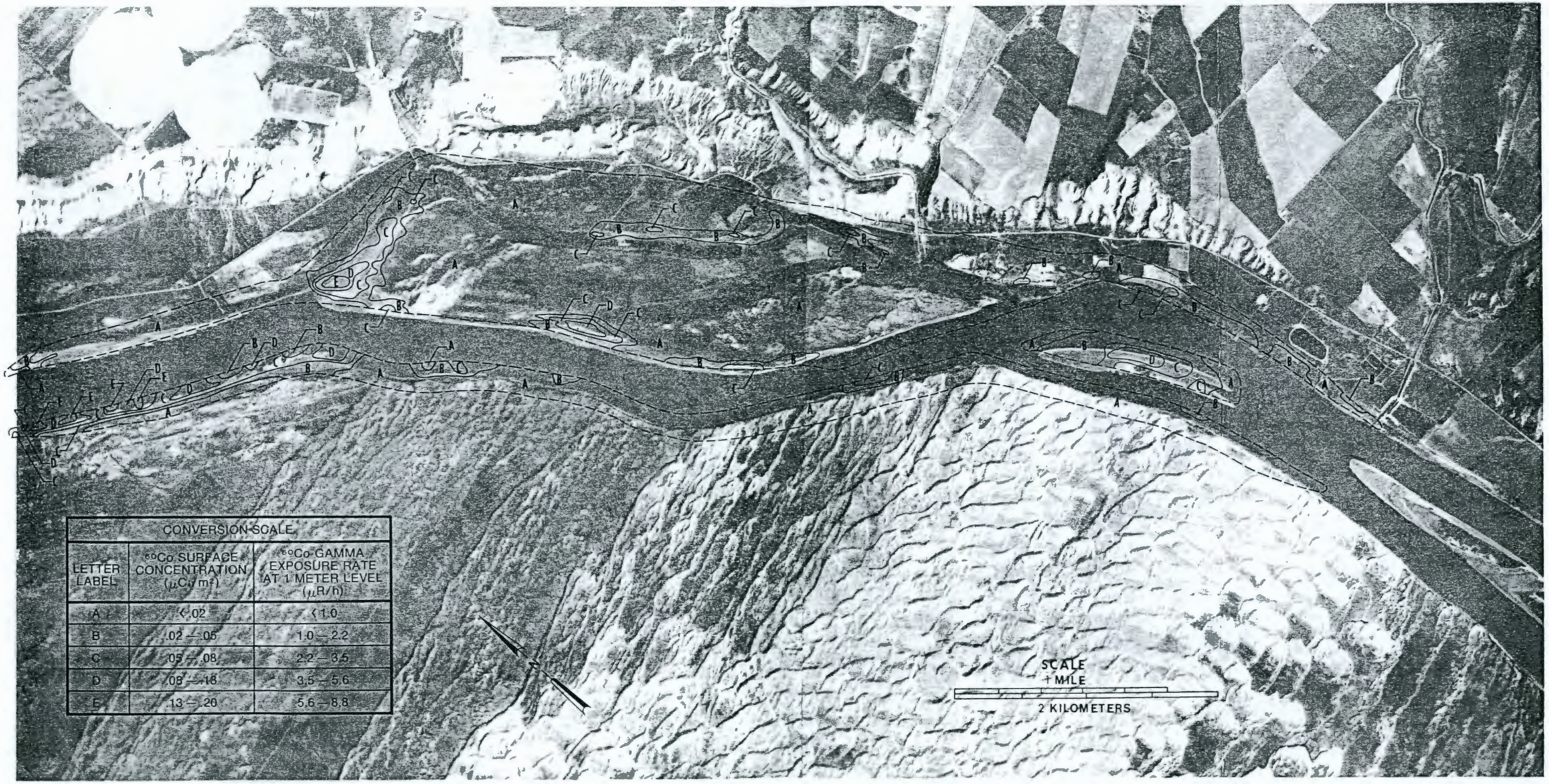

Figure 57. Concentration and gamma exposure rate isopleths for ^{60}Co derived from the aerial survey data obtained during March and April 1974 along the Columbia River in the vicinity of Savage Island. The normal background exposure rate is approximately 10 μR/h in this area.

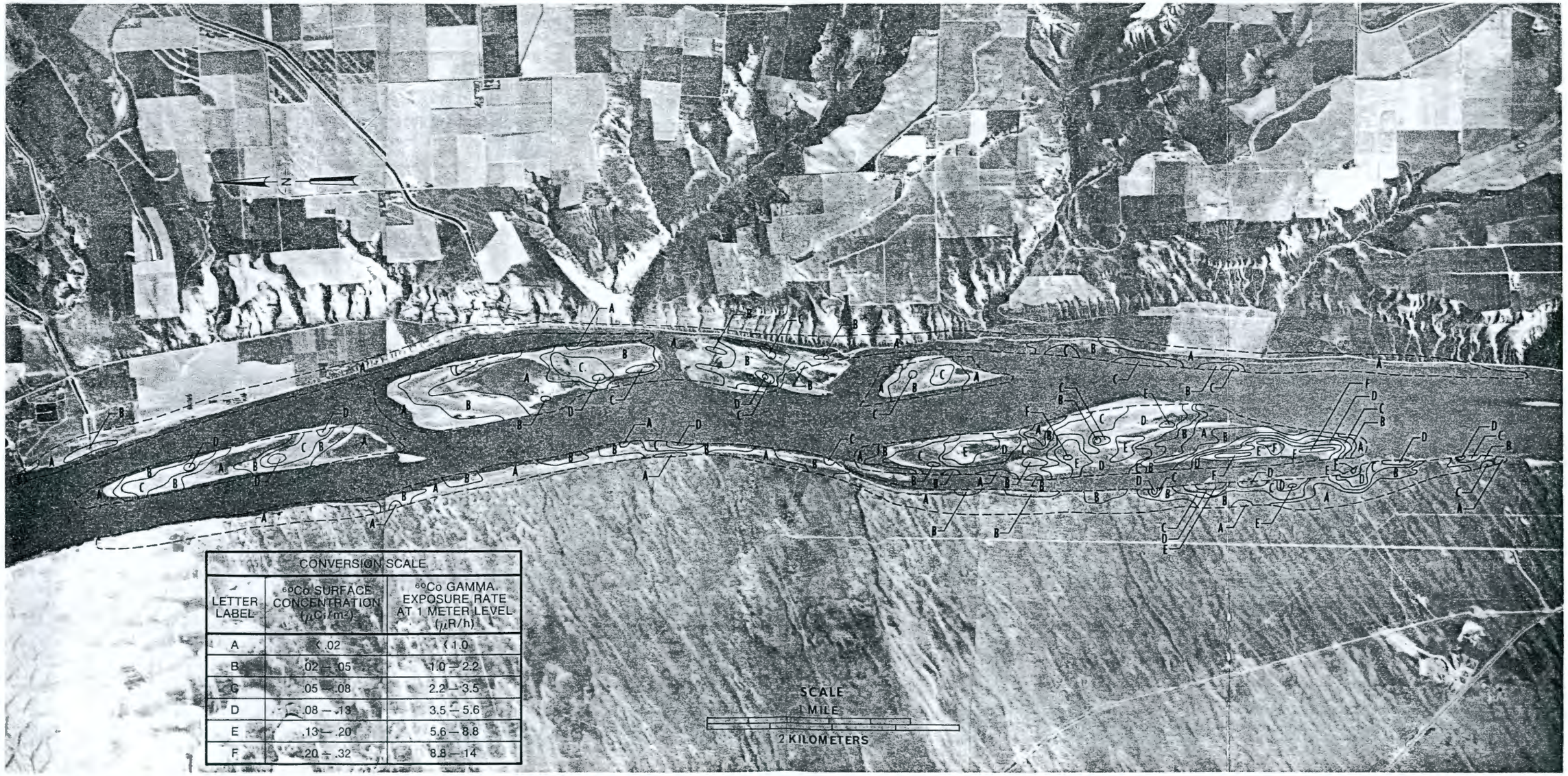

Figure 58. Concentration and gamma exposure rate isopleths for ^{60}Co derived from the aerial survey data obtained during March and April 1974 along the Columbia River in the vicinity of Wooded Island. The normal background exposure rate is approximately 10 $\mu R/h$ in this area.

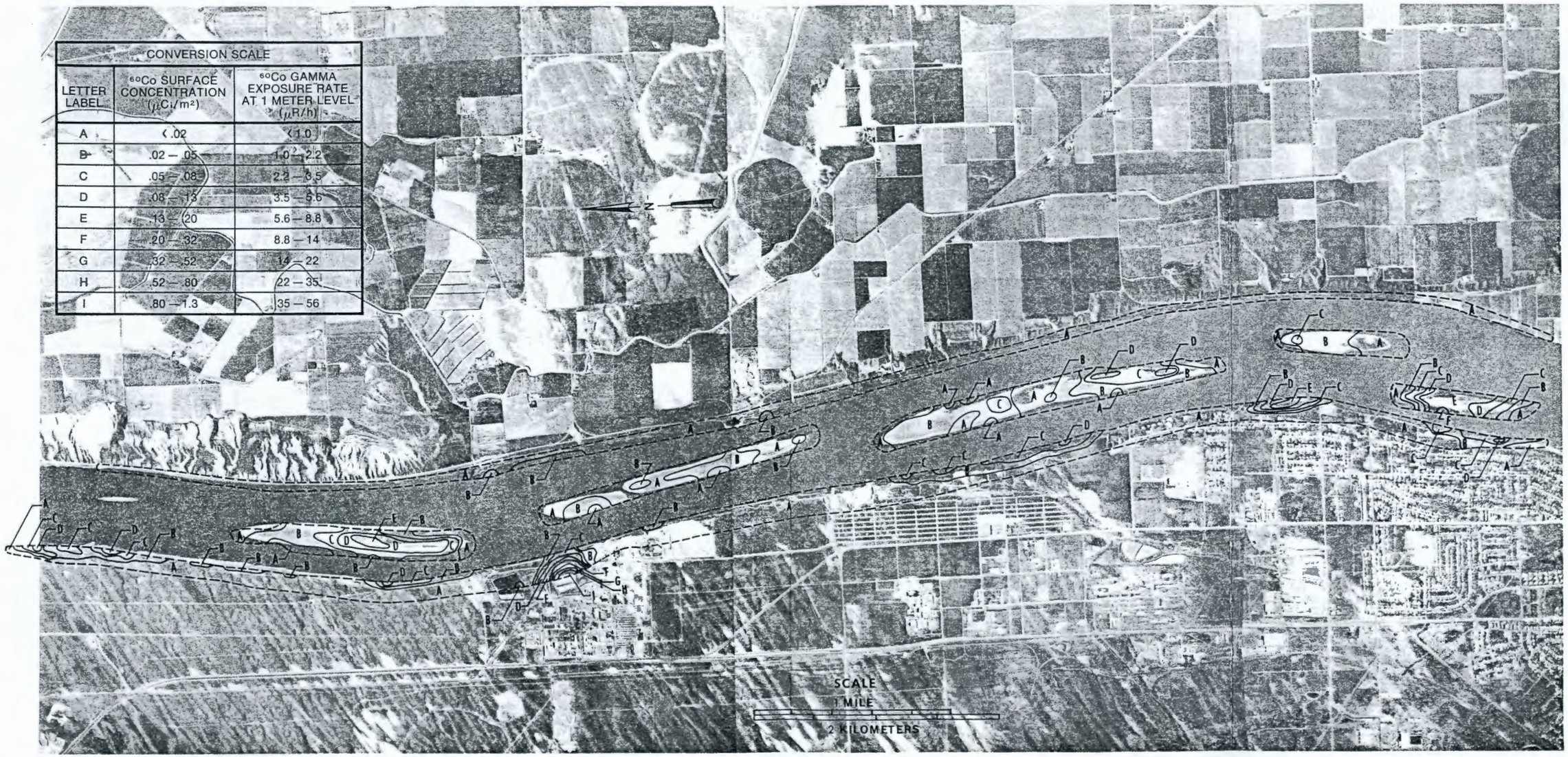

Figure 59. Concentration and gamma exposure rate isopleths for ^{60}Co derived from the aerial survey data obtained during March and April 1974 along the Columbia River between the 300 Area and North Richland. The normal background exposure rate is approximately 10 μR/h in this area.

Figure 60. Concentration and gamma exposure rate isopleths for ^{60}Co derived from the aerial survey data obtained during March and April 1974 along the Columbia River near its intersection with the Yakima River. The normal background exposure rate is approximately 10 μR/h in this area.

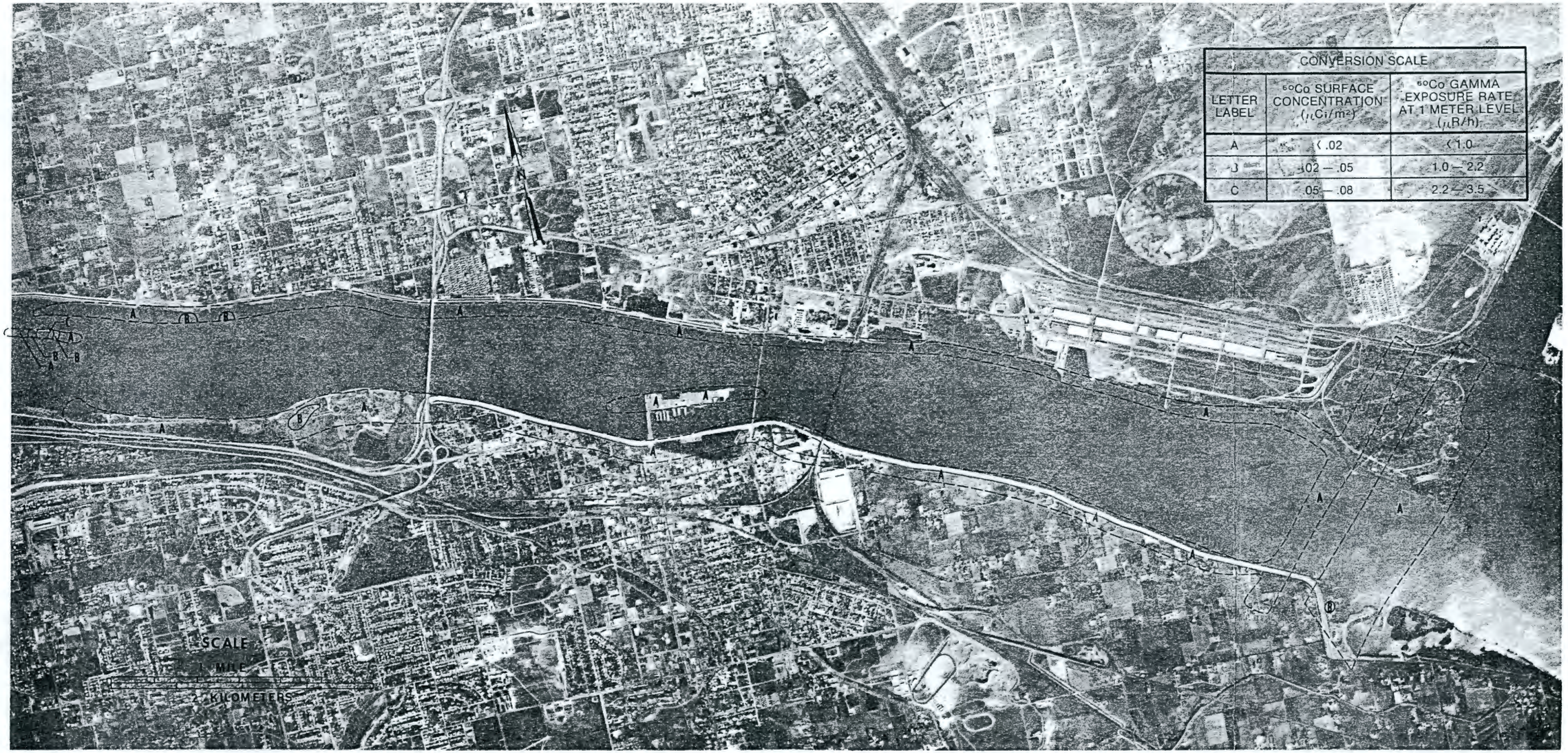

Figure 61. Concentration and gamma exposure rate isopleths for ^{60}Co derived from the aerial survey data obtained during March and April 1974 along the Columbia River between Pasco and Kennewick. The normal background exposure rate is approximately 10 $\mu R/h$ in this area.

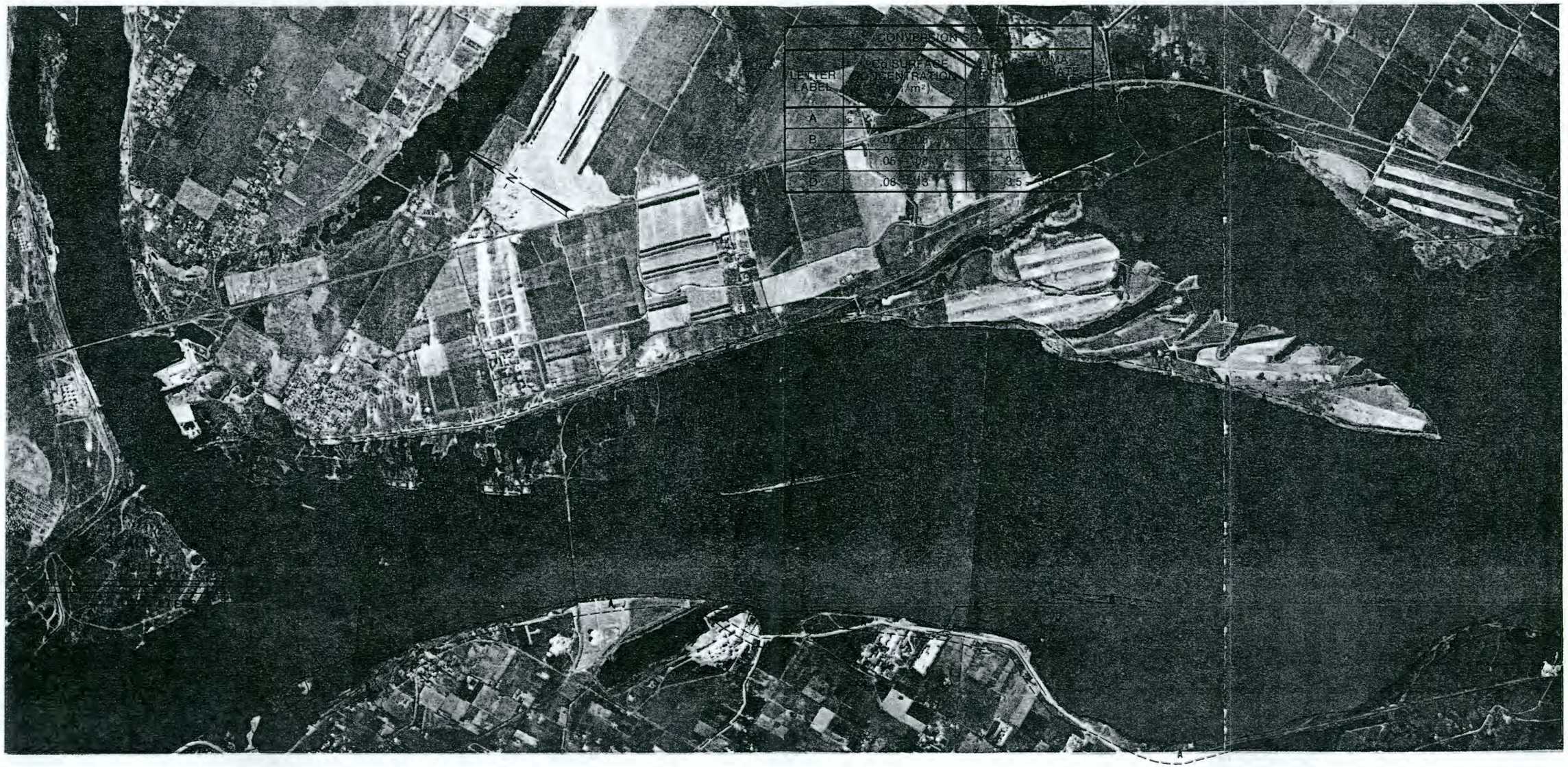

Figure 62. Concentration and gamma exposure rate isopleths for ^{60}Co derived from the aerial survey data obtained during March and April 1974 along the Columbia River near its intersection with the Snake River. The normal background exposure rate is approximately 10 μR/h in this area.

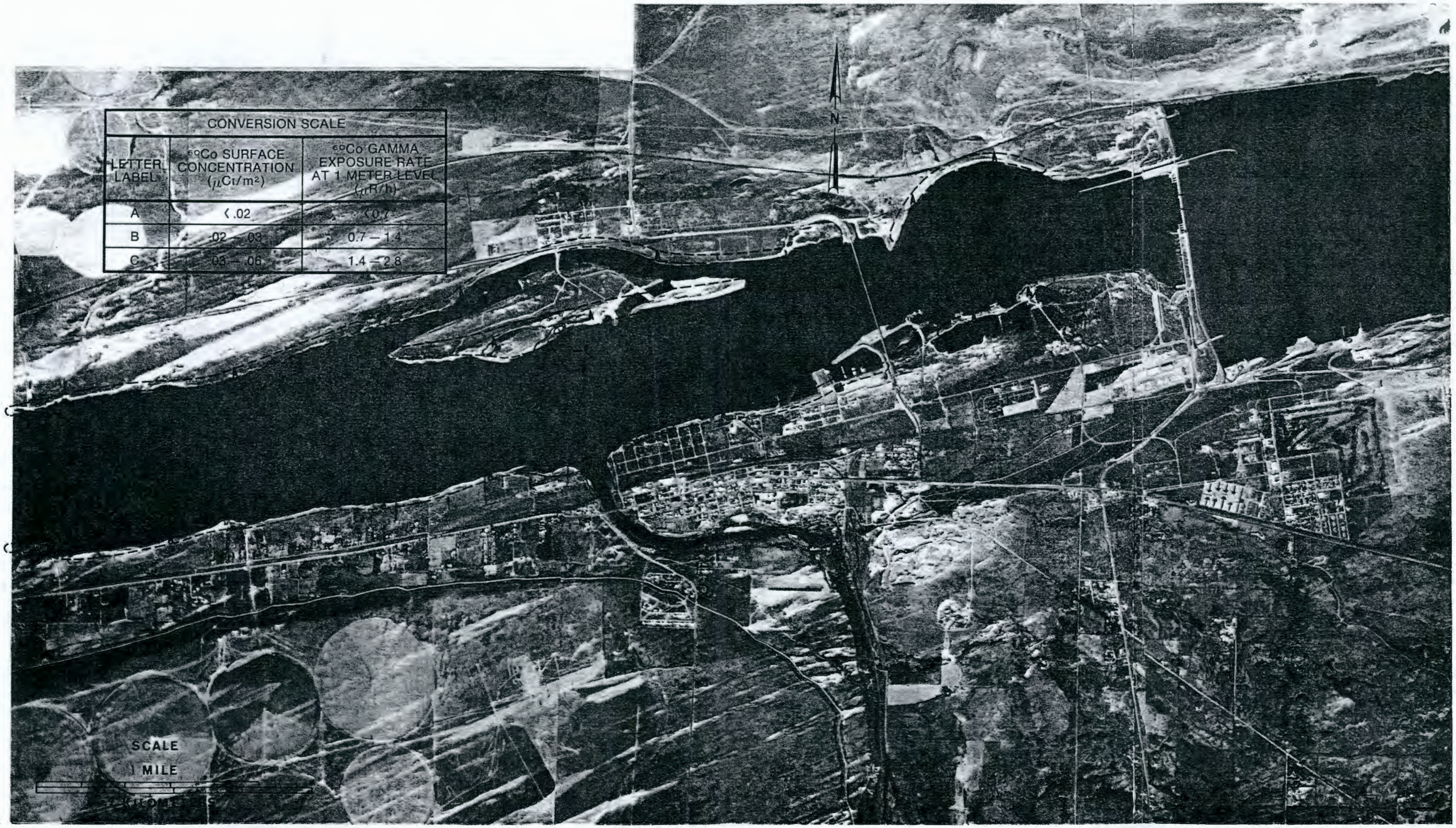

Figure 63. Concentration and gamma exposure rate isopleths for ^{60}Co derived from the aerial survey data obtained during March and April 1974 along the Columbia River just below McNary Dam. The normal background exposure rate is approximately 10 $\mu R/h$ in this area.

Figure 64. Concentration and gamma exposure rate isopleths for ^{60}Co derived from the aerial survey data obtained during March and April 1974 along the Columbia River near Irrigon. The normal background exposure rate is approximately 10 $\mu R/h$ in this area.

contractor at Hanford) show the residual activity is mainly due to ^{60}Co, with some ^{137}Cs occurring in the areas of highest ^{60}Co activity (7). Trace amounts of ^{54}Mn, ^{152}Eu and ^{154}Eu were also observed. Based upon surveys conducted on foot with portable instruments, Battelle concluded in the 1973 Environmental Monitoring Report (BNWL-1811) that the potential radiation dose to members of the public using the river for recreation would be less than one millirem per year. This value may be compared to the approximately 90 millirem per year whole body radiation dose received by the local population from external radiation due to non-Hanford sources (fallout and natural radioactivity)

3.7 Special Surveys

3.7.1 ^{241}Am Survey

A special low energy survey was conducted on June 2, 1973 over a portion of the 200-West Area centered on the U-pond. This was an attempt to detect low level plutonium activity in this controlled area via the 60 keV gamma ray from ^{241}Am, a decay product of ^{241}Pu. The ^{241}Am was expected to give only an approximation of the plutonium since some of the low level effluent released into the pond came from locations within the plutonium handling facilities where the americium and plutonium may have been separated.

The survey was flown at an altitude of 30 meters, with 30 meter line spacings, using the Navy helicopter. Electronic gain was adjusted for this survey so that the full energy scale corresponded to a gamma ray energy of 300 keV (compared to 3 MeV in the normal surveys).

The results are shown in Figure 65. ^{241}Am is clearly seen along the open ditch leading from the plutonium handling facilities. In addition, the plutonium scrap storage facility is also observed. The ^{241}Am information, however, was masked by the high count rates due to ^{137}Cs over the U-pond area. Sixteen detectors were turned on for the ^{241}Am survey. At an altitude of 30 meters, the ^{137}Cs activity gave a count rate in excess of one million counts per second over the U-pond area. The resulting spectral distortion due to pulse pile-up made it impossible to extract meaningful ^{241}Am data. During the normal (3 MeV) survey conducted over this area in October, 1973, only a single detector was used at an altitude of 45 meters to reduce the count rate problem.

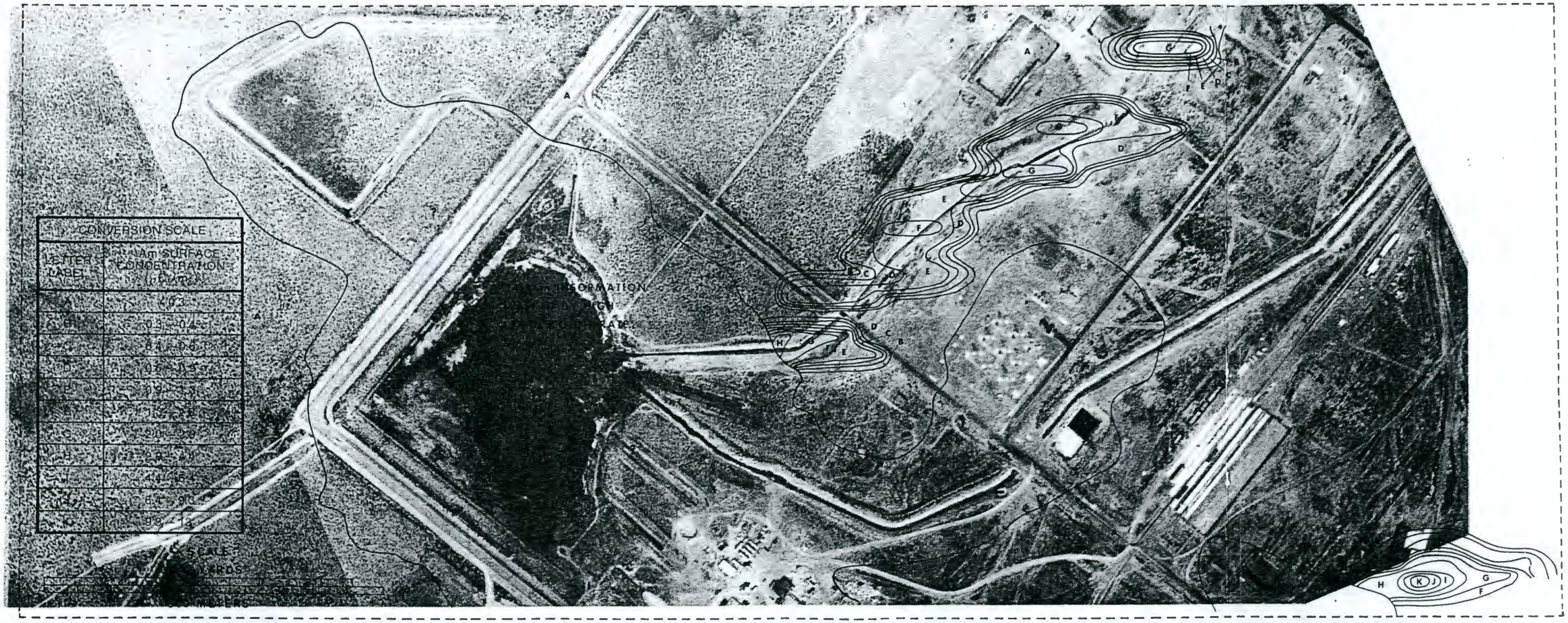

Figure 65. Concentration isopleths for ^{241}Am obtained during a special low energy survey conducted on June 2, 1973, over a portion of the 200-West Area centered on the U-pond.

3.7.2 Neutron Survey

Another special survey was flown on October 15, 1973 over a portion of the 200-West Area in an attempt to measure low level plutonium within the U-pond area. In this survey, BF_3 neutron detectors, having a total thermal neutron sensitivity of 6000 cps per n/cm^2-sec., were mounted on the helicopter in place of the gamma detectors. The survey was flown at an altitude of 30 meters, with 45 meter line spacings. Figure 66 shows the results of this survey. The only neutron activity observed was that due to shine from the plutonium handling facilities. No activity was detectable over the U-pond area within the detectability limits of the aerial system.

3.7.3 Ge(Li) Survey

Due to the count rate limitations of the acquisition system, a large portion of the 200-West Area was surveyed with a single 12.7 cm diameter by 5 cm thick NaI (Tℓ) detector during the 45 meter altitude helicopter survey. Count rates in excess of 50,000 cps, mainly due to ^{137}Cs, were still encountered over several areas however. The resulting pulse pile-up of the ^{137}Cs gamma ray signals into the ^{60}Co photopeak window made it impossible to extract meaningful ^{60}Co photopeak count rate data using the stripping procedures described in Section 2. For this reason another aerial survey was conducted over the center portion of the 200-West Area on March 29, 1974 using a high resolution lithium-drifted germanium [Ge(Li)] detector.

The major advantage of a Ge(Li) detector is its high resolution. An improvement in the photopeak full-width-at-half-maximum (FWHM) value by factors of 40 to 50 is common between Ge(Li) detectors and NaI (Tℓ) detectors. The Ge(Li) detectors suffer compared to NaI(Tℓ) detectors for aerial applications due to the relatively small volumes attainable for a single detector (leading to poor counting statistics for a moving aerial platform) and the large expense necessary to fabricate a large volume array. Over the regions of interest within the 200-West Area, however, the gamma ray flux was sufficient to allow the use of a single Ge(Li) detector.

The Ge(Li) detector survey was flown at an altitude of 45 meters with the detector located inside the helicopter. The detector had an efficiency of 14.5% with a total active volume of 77 cm^3. This detector had not been calibrated for an aerial survey, so the results for ^{137}Cs and ^{60}Co are expressed in terms of their photopeak count rate data at 662 keV

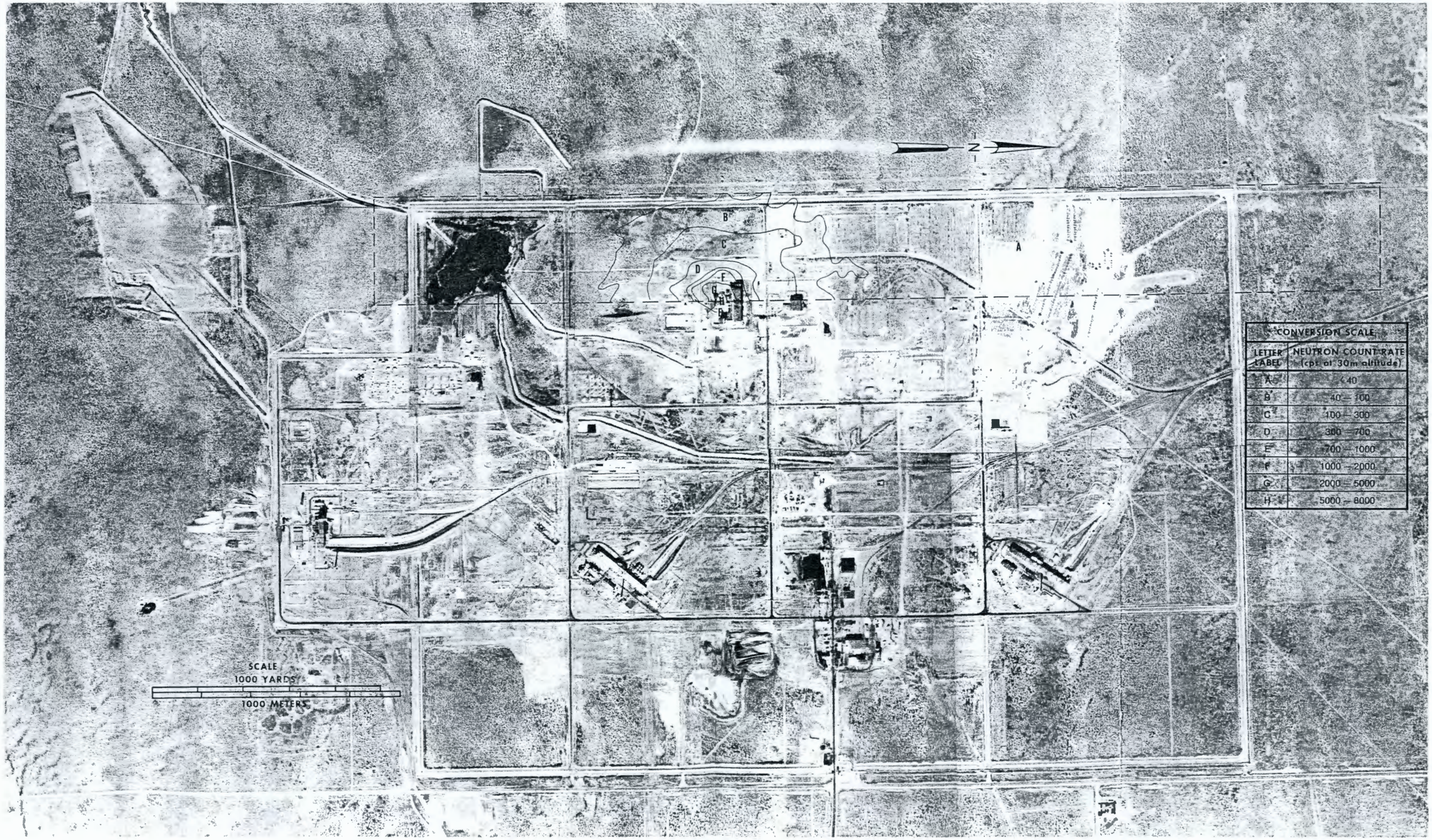

Figure 66. Isopleth map of the neutron count rate at 30-meter altitude obtained during a special survey flown on October 15, 1973, over a portion of the 200-West Area. These results were obtained using an array of BF_3 detectors having a thermal neutron sensitivity of 6000 cps per n/cm^2-sec.

and 1333 keV, respectively. No background subtraction was necessary for the Ge(Li) survey since, on the average, only 1 count every 4 seconds and 1 count every 30 seconds for the ^{137}Cs and ^{60}Co photopeak windows, respectively, were recorded due to natural background radiation. The contribution due to Compton scattered gamma rays from ^{60}Co were removed from the ^{137}Cs photopeak window using the stripping technique described in Section 2.

The aerial survey results are shown in Figures 67, 68 and 69. Figure 67 gives the total gamma ray count rate, at a 45 meter altitude, for gamma ray energies between 40 keV and 1500 keV. The results for ^{137}Cs and ^{60}Co are given in Figures 68 and 69, respectively. These results can be compared with Figures 34 and 35 which were based on the NaI(Tℓ) survey. The two "gross count" isopleth maps (Figures 34 and 67) compare quite well. The same general areas of gamma radioactivity appear in both Figures with the exception of the two transient sources which were present during the NaI(Tℓ) survey and the activity associated with the plutonium handling facilities. In the later case sufficient additional shielding was present with the detector located inside the helicopter to mask the 60 keV gamma ray signal from ^{241}Am. Due to the lower counting rates and improved resolution, the Ge(Li) results could easily be processed for both ^{60}Co and ^{137}Cs. The locations of areas containing ^{60}Co, described in the text in Section 3.3.1, can be seen in Figure 69. No isotopes other than ^{137}Cs and ^{60}Co were identified from the Ge(Li) detector data.

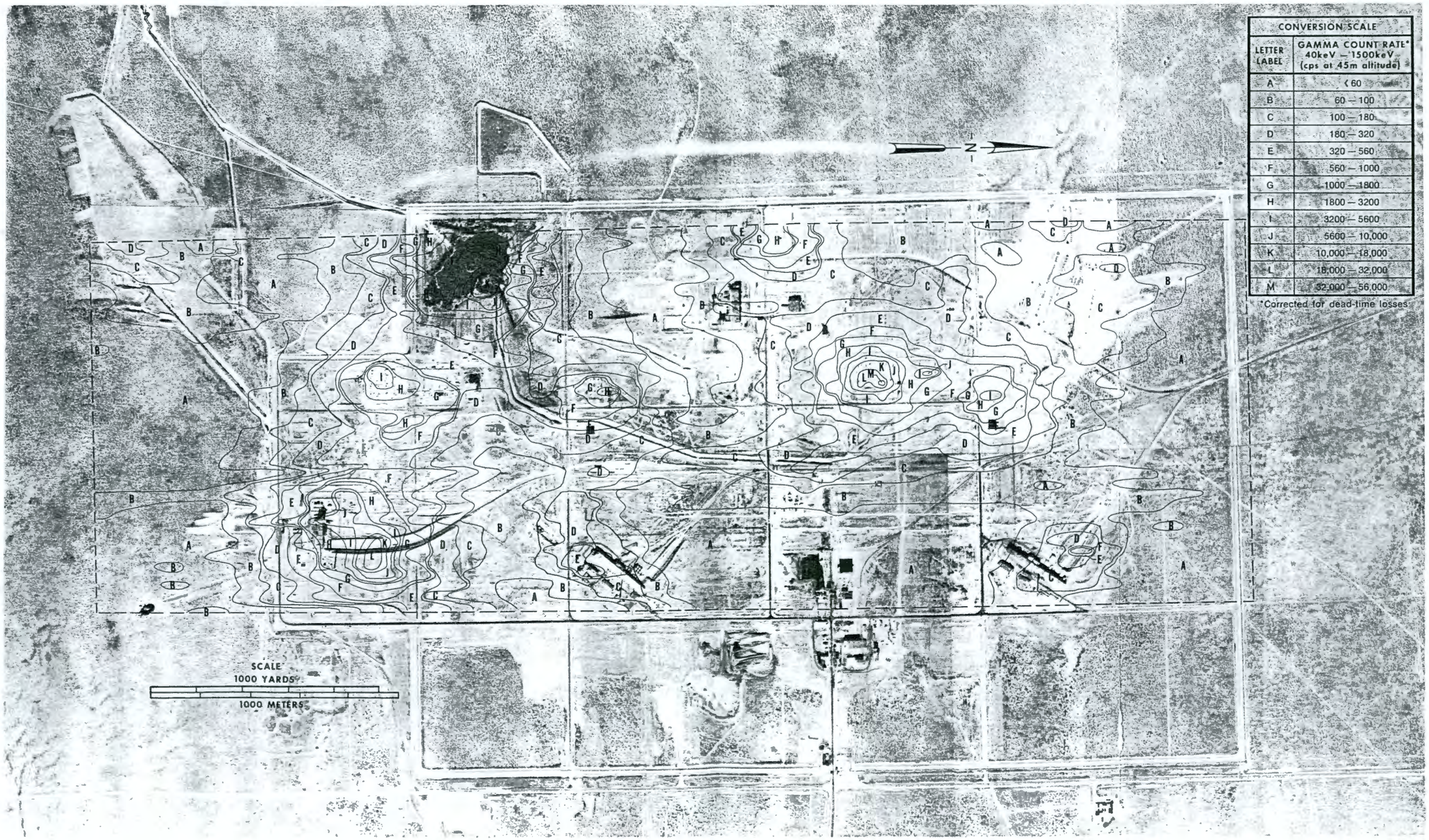

CONVERSION SCALE	
LETTER LABEL	GAMMA COUNT RATE* 40keV — 1500keV (cps at 45m altitude)
A	< 60
B	60 — 100
C	100 — 180
D	180 — 320
E	320 — 560
F	560 — 1000
G	1000 — 1800
H	1800 — 3200
I	3200 — 5600
J	5600 — 10,000
K	10,000 — 18,000
L	18,000 — 32,000
M	32,000 — 56,000

*Corrected for dead-time losses.

Figure 67. Isopleth map of the total gamma ray count rate between 40 keV and 1500 keV (at an altitude of 45 meters) obtained during a special survey flown on March 29, 1974 over a portion of the 200-West Area. These results were obtained with a 77 cm^3 Ge(Li) detector, having an efficiency of 14.5%, mounted inside the helicopter.

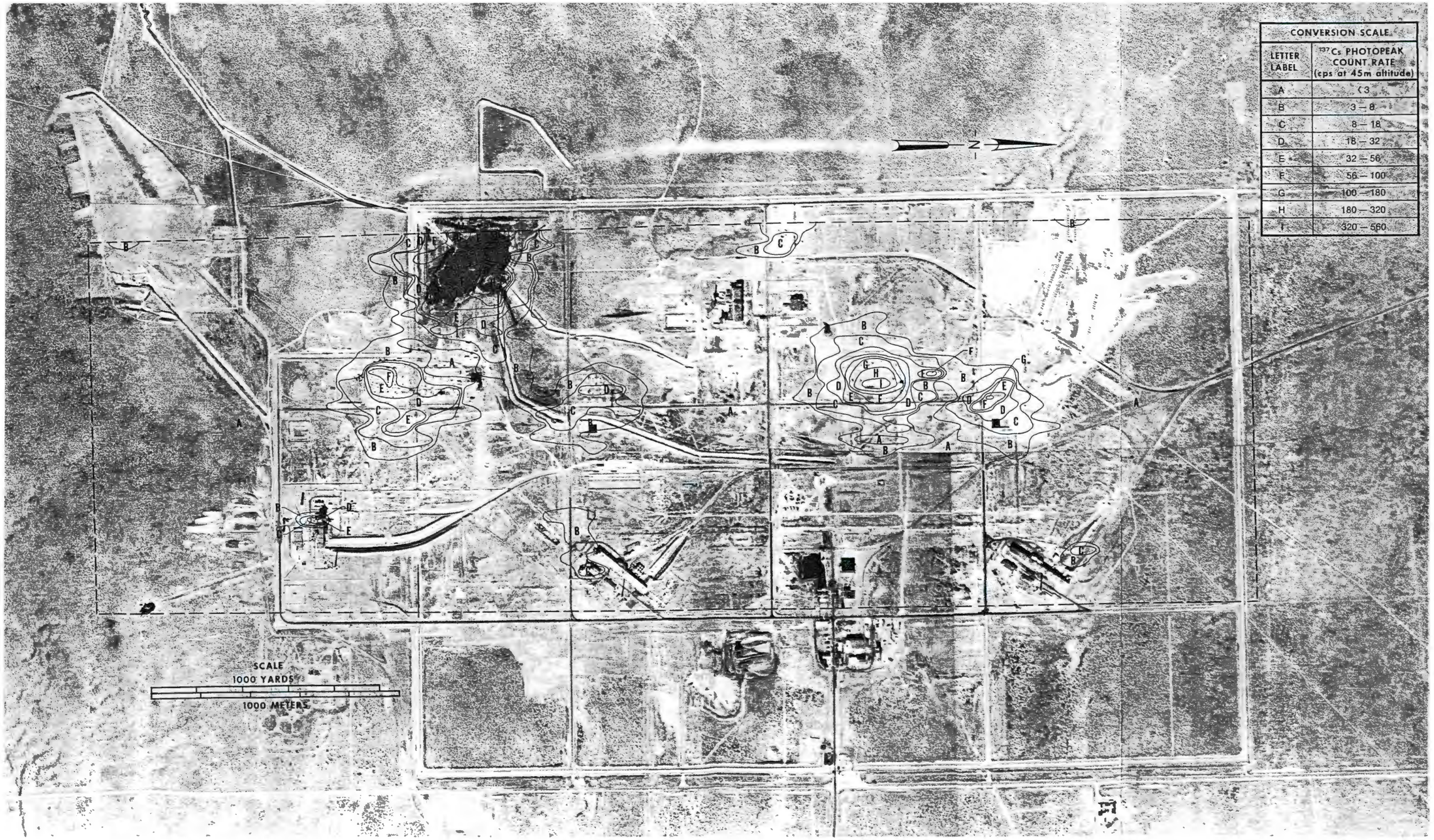

Figure 68. Isopleth map of the ^{137}Cs photopeak count rate (at an altitude of 45 meters) obtained during a special survey flown on March 29, 1974 over a portion of the 200-West Area. These results were obtained with a 77 cm^3 Ge(Li) detector, having an efficiency of 14.5%, mounted inside the helicopter.

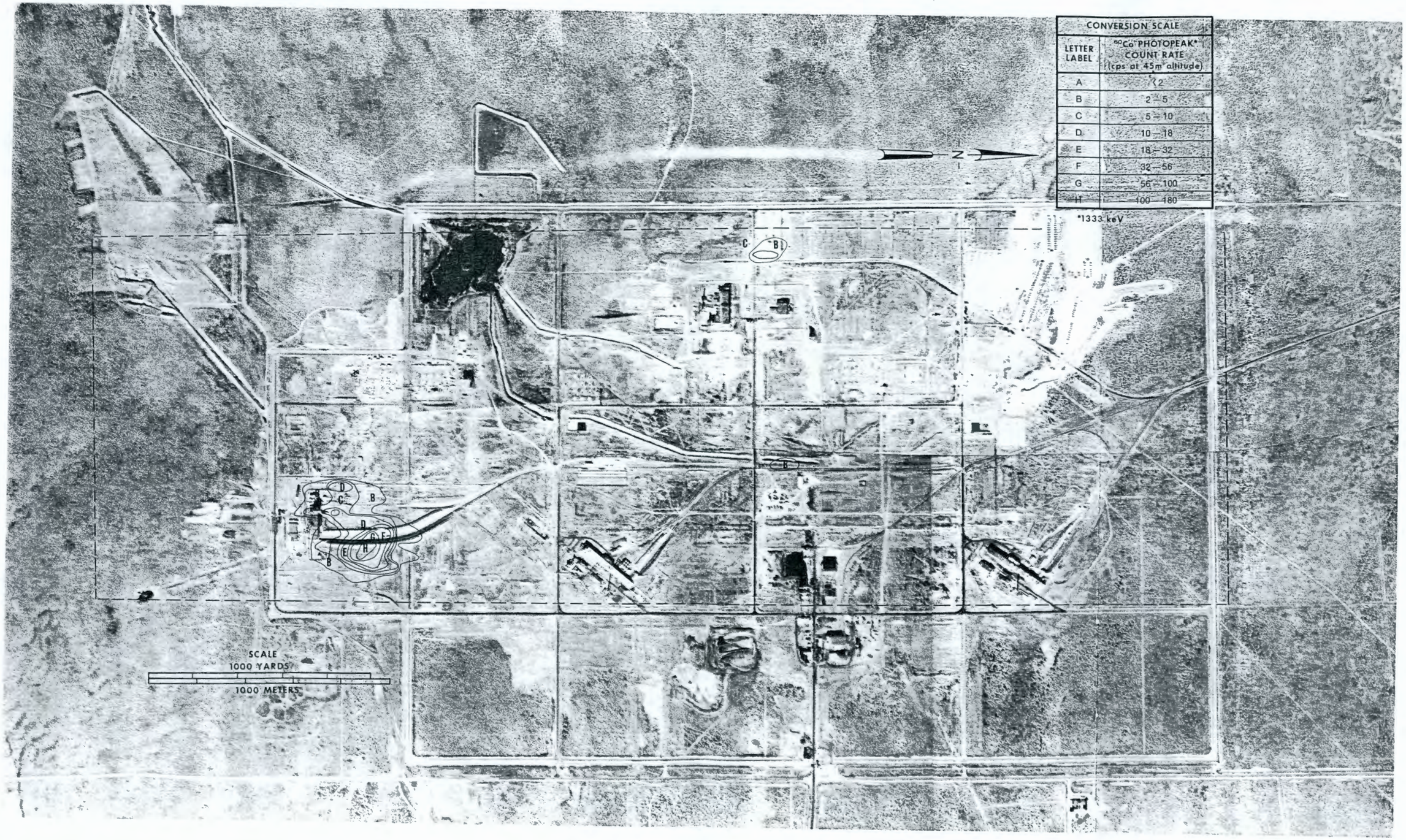

Figure 69. Isopleth map of the ^{60}Co photopeak count rate (at an altitude of 45 meters) obtained during a special survey flown on March 29, 1974 over a portion of the 200-West Area. These results were obtained with a 77 cm^3 Ge(Li) detector, having an efficiency of 14.5%, mounted inside the helicopter.

4. SUMMARY

During the four aerial surveys conducted over the Hanford Reservation between May 1973 and April 1974 survey lines in excess of 6000 kilometers were flown. These included detailed, low altitude (45 meter) surveys over all the major facilities within the site, a large area high altitude (150 meter) survey over the entire site and a low altitude (45 meter) detailed survey over the Columbia River shoreline, slough areas and river islands. The river survey extended from the Vernita Bridge upstream of the site to the intersection of the Snake and Columbia Rivers approximately 35 kilometers downstream from the site boundary. These surveys provide a complete documentation of all areas within and adjacent to the site containing gamma emitting radionuclides associated with past and present Hanford operations. (The minimum detectable level of the ARMS detector system is approximately a factor of ten lower than that due to normal background radiation.)

The aerial survey detected the presence of ^{137}Cs, ^{60}Co, ^{22}Na, ^{241}Am and ^{234m}Pa, with ^{137}Cs and ^{60}Co being most prevalent. Over the reactor facilities, located within the 100 Areas, the major portion of the gamma ray activity observed was due to ^{60}Co. This activity was associated with the reactor blocks, with small cribs and liquid waste disposal trenches in the vicinity of the reactor buildings and with the retention basins, overflow trenches and outfall structures associated with the cooling water effluent (for all the reactors except N Reactor, which has a closed primary cooling loop). In addition, activity was observed over several solid waste burial grounds, mainly where an open pit existed containing radioactive material. Within the 200 Area Plateau, where the reactor fuel processing and waste management facilities are located, the predominant isotope observed was ^{137}Cs. Activity within this area was generally associated with the various handling, decontamination and storage facilities, with solid and liquid waste burial grounds and low level activity associated with contaminated cooling water ponds. Both ^{137}Cs and ^{60}Co were identified in the above ground liquid waste handling facilities within the 300 Area where reactor fuel manufacturing facilities and research and development laboratories are located. ^{234m}Pa was also observed within the 300 Area where large amounts of depleted uranium were stored.

The only gamma radioactivity observed during the four aerial surveys which was not located within a radiation control area was that detected at occasional locations along the shoreline and islands

of the Columbia River. This activity resulted from a long term build-up of low level activity released into the Columbia River during operation of the single-pass reactors (the last of which was deactivated during January 1971). The highest activity observed within the site boundary occurred along the slough areas between the 100-H Area and the old Hanford townsite. Radiation levels up to 22 μR/h due to ^{60}Co and 3μR/h due to ^{137}Cs were observed. The highest activity observed in areas accessible to the public occurred on the islands between the old Hanford townsite and Pasco. Maximum levels up to 14μR/h due to ^{60}Co were observed, with no detectable ^{137}Cs activity. (The normal background exposure rate is approximately 10 μR/h in the Hanford vicinity.)

These results, described in detail in Section 3, represent the most comprehensive ARMS survey conducted to date over an ERDA facility. Periodic resurveys over selected areas within and adjacent to the Hanford Reservation are anticipated in the future as an aid to local personnel in their efforts to maintain an up-to-date inventory of the radiological contamination within the Hanford environment.

APPENDIX

Derivation of Conversion Factors Relating Aerial Measurements to Ground Concentration For a Variety of Source Geometries

The quantitative results given in Section 3 are expressed in terms of radioactivity and gamma exposure rate isopleths for ^{137}Cs and ^{60}Co. These results were derived assuming a uniform surface concentration of radioactivity over an infinite smooth plane (see Section 2.5). For those areas where the activity is not distributed uniformly over the surface, ground level results can be inferred from the airborne results more accurately if the actual source distribution geometry is known. This information can be obtained through ground sampling in the area of interest. Once this information is known, more precise conversion factors can be applied to the photopeak count rate data. (This is especially important in cases where the total activity contained within a given area is derived using the aerial results). The method employed in Section 2.5 for a uniform surface distribution of radioactivity will be extended in this appendix to an exponential depth distribution and a uniform volume distribution of radioactivity in the soil.

As in Section 2.5, an effective detector area is defined from data taken by hovering over a point source of known strength. For this case, the photopeak count rate (CR_p) in the detector is given by

$$CR_p = \frac{S_0 A}{4\pi h^2} e^{-h/\lambda_a}, \qquad (A.1)$$

where

S_0 = source strength in gammas per second,

h = height of detector above the source,

λ_a = gamma ray mean free path in air and

A = effective detector area for normal incidence.

This effective area takes into account factors such as gamma ray attenuation in the detector housing and the photopeak efficiency of the detector.

Consider first a radioelement distributed exponentially with depth in the soil. The activity per unit volume, at a depth z, is given by

$$\eta_v = \eta_v^o e^{-\alpha z} , \tag{A.2}$$

where

η_v^o = activity per unit volume of soil at the surface and

α = reciprocal of the relaxation depth.

The photopeak count rate (CR) of a detector at any survey altitude d above the surface (see Figure A.1) is then given by

$$CR = \int_0^\infty \int_0^\infty \frac{\eta_v A^*}{4\pi r^2} \exp\left[-\left(\frac{r_a}{\lambda_a} + \frac{r_s}{\lambda_s}\right)\right] 2\pi x\,dx\,dz , \tag{A.3}$$

where

λ_s, λ_a = gamma ray mean free path in soil and air, respectively,

$r = \sqrt{x^2 + (d + z)^2}$ = the distance from each element of differential volume to the detector position and

A^* = effective detector area for gamma rays incident at an angle

$$\theta = \arccos\left(\frac{d + z}{r}\right).$$

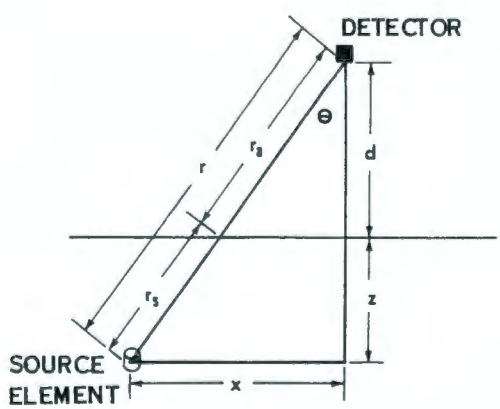

Figure A.1. Geometry used in the derivation of conversion factors relating aerial photopeak count rate data to ground concentrations for exponential and uniform volume depth distributions of radioactivity in the soil.

Here the distance r is divided into that part within air, r_a, and that part within the soil, r_s.

The total activity in an infinitely deep column of soil of unit cross-sectional area is given by

$$\eta_A = \int_0^\infty \eta_V \, dz = \int_0^\infty \eta_V^o \, e^{-\alpha z} \, dz = \frac{\eta_V^o}{\alpha} \quad . \tag{A.4}$$

Using this result, Eq. A.3 can be rewritten as

$$CR = \int_0^\infty \int_0^\infty \frac{\alpha \eta_A \, e^{-\alpha z} \, A^*}{4\pi r^2} \exp\left[-\left(\frac{r_a}{\lambda_a} + \frac{r_s}{\lambda_s}\right)\right] 2\pi x \, dx \, dz \quad . \tag{A.5}$$

As in the case of the uniform surface distribution described in Section 2.5, two limiting values of the detector angular response can be assumed. For an isotropic angular response the effective area A^* equals A and for a cosine angular response the effective area A^* equals $A \cos\theta$. Equation A.5 can then be solved for these two limiting cases. The isotropic angular response will be considered first.

Since

$$\cos\theta = \frac{d}{r_a} = \frac{d+z}{r} \quad ,$$

the distances r_a and r_s can be rewritten as

$$r_a = \frac{d}{d+z} \quad r$$

$$r_s = \frac{z}{d+z} \quad r \quad .$$

Keeping d and z fixed, Eq. A.5 can be written as

$$CR = \int_0^\infty \frac{\alpha \eta_A A}{2} \left[\int_{d+z}^\infty \frac{\exp\left\{ - r \left[\left(\frac{d}{d+z}\right) \frac{1}{\lambda_a} + \left(\frac{z}{d+z}\right) \frac{1}{\lambda_s} \right] \right\}}{r} \, dr \right] \times e^{-\alpha z} \, dz \quad . \tag{A.6}$$

By defining

$$y = \left[\left(\frac{d}{d+z}\right)\frac{1}{\lambda_a} + \left(\frac{z}{d+z}\right)\frac{1}{\lambda_s}\right] r \ ,$$

Eq. A.6 can be put into the form

$$CR = \int_0^\infty \frac{\alpha \eta_A A}{2} \left[\int_{\left(\frac{d}{\lambda_a}+\frac{z}{\lambda_s}\right)}^\infty \frac{e^{-y}}{y}\, dy \right] e^{-\alpha z}\, dz \ . \qquad (A.7)$$

Recalling the exponential integral, defined as

$$E_n(a) \equiv a^{n-1} \int_a^\infty \frac{e^{-x}}{x^n}\, dx \ ,$$

Eq. A.7 can be written as

$$CR = \frac{\alpha \eta_A A}{2} \int_0^\infty e^{-\alpha z} E_1\left(\frac{d}{\lambda_a} + \frac{z}{\lambda_s}\right) dz \ . \qquad (A.8)$$

Eliminating the effective area between Eq.'s A.1 and A.8 , the total activity per unit area for an infinitely deep column of soil is given by

$$\eta_A = \left[\frac{S_0\, e^{-h/\lambda_a}}{2\pi h^2\, \alpha (CR_p) \int_0^\infty e^{-\alpha z} E_1 \left(\frac{d}{\lambda_a} + \frac{z}{\lambda_s}\right) dz} \right] CR \ . \qquad (A.9)$$

For the cosine angular response, an additional factor of $\left(\frac{d+z}{r}\right)$ must be included in Eq. A.6. The results for this case are given by

$$\eta_A = \left[\frac{S_0 \, e^{-h/\lambda_a}}{2\pi h^2 \alpha (CR_p) \int_0^\infty e^{-\alpha z} \, E_2 \left(\frac{d}{\lambda_a} + \frac{z}{\lambda_s}\right) dz} \right] CR \, , \tag{A.10}$$

where the only change occurs in the order of the exponential integral.

The expression within the bracket of Eq. A.9 and Eq. A.10 may be evaluated by numerical integration for any relaxation depth, $1/\alpha$, and any survey altitude, d, by using the results of the calibration hover over a known point source (at an altitude h), the tabulated values of the exponential integrals and representative values for the air and soil density.

Next consider a radioactive source distributed uniformly with volume in the soil. The photopeak count rate (CR) obtained at an altitude d above the surface (see Figure A.1) is given by

$$CR = \int_0^{\pi/2} \int_{d/\omega}^{\infty} \frac{nA^*}{4\pi r^2} \exp\left[-\left(\frac{d}{\omega}\right) \frac{1}{\lambda_a} - \left(r - \frac{d}{\omega}\right) \frac{1}{\lambda_s} \right] \times 2\pi r^2 \sin\theta \, dr \, d\theta \, , \tag{A.11}$$

where

n = activity per unit volume,
A^* = effective detector area for gamma rays incident at an angle θ,
ω = $\cos\theta$,
r = the distance from each element of differential volume to the detector position and
λ_a, λ_s = gamma ray mean free path in air and soil, respectively.

Integrating over r, Eq. A.11 becomes

$$CR = \int_0^{\pi/2} \frac{nA^* \lambda_s}{2} \exp\left[-\left(\frac{d}{\omega}\right) \frac{1}{\lambda_a} \right] \sin\theta \, d\theta \, . \tag{A.12}$$

Again, the two limiting cases for A^* can be considered. For the isotropic detector response A^* equals A. Using the substitution

$$y = \left(\frac{d}{\omega}\right) \frac{1}{\lambda_a} ,$$

Eq. A.12 can be rewritten as

$$CR = \frac{nA\lambda_s}{2} \frac{d}{\lambda_a} \int_{(d/\lambda_a)}^{\infty} \frac{e^{-y}}{y^2} dy$$

or

$$CR = \frac{nA\lambda_s}{2} E_2 \left(\frac{d}{\lambda_a}\right) . \tag{A.13}$$

Eliminating the effective area between Eq. A.1 and Eq. A.13, the activity per unit mass is given by

$$\frac{n}{\rho} = \left[\frac{S_0 e^{-h/\lambda_a}}{2\pi h^2 (CR_\rho) \lambda_s \rho E_2 (d/\lambda_a)} \right] CR , \tag{A.14}$$

where ρ is the soil density.

For a cosine angular response A^* equals $A \cos\theta$. In this case Eq. A.13 becomes

$$CR = \frac{nA\lambda_s}{2} E_3 \left(\frac{d}{\lambda_a}\right) . \tag{A.15}$$

Eliminating A between Eq. A.1 and Eq. A.15 leads to

$$\frac{n}{\rho} = \left[\frac{S_0 e^{-h/\lambda_a}}{2\pi h^2 (CR_\rho) \lambda_s \rho E_3 (d/\lambda_a)} \right] CR . \tag{A.16}$$

The expression within the bracket of Eq. A.14 and Eq. A.16 can be evaluated for any survey altitude d by using the results of a calibration hover over a known source, the tabulated values for the exponential integrals and representative values for the air and soil density.

Table A.1 contains conversion factors for the 40 NaI (Tℓ) detector array, at a survey altitude of 45 meters, for all the source geometries considered. In each case the conversion factor given is an average between the calculated values assuming an isotropic and a cosine detector angular response. Three relaxation depths (0.1, 1.0 and 10 centimeters) were considered in the exponential distribution case. Also given in Table A.1 are the corresponding exposure rate conversion factors (at the one meter level) for each source geometry considered. These were obtained from tables given in reference 4. The values for the gamma ray mean free path in soil were also obtained from reference 4 assuming a soil density of 1.6 with a 10% soil moisture content.

The concentration and exposure rate values given in Section 3 can be converted to more realistic values (in cases where the actual source distribution geometry is known) by multiplying the "surface" concentration values by the appropriate conversion factor ratio using Table A.1. This must be done to obtain an accurate value for the total activity contained within an area using the aerial results.

It is interesting to note that the exposure rate conversion factors are relatively insensitive to the depth distribution over a wide range of values. For relaxation depths greater than 1 cm (down to the extreme case of a uniform volume distribution), the exposure rate conversion factors are essentially constant. The greatest difference occurs in going from a surface distribution to a volume distribution extending over a depth of a few centimeters. Thus, it is not necessary to know the exact depth distribution to obtain a good measure of the exposure rate at the 1 meter level.

Table A.1 Conversion factors relating aerial photopeak count rate data to radionuclide concentration on the ground for a variety of source distribution geometries.

Radio-nuclide	Conversion Factor[a]								
	Point Source on Surface $\left[\frac{\mu Ci}{cps}\right]$		Uniform Surface Distribution		Exponential Distribution			Uniform Volume Distribution	
	Directly under aircraft	At lateral distance of 22 m	$\left[\frac{\mu Ci/m^2}{cps}\right]^b$	$\left[\frac{\mu R/h}{cps}\right]^c$	Relaxation depth [cm]	$\left[\frac{\mu Ci/m^2}{cps}\right]^b$	$\left[\frac{\mu R/h}{cps}\right]^c$	$\left[\frac{pCi/g}{cps}\right]^b$	$\left[\frac{\mu R/h}{cps}\right]^c$
^{137}Cs	5.4	7.1	$5.6(10^{-4})$	$5.9(10^{-3})$	0.1	$5.8(10^{-4})$	$5.4(10^{-3})$	$7.1(10^{-3})$	$4.4(10^{-3})$
					1.0	$7.0(10^{-4})$	$4.3(10^{-3})$		
					10	$1.8(10^{-3})$	$4.2(10^{-3})$		
^{60}Co	3.5	4.6	$3.2(10^{-4})$	$1.4(10^{-2})$	0.1	$3.4(10^{-4})$	$1.3(10^{-2})$	$3.2(10^{-3})$	$9.1(10^{-3})$
					1.0	$4.0(10^{-4})$	$1.0(10^{-2})$		
					10	$8.9(10^{-4})$	$8.9(10^{-3})$		

[a] Conversion factors are given for the forty 12.7 cm x 5 cm NaI(Tℓ) detector array at an altitude of 45 meters, assuming an air density of 1.153 g/ℓ and a soil density of 1.6 g/cm^3 (10% soil moisture content). All results given are an average between those computed for an isotropic and for a cosine detector angular response (see text).

[b] Assuming a smooth air-ground interface (ie. no surface roughness).

[c] At the 1 meter level.

REFERENCES

1. Goldstein, H., Fundamental Aspects of Reactor Shielding (Addison - Wesley Publishing Company, 1959).

2. E.G.&G. 1183-1617, Research and Development FY 1973 Final Report, AEC Contract No. AT(29-1)-1183, November 1973 (73-10).

3. E.G.&G. 1183-1563, Research and Development FY 1972 Final Report, AEC Contract No. AT(29-1)-1183, September 1972 (72-05).

4. Beck, H. L., DeCampo J. and Gogolak C., In Situ Ge(Li) and NaI (Tℓ) Gamma-Ray Spectrometry, HASL-258 (1972).

5. Bruns, L. E., Aerial Gamma Survey by Helicopter to Measure Surficial Contamination, ARH-SA-176 (1974).

6. Bramson, P. E., Corley, J. P. and Nees, W. L., Environmental Status of the Hanford Reservation for CY-1972, BNWL - B-278 (1973).

7. Nees, W. L. and Corley, J. P., Environmental Surveillance at Hanford for CY-1973, BNWL-1811 (1974).

DISTRIBUTION LIST

ERDA/DSSC

L. J. Deal (25)

ERDA/RL

M. W. Tiernan (25)

ERDA/NV

J. A. Koch
R. R. Loux
R. B. Purcell
R. J. Peterson (5)

ERDA/TIC

T. B. Abernathy (2)

EG&G

H. M. Borella (2)
J. F. Doyle
R. L. Lynn
E. J. Story
ARMS Library (50)
LVAO Library
SBO Library (2)